2019

PRECLINICAL TARGETING OF TREM2 FOR THE TREATMENT OF ALZHEIMER'S DISEASE-TYPE PATHOLOGY IN A TRANSGENIC MOUSE MODEL

Brittani Rae Price
University of Kentucky, brpr222@g.uky.edu
Digital Object Identifier: https://doi.org/10.13023/etd.2019.254

STUDENT AGREEMENT:

I represent that my thesis or dissertation and abstract are my original work. Proper attribution has been given to all outside sources. I understand that I am solely responsible for obtaining any needed copyright permissions. I have obtained needed written permission statement(s) from the owner(s) of each third-party copyrighted matter to be included in my work, allowing electronic distribution (if such use is not permitted by the fair use doctrine) which will be submitted to UKnowledge as Additional File.

I hereby grant to The University of Kentucky and its agents the irrevocable, non-exclusive, and royalty-free license to archive and make accessible my work in whole or in part in all forms of media, now or hereafter known. I agree that the document mentioned above may be made available immediately for worldwide access unless an embargo applies.

I retain all other ownership rights to the copyright of my work. I also retain the right to use in future works (such as articles or books) all or part of my work. I understand that I am free to register the copyright to my work.

REVIEW, APPROVAL AND ACCEPTANCE

The document mentioned above has been reviewed and accepted by the student's advisor, on behalf of the advisory committee, and by the Director of Graduate Studies (DGS), on behalf of the program; we verify that this is the final, approved version of the student's thesis including all changes required by the advisory committee. The undersigned agree to abide by the statements above.

Brittani Rae Price, Student

Dr. Donna M. Wilcock, Major Professor

Dr. Kenneth S. Campbell, Director of Graduate Studies

PRECLINICAL TARGETING OF TREM2 FOR THE TREATMENT OF ALZHEIMER'S DISEASE-TYPE PATHOLOGY IN A TRANSGENIC MOUSE MODEL

DISSERTATION

A dissertation submitted in partial fulfillment of the
requirements for the degree of Doctor of Philosophy in the
College of Medicine
at the University of Kentucky

By
Brittani Rae Price

Lexington, Kentucky

Director: Dr. Donna M Wilcock, Professor of Physiology

Lexington, Kentucky

2019

ABSTRACT OF DISSERTATION

PRECLINICAL TARGETING OF TREM2 FOR THE TREATMENT OF ALZHEIMER'S DISEASE-TYPE PATHOLOGY IN A TRANSGENIC MOUSE MODEL

Alzheimer's disease (AD) is defined as a progressive neurodegenerative disorder and is characterized by a devastating mental decline. There are three pathological hallmarks of the disease necessary for its diagnosis, these are extracellular amyloid plaques comprised of beta-amyloid (Aβ) protein, intracellular neurofibrillary tangles comprised of hyperphosphorylated tau protein, and marked neuronal loss. Active immunization against $A\beta_{1-42}$ or passive immunization with monoclonal anti-Aβ antibodies has been shown to reduce amyloid deposition and improve cognition in transgenic mouse models of AD, aged beagles, and nonhuman primates. Unfortunately, due to cerebrovascular adverse events, both active and passive immunization strategies targeting Aβ have failed in clinical trials. It is, therefore, necessary to identify novel amyloid-clearing therapeutics that do not induce cerebrovascular adverse events. We hypothesized that neuroinflammatory modulation could be a potential novel target.

Triggering receptor expressed on myeloid cells-2 (TREM2) is a lipid and lipoprotein binding receptor expressed exclusively in the brain by microglia. Homozygous TREM2 loss of function mutations cause early-onset progressive presenile dementia while heterozygous, function-reducing point mutations triple the risk of sporadic, late-onset AD. Heterozygous TREM2 point mutations, which reduce either ligand binding or cell surface expression, are associated with a reduction in the number of microglia surrounding amyloid plaques, microglial inability to phagocytose compact Aβ deposits and form a barrier between plaques and neurons, an increase in the number of phospho- tau-positive dystrophic neurites and increased tau in the cerebrospinal fluid. Heterozygous mutations also double the rate of brain atrophy and decrease the age of AD onset by 3-6 years. Although human genetics support the notion that loss of TREM2 function

exacerbates neurodegeneration, it is unclear whether activation of TREM2 in a disease state is beneficial.

The work we present here characterizes a TREM2 agonizing antibody as a potential therapeutic for amyloid reduction. We found that its administration results in immune modulation, recruitment of microglia to the site of amyloid plaques, reduced amyloid deposition and improvement in spatial learning and novel object recognition memory in the 5xFAD model of AD. More specifically, we show that intracranial injection of TREM2 agonizing antibodies into the frontal cortex and hippocampus of 5xFAD mice leads to clearance of diffuse and compact amyloid. We also show that systemic injection of TREM2 agonizing antibodies weekly over a period of 14 weeks results in clearance of diffuse and compact amyloid as well as elevated plasma concentrations of $A\beta_{1\text{-}40}$ and $A\beta_{1\text{-}42}$. Furthermore, systemic administration of these antibodies led to immune modulation and enhanced cognitive performance on radial arm water maze and novel object recognition tests. Importantly, we show the TREM2 agonizing antibody does not induce the adverse cerebrovascular events known to accompany amyloid modifying therapies. Though systemic administration of both TREM2 agonizing and anti-$A\beta$ antibodies does not further enhance amyloid clearance or cognitive performance, co-administration mitigates the adverse cerebrovascular events associated with anti-$A\beta$ antibodies.

Collectively, these data indicate TREM2 activators may be an effective therapeutic target for the treatment of AD.

KEYWORDS: Alzheimer's Disease, Immunotherapy, Microglia, TREM2, Adverse Cerebrovascular Events.

Brittani Rae Price
April 15, 2019

PRECLINICAL TARGETING OF TREM2 FOR THE TREATMENT OF ALZHEIMER'S DISEASE-TYPE PATHOLOGY IN A TRANSGENIC MOUSE MODEL

By

Brittani Rae Price

Donna M Wilcock, Ph.D.

Director of Dissertation

Kenneth S Campbell, Ph.D.

Director of Graduate Studies

April 15, 2019

Dedicated to those that thought my dreams were unattainable, your doubt was my inspiration.

ACKNOWLEDGEMENTS

First and foremost, I'd like to thank all those that believed in and encouraged me along the way. I would not be here without your continued love and support.

Donna, I can't even begin to thank you. Thank you for taking a chance on me, encouraging me, and challenging me. Thank you for allowing me to pursue everything I wanted to learn and accomplish, and for fueling me with caffeine, seltzer water, and wine as I did it. Above everything else, thank you for believing in me even when I didn't believe in myself. I've said it before, and I'll say it again: when I grow up, I want to be like you. If I am ever half the woman or half the scientist you are, I will consider both my life and career a success.

Tiffany, I'm at loss for words (which, as you know, rarely happens). I can't begin to thank you for your patience while teaching me various techniques and answering my incessant questions. Thank you for accompanying me on countless trips to Speedway for diet coke and sour patch kids, for willingly wandering the streets of Dresden just so I could find a reasonably sized coffee, and for vouching to the Holland TSA agent that I am in no way a flight risk. Thank you for listening to me rant, for letting me eat lunch in your office, and for your willingness to partake in shenanigans from time to time. There is no one I'd rather be stranded in a foreign country with, clean out a (rather toxic) cold room with, or manage 300 abnormally aggressive mice with. You have become one of my very best friends and I couldn't have made it this far without your encouragement. I owe you my sanity.

Erica, thank you for being such an excellent role model, for always sharing advice and feedback, and for teaching me to run RAWM (I think it's safe to say which of those I'm least thankful for). Thank you for being equally as dramatic as I am, for loving Tim Horton's as much as I do, and for appreciating the use of a well-played GIF as much as I do. Thank you for partaking in and supporting the shenanigans Tiffany and I design, and for letting me serenade you with one hit wonders from the early 2000s. Sorry I made you listen to *Song of the South* on repeat that one time, I thought you would like it. Like Tiffany, you've become one of my best friends and I couldn't have made it this far without you. But don't worry, we both know I'll be embarrassing you for years to come.

Chelsea, thank you for being equally as passionate about improving the gradual school experience as I am. I'm so proud of the work we've done and will do. Despite the numerous frustrations we faced, you never considered giving up—you're amazing, thank you. I could not have asked for a better partner, we truly are a dream team. Any chance I can recruit you to Boston?

Mom, you have always worked incredibly hard and put my needs above your own. It is because of you that I understand what hard work looks like. It is because of your example that I have made it to where I am today. Thank you. Oh, and thank you for introducing me to wine, it has been quite helpful throughout the writing process.

Dad, you taught me how to dribble a basketball, wash a car, do a proper squat, and the importance of keeping my word. Most importantly, you taught me how to persevere in spite of the limitations others set for me. You have always

believed in me and for that, I am forever grateful. It is an honor to be your daughter.

Morgan, thank you for your unwavering support, unnecessarily long snapchats, and love of coffee and breakfast food. You're constantly making me laugh and remind me not to take life or myself too seriously. Although I begged mom to return you when I was 5, I'm proud to be your big sister.

Johnny, thank you for being patient when I chose to work weekends or stay up late to read, write, or study. Thank you for agreeing to uproot yourself and move to Boston this May. And thank you for never doubting me. I could not have done this without you, or your willingness to make me a fresh pot of coffee any time I asked. You're an incredible partner and dog-dad, I can't wait to see what our future holds.

TABLE OF CONTENTS

LIST OF FIGURES

Chapter 1

Introduction

Alzheimer's Disease

The term dementia is used to describe cognitive impairment severe enough to impact activities of daily living, otherwise referred to as basic self-care tasks, such as routine meals, oral care, bathing, etc. Considering dementia is an umbrella term used to describe a clinical syndrome, it should be understood that the dementia phenotype can be attributed to a number of distinct diseases. Of the diseases that cause dementia, Alzheimer's disease is the most common etiology accounting for roughly 60% of all dementia cases [1]. First described by German psychiatrist Alois Alzheimer in 1906, Alzheimer's disease (AD) is a progressive neurodegenerative disease characterized by a devastating mental decline and serves as the sixth leading cause of death in the United States today [1, 2].

Although AD symptoms vary widely among individuals, the most common initial symptom is a worsening ability to remember new information [1]. Other common symptoms include: memory loss resulting in a disruption of daily life, trouble planning or solving problems, difficulty completing routine tasks, confusion regarding time or place, challenges understanding images and visual-spatial relationships, misplacing items and losing the ability to retrace one's steps, disinhibition, reclusive behavior, alterations in mood and personality, and increased anxiety, agitation and sleep disturbances [1]. Like the symptoms themselves, the rate at which symptoms progress from mild to severe varies widely among affected individuals. Currently, there is no single test for a clinical diagnosis

of probable AD. Rather, diagnosis requires a comprehensive medical evaluation for which the patient must provide a medical and family history, undergo cognitive tests, physical and neurological examinations, blood tests, and neuroimaging. Currently, a clinical diagnosis of AD can only be confirmed by pathological assessment at the time of autopsy.

Pathologically confirmed AD diagnoses require the presence of three hallmark pathologies: extracellular amyloid plaques comprised of the amyloid-beta (Aβ) protein, neurofibrillary tangles comprised of intraneuronal inclusions of hyperphosphorylated tau protein, and marked neuronal loss [3]. The pathogenic Aβ peptide is derived from the larger amyloid precursor protein (APP), which is cleaved by α, β, and γ secretases. Approximately 90% of cellular APP is cleaved by α secretase, generating sAPPα and the CTFα fragment [4]. Subsequent γ-secretase cleavage of CTFα produces a benign, truncated fragment that does not aggregate [4]. By contrast, the remaining 10% of cellular APP is sequentially cleaved by the β and γ secretases. β secretase first cleaves APP at amino acid 671 to release a large secreted derivative, sAPPβ [4]. The resulting CTFβ fragment remains membrane-bound where it is then rapidly cleaved by γ secretase to generate the Aβ peptide [4]. However, unlike cleavage by β secretase, cleavage by γ secretase can occur at either amino acid 711 or 713 and is therefore somewhat imprecise [4]. This imprecise cleavage generates Aβ peptides of varying amino acid lengths ($A\beta_{1-40}$ and $A\beta_{1-42}$, respectively) and accounts for the C-terminal heterogeneity of the Aβ peptide population. The slightly longer 42 amino acid species of Aβ ($A\beta_{1-42}$) is more hydrophobic and fibrillogenic then shorter Aβ species

[4]. As a result, $A\beta_{1-42}$ is the principal species deposited in amyloid plaques. However, accumulation of the Aβ peptide is not limited to amyloid plaques of the brain parenchyma but is also observed in the brain vasculature as cerebral amyloid angiopathy (CAA). In contrast to parenchymal depositions comprised primarily of $A\beta_{1-42}$, CAA contains both $A\beta_{1-40}$ and $A\beta_{1-42}$, with $A\beta_{1-40}$ being the major isoform present [5]. $A\beta_{1-40}$ has also been reportedly shown to colocalize with $A\beta_{1-42}$ in parenchymal deposits of amyloid. It is important to note Aβ can also be deposited as diffuse plaques, often thought to be an intermediate step in the formation of the compact amyloid plaques referred to above.

By contrast, neurofibrillary tangles (NFTs) are intraneuronal cytoplasmic bundles of paired, helically wound filaments comprised of hyperphosphorylated tau protein [6]. Under physiological conditions, tau modulates the stability of axonal microtubules. Tau contains 85 phosphorylation sites and so it is not surprising phosphorylation at any of these sites profoundly impacts its function [7]. Under pathological conditions such as AD, tau becomes hyperphosphorylated, reducing its affinity for microtubules and destabilizing the cytoskeleton of the affected neuron [7]. Additionally, hyperphosphorylation of tau promotes aberrant assembly of tau into insoluble aggregates that induce synaptic dysfunction and neuronal cell death.

Topographic Distribution of AD-Associated Pathology

Throughout the progression of AD, amyloid plaques and neurofibrillary tangles are initially observed in different areas of the brain: amyloid pathology is first observed in the neocortex whereas neurofibrillary tangles are first observed in allocortical structures [3, 8-11]. As to be expected, the distribution patterns of amyloid and neurofibrillary tangle pathology also differ throughout disease progression. In 1995, a landmark paper by Braak and Braak characterized the regional distribution of neurofibrillary tangles, known today as the six-part Braak staging system of AD [3]. According to Braak staging, the distribution pattern of neurofibrillary tangles in AD begins in the transentorhinal cortex (stages I) then advances to include the CA1 region of the hippocampus (stage II) and limbic structures such as the subiculum (stage III) and amygdala and thalamus (stage IV) [3]. This expansion of pathology continues until virtually all subdivisions of the cerebral cortex are consumed with neurofibrillary tangle pathology (stages V-VI) [3]. Conversely, amyloid plaques accumulate mainly in the neocortex. While the spatiotemporal pattern of progression of amyloid deposition is less predictable than that of neurofibrillary tangles, in 2002 Thal et al. proposed a staging system that is still in use today [10]. Thal staging proposes 5 stages: 1) Stage 1, characterized by the accumulation of amyloid deposits in the neocortex, 2) Stage 2, involves additional amyloid deposition in the entorhinal cortex, hippocampus, and amygdala, 3) Stage 3, involves additional deposition in the striatum, thalamus, hypothalamus and white matter, 4) Stage 4, involves additional deposition in the

red nucleus, reticular formation of the medulla oblongata and the substantia nigra, and 5) Stage 5, involves additional deposition in the pons and cerebellum [10].

The Amyloid Cascade Hypothesis

To date, AD pathogenesis is widely believed to be driven by the production and deposition of the Aβ peptide in amyloid plaques. First conceptualized by John Hardy and Gerald Higgins in 1992, the amyloid cascade hypothesis proposes neurofibrillary tangles, neuronal loss, vascular damage, and dementia are the direct result of Aβ deposition in the form of diffuse and compact, neuritic plaques [12]. More specifically, this hypothesis suggests the pathological progression of AD follows a temporal sequence with Aβ deposition triggering neurofibrillary tangle formation, synaptotoxicity, mitochondrial dysfunction, chronic neuroinflammation arising from aberrant activation of microglia and astrocytes, and ultimately dementia (Figure 1.1) [13, 14]. Despite growing controversy surrounding this hypothesis, it continues to provide the main theoretical construct for AD due to a large body of supporting evidence.

Much of the support for the amyloid cascade hypothesis is derived from genetic mutations known to cause familial, early-onset AD (EOAD) which is characterized by a mean age of onset of less than 65 years. Mutations in either APP or the core catalytic subunit of γ-secretase, presenilin 1 (PSEN1) or presenilin 2 (PSEN2), either increase the overall production of Aβ or increase the production of $A\beta_{1-42}$ specifically. Granted, EOAD accounts for only 5% of AD cases. Additional support for the amyloid cascade hypothesis comes from the most significant

genetic risk factor for late-onset AD (LOAD), apolipoprotein E (ApoE), a plasma protein involved in the transport of cholesterol and other lipids. The ApoE gene contains several single-nucleotide polymorphisms (SNPs) resulting in three common isoforms of ApoE: ApoE2 (cys112, cys158), ApoE3 (cys112, arg158), and ApoE4 (arg112, arg158) [15]. Though the three isoforms differ only by one or two amino acids, these differences profoundly influence ApoE structure and function [15, 16]. Of the three isoforms, ApoE3 is the most common and is not believed to play a significant role in AD. While ApoE2 is associated with a lower risk for AD, possession of an ApoE4 allele is the strongest genetic risk factor for LOAD and CAA or a combination of both disorders, given it impairs Aβ clearance in the brain [15, 17, 18]. Yet, possession of the ApoE4 allele does not guarantee that a person will develop LOAD, simply that they have a significantly increased risk compared to someone with no ApoE4 alleles. Overall, genetic risk factors and mutations for LOAD and EOAD, respectively, support the amyloid cascade hypothesis given they increase Aβ deposition either by enhancing amyloidogenic processing of APP or by inducing disruption in Aβ clearance mechanisms.

Further support for the amyloid cascade hypothesis comes from individuals with Down syndrome. First described by J. Langdon Down in 1866 and identified as a chromosome 21 trisomy by Jerome Lejeune in 1959, Down syndrome is one of the most common causes of intellectual disability [19-21]. It's well known that Down syndrome is characterized by facial dysmorphology, deficits in the immune and endocrine systems and delayed cognitive development, but a lesser known feature of Down syndrome is that affected adults experience an increased risk for

developing AD as they age. Coinciding with this age-dependent risk, almost all Down syndrome adults over the age of 40 exhibit neuropathology sufficient for an AD diagnosis [21]. This is because APP is located on chromosome 21 and the most common form of Down syndrome, trisomy 21, leads to an overexpression of APP. In Down syndrome individuals with complete trisomy 21, extracellular Aβ accumulates in diffuse plaques starting at age 30 [21, 22], after which amyloid plaques and neurofibrillary tangles continue to rapidly accumulate until they reach a threshold sufficient for AD diagnosis by age 40 [21, 23]. Conversely, individuals with partial trisomy of chromosome 21 that does not result in duplication of the APP locus develop Down syndrome but not AD [24], whereas individuals presenting only small internal chromosome 21 duplications that result in three copies of APP develop EOAD but do not develop Down syndrome [25]. Thus, overexpression of APP is strongly linked to Aβ deposition in adult life.

Additional support for the amyloid cascade hypothesis arises from studies of Aβ-induced synaptic dysfunction and synaptotoxicity. Synaptic plasticity is the process by which specific patterns of synaptic activity alter synaptic strength over time. Long-term potentiation (LTP) is a form of activity-dependent plasticity which results in the enhancement of synaptic transmission, whereas long-term depression (LTD) is a form of activity-dependent plasticity that leads to reduced efficacy of synaptic transmission. Both LTP and LTD are important for learning and memory. LTP and LTD are regulated by the activity of two ionotropic receptors for glutamate: N-methyl-D-aspartate receptors (NMDARs) and α-amino-3-hydroxy-5-methyl-4-isoxazolepropionic acid receptors (AMPARs). Induction of LTP requires

activation of NMDARs, leading to large post-synaptic increases in Ca^{2+} and activation of downstream signaling events that involve re-localization of new AMPARs to the plasma membrane [26]. AMPARs are redistributed to the plasma membrane to potentiate the synapse (LTP) or removed from the plasma membrane to weaken the synapse (LTD). Studies suggest that A□-induced excitotoxicity results from aberrant stimulation of NMDARs, likely resulting from impaired regulation of glutamate levels [14, 27, 28]. Excess glutamate in the synaptic cleft may desensitize NMDARs, preventing sufficient post-synaptic Ca^{2+} influx and LTP induction [29]. Furthermore, increased Aβ levels have been associated with increased AMPAR internalization and thus enhanced LTD [30]. These studies are further supported by others demonstrating that preventing the overstimulation of NMDARs with partial antagonists mitigates axonal transport deficits in primary neuronal cultures and hippocampal slices from rats and mice [31, 32]. Coincident with these studies, partial NMDAR antagonism is said to account for the beneficial clinical effect of memantine when prescribed for AD [33].

Finally, support for the amyloid cascade hypothesis comes from two rat studies. In 2008, Shankar et al. demonstrated that injection of $A\beta_{1-42}$ directly isolated from AD brains leads to impaired synaptic plasticity and memory in otherwise healthy rats [34, 35]. In 2011, Jin et al. demonstrated that human $A\beta_{1-42}$ oligomers induced hyperphosphorylation of tau in cultured rat neurons [34].

Despite compelling evidence in support of the amyloid cascade hypothesis, data from a number of studies are inconsistent with its linear structure. One major objection for the amyloid cascade hypothesis is the fact that Aβ deposition can

occur in nondemented elderly individuals. In fact, one study found that only 17% of nondemented elderly individuals had few or no degenerative brain changes at the time of autopsy [36], while another demonstrated that between 20-40% met criteria for neuropathological diagnosis of AD despite having an average MMSE score of 28.1 prior to death [37]. Furthermore, amyloid-PET studies have shown that a substantial amyloid burden can be observed in the brains of nondemented elderly individuals [38, 39], supporting the estimate that 10-30% of this patient population has amyloid-positive brain scans [40]. Granted, the most compelling argument against the amyloid cascade hypothesis is derived from numerous failed Aβ-targeted immunotherapy trials.

In 2002, a participant of the first active $A\beta_{1-42}$ immunotherapy trial (AN1792) died due to conditions unrelated to the vaccine, thereby allowing neuropathologists to examine the effects of $A\beta_{1-42}$ immunotherapy for the first time. The autopsy revealed extensive areas of the cerebral cortex were devoid of plaques, although plaques remained present in other cortical areas along with residual tau pathology [41]. A follow-up study examined 9 additional participants of the AN1792 trial and found that those receiving the vaccine presented a reduction in Aβ load compared to unimmunized controls, though reductions in Aβ load and the degree of plaque removal was variable [42]. Unfortunately, despite enhanced clearance and subsequent reductions in $A\beta_{1-42}$, a long-term clinical follow up study found AN1792 participants experienced no cognitive benefits [43]. Rather, this study showed that all participants exhibited progressive cognitive decline until the time of death, including 2 participants that presented virtually no plaque pathology at the time of

autopsy [43, 44]. To date, these findings have been corroborated by several other groups [45-47]. Similarly, passive immunotherapy trials have also failed.

These studies suggest that amyloid deposition and the dementia characteristic of AD are mutually exclusive and therefore serve as a substantial challenge to the amyloid cascade hypothesis. However, it is important to note that these data do not negate the fact that $A\beta_{1-42}$ is toxic, but rather suggest the field reconsider its reliance on what has potentially become an overwhelming dogma.

Transgenic Mouse Models of AD

Transgenic mouse models became an aim for researchers following the discovery of genetic mutations in the APP, PS1, and PS2 genes causative of EOAD. In 1996 Duff et al. reported that mice overexpressing the M146L mutation in PS1 showed a selective increase in brain $A\beta_{1-42}$ compared to wildtype littermates, however, these mice did not deposit amyloid in diffuse or compact plaques [48]. Fortunately, mice expressing mutations in the APP gene showed greater promise.

First described by Games et al., the PDAPP mouse is one of the earliest transgenic mouse models of AD. The PDAPP model expresses APP 695, APP 751 and APP 770 with the Indiana mutation (V717F) under the control of the platelet-derived growth factor (PDGF) promoter [49]. Starting at 4 months of age, this model exhibits cognitive deficits in a variety of tasks. In fact, cognitive deficits are observed prior to amyloid deposition which is first seen between 4 and 6 months of age, accelerates rapidly between 7 and 9 months of age, and reveals significant

numbers of both diffuse and compact deposits in the frontal cortex and hippocampus by 12 months of age [49]. GFAP-positive astrocytes and activated microglia have also been shown to associate with plaques in this model [49]. Interestingly, while there are no paired helical filaments or aggregates present in this model, phosphorylated tau immunoreactivity has been observed in dystrophic neurites after 14 months of age [50].

To date, one of the most well characterized and widely used mouse models of AD is the Tg2576 model. Developed by Karen Hsiao Ashe, the Tg2576 model overexpresses the APP 695 with the Swedish mutation (KM670/671NL) under the control of the hamster prion protein promoter [51]. Tg2576 mice have detectable diffuse and compact amyloid deposits by 6 months of age and exhibit extensive parenchymal plaque deposition by 11-13 months of age [52]. The Tg2576 model has also been shown to exhibit an increase in microglial density and size in plaque forming areas [53], synaptic loss by 4.5 months of age [54], and deficits in LTP by 5 months of age [55]. Some studies show Tg2576 mice have impaired spatial learning and deficits in working memory and contextual fear conditioning by 6 months of age, while others report normal cognition at this age with progressive impairment starting at 12 months of age. It may be noted this discrepancy likely arises because the mice carry the $Pde6b^{rd1}$ retinal degeneration allele that may induce light sensitivity or blindness and affect the results of behavioral testing.

In an effort to produce a transgenic model that demonstrated reproducible cognitive and memory deficits, the M146L PS1 mouse was crossed with the Tg2576 APP mouse to create the PS/APP mouse. First described by Holcomb et

al. in 1998, the PS/APP model exhibits an early, selective increase in brain levels of $A\beta_{1-42}$ followed by accelerated $A\beta$ deposition, with amyloid plaques occupying large areas of the neocortex and hippocampus by 16 months of age [56]. Coincident with plaque deposition, there is a substantial increase in plaque-associated microglia and astrocytes, indicating a substantial neuroinflammatory response between 6 and 16 months of age [57]. Importantly, PS/APP mice exhibit reproducible age-dependent behavioral deficits as assessed by both the Morris and radial arm water mazes [58]. Interestingly, while neurofibrillary tangles are not observed in this model, hyperphosphorylated tau is detectable as punctate deposits near amyloid plaques in the cortex and hippocampus starting at 24 weeks of age [59]. Additionally, neuronal loss in the CA1 region of the hippocampus has been demonstrated in 22-month-old PS/APP mice [60].

Although the aforementioned models exhibit amyloid plaque pathology similar to that observed in AD, they develop this pathology slowly. In 2006, in an effort to accelerate the development of amyloid pathology and investigate the effects of very high cerebral $A\beta_{1-42}$ levels, Oakley et al. generated the 5xFAD model of AD. 5xFAD mice express 3 APP mutations (Swedish K670N/M671L, Florida I716V, and London V717I) and 2 PS1 mutations (M146L and L286V), each driven by the mouse Thy1 promoter [61]. As a result of expressing 5 distinct AD-associated mutations, the 5xFAD model rapidly develops severe amyloid pathology. These mice accumulate intraneuronal $A\beta_{1-42}$ starting at 1.5 months of age with amyloid deposition rapidly following at 2 months and continuing to increase with age. Gliosis begins at 2 months of age coincident with plaque

deposition, synapse degeneration is then observed by 4 months of age along with neuronal loss and behavioral deficits [61].

Although these amyloid-depositing models are useful for testing therapies targeting amyloid specifically, they fail to incorporate neurofibrillary tangle pathology. As a result, the P301L tau transgenic model was developed in the lab of Mike Hutton in 2000. P301L mice carry a transgene encoding human tau that contains the P301L mutation under the control of the mouse prion promoter [62]. This model develops neurofibrillary tangle pathology in an age and gene-dose dependent manner; by 4.5 months of age in homozygotes and 6.5 months of age in heterozygotes [62]. Unfortunately, due to the expression of P301L tau in the brain stem and spinal cord, this model also develops motor deficits that render the mice completely paralyzed by 12 months of age [62]. Moreover, mice show differential expression between males and females, with females having 3-4 times greater expression of P301L tau [62]. Despite these disadvantages, it has been shown that crossing the P301L mouse with the Tg2576 mouse (APPSwe-Tau model) enhances forebrain neurofibrillary tangle pathology, further suggesting the presence of Aβ influences the extent of neurofibrillary pathology [63]. However, it should be noted that this model exhibits motor disturbances similar to those observed in the P301L mouse [63].

Fortunately, the 3xTg model displays both plaque and tangle pathology without any physical or behavioral abnormalities. The 3xTg model was generated by injecting single-cell embryos from mice with knock-in of PS1 with the M146V mutation with two human transgenes (APP with the Swedish mutation and tau with

the P301L mutation), both under the control of the mouse Thy1.2 promoter [64]. Extracellular Aβ deposits are evident by six months of age, with tau pathology apparent by 12 months of age [65]. 3xTg mice also demonstrate age-dependent LTP impairment although this occurs prior to the development of any AD-like pathology [64]. Cognitive impairment has been shown to manifest by 4 months of age as a deficit in long-term retention, however, neither amyloid nor tau pathology is present at this time point [66].

Though these models have been pivotal for our current understanding of AD, because the vast majority of AD cases arise not from autosomal dominant mutations causative of EOAD but through a complex interaction of polymorphisms and environmental risk factors that accrue over time, significant progress remains to be made in the creation of the ideal mouse model.

Behavioral Analyses of Transgenic Mice

As previously discussed, AD symptoms center on cognitive impairment, thus any proposed clinical therapy will only be deemed effective if it improves learning and memory. As such, cognitive assessment is crucial in preclinical studies. Several behavioral paradigms have been developed to assess cognitive impairment in mice.

First described by Richard Morris in 1982, the Morris water maze is consistently used to assess memory retention [67]. The test is comprised of a water pool with a hidden escape platform that the mouse must locate using either local or contextual clues. This test takes advantage of a mouse's natural aversion

to water and swimming, using this aversion to encourage mice to seek out the hidden platform. Measurements include the time taken to locate the platform (escape latency) and the time spent in the quadrant where the platform was once removed (probe trials) [67]. The Morris water maze has been shown to be heavily hippocampal dependent given lesions to the hippocampus or its cholinergic inputs significantly impair performance [67].

A commonly used modification of the Morris water maze is known as the radial arm water maze (RAWM). The RAWM consists of a circular pool with six swim alleys (arms) radiated out from an open central area and a submerged escape platform at the end of one of the arms. Similar to the Morris water maze, the mouse must locate the escape platform using spatial cues present on the walls of the testing room. Mice complete thirty trials over the course of two days, during which the platform remains in the same arm (goal arm) for each mouse but the arm in which the mouse starts each trial is different [68]. Alternating the start arm requires the mouse to use the visual cues to remember where the platform is [69]. Both the time taken to find the platform and the number of wrong arms entered (errors) is measured [68]. Like the Morris water maze, the RAWM is a heavily hippocampal dependent spatial learning and memory task.

In contrast to the Morris and radial arm water mazes described above, novel object recognition (NOR) is a short-term memory task that exploits a mouse's innate predisposition to explore new objects [70]. NOR is comprised of two phases of testing: a familiarization phase and a test phase. During the familiarization phase, the mouse is presented with, and explores, two identical copies of an object

(object A) in the test environment. Following a delay period, the mouse undergoes the test phase which involves presenting a new copy of object A and a novel object B in the same test environment. If the mouse preferentially orients to and explores object B, an inference is made that the mouse recognized object A as familiar, thereby displaying a sensitivity to discriminate old from new [71]. On the other hand, if the mouse orients to and explores both objects A and B equally, it is assumed that the mouse is unable to perform the recognition discrimination [71]. NOR task performance is quantified using the Discrimination Ratio (DR), which reflects the duration of exploration of the novel object compared to the familiar object as a proportion of the mouse's total exploration time [72]. NOR has been shown to be heavily dependent upon the integrity of the perirhinal cortex given that lesions of the perirhinal cortex reliably lead to NOR task performance deficits [73].

Another widely used behavioral paradigm for assessing memory is known as contextual fear conditioning. Contextual fear conditioning is employed using an aversive stimulus, commonly a small electric shock, coupled to sound. Throughout this task mice learn to freeze when the sound is heard as it is associated with the aversive stimulus and the extent of freezing is then measured [74]. If a mouse fails to freeze it is assumed it exhibits impaired memory of the preceding events [75]. While this task is highly dependent upon the integrity of the amygdala it is also sensitive to disruptions in hippocampal function.

Targeting Neuroinflammation for the Treatment of Alzheimer's Disease

In addition to its three hallmark pathologies, AD is characterized by an extensive neuroinflammatory response, of which microglia and astrocytes are the principal regulators. This pathological feature of AD was uncovered by autopsy reports from the 1980s demonstrating the presence of immune-related antigens and cells surrounding amyloid plaques in the brains of AD and Down syndrome patients [76-78]. While these initial reports challenged the previously assumed view that the brain was immunologically privileged due to the blood-brain-barrier (BBB), additional reports from the 1990s led to the concept of neuroinflammation [79-81]. Today, neuroinflammation is at the forefront of AD research, both for its contribution to the neurodegenerative process and for its role in the clearance of AD lesions.

As the brain's resident macrophages, microglia are crucial contributors to homeostasis and immune defense. Under homeostatic conditions, microglia regulate neuronal proliferation and differentiation as well as synaptogenesis [82, 83]. Additionally, as part of the innate immune system, microglia constantly survey the brain parenchyma for signals of external danger [84]. del Rio-Hortega first identified microglia in 1932, describing them as a small population of phagocytic migratory cells within the CNS [85]. It wasn't until 1939 that he coined the term microglia. Because microglia exhibit morphology and phagocytic capacity similar to that of macrophages, del Rio-Hortega hypothesized microglia may be derived from blood monocytes [85]. These observations ultimately gave way to the long-supported prevailing viewpoint that microglia, like macrophages, are of monocyte

origin. However, a landmark study published in 2010 by Florent Ginhoux and colleagues proved this viewpoint false. In this study, Ginhoux et al. used fate-mapping analysis to reveal that microglia are derived from primitive yolk-sac macrophages and subsequent studies have shown that microglia self-renew via local proliferation under homeostatic conditions [86, 87]. Conversely, in the context of neurodegeneration, bone marrow-derived (BM) macrophages can infiltrate the CNS, however, this infiltration has been shown to require BBB disruption as well as the induction of specific chemokines [88-90].

del Rio-Hortega's original characterization of microglia also described the cell's ability to respond to brain injury by migrating to sites of tissue damage, undergoing marked changes in morphology, proliferating, and engulfing tissue debris [85]. It wasn't until the 1980s when methods for culturing microglia in vitro and reagents for visualizing cells in situ were developed, that subsequent studies identified two principal forms of microglia: amoeboid or "activated" microglia and ramified or "resting" microglia. Activated microglia were described as being morphologically similar to monocytes and macrophages whereas resting microglia were described as having processes [91]. One study compared microglial cultures to macrophages and demonstrated a number of similarities in morphology, cellular functions, cell surface antigens and immunohistochemical properties [91].

Macrophages are leukocytes that monitor their tissue environment and respond rapidly to perturbations based on the stimuli they are presented with. The heterogeneity of their responses warranted a phenotypic classification system in which macrophages are said to be polarized to either an M1 or M2 phenotype.

Macrophages activated by IFN-γ or TNFα secrete proinflammatory cytokines, produce reactive oxygen and nitrogen species, and are considered to be classically activated, M1 macrophages. It is important to note that M1 macrophages exhibit high microbicidal activity and therefore serve as an important defense mechanism that can cause damage if not tightly regulated [92]. Conversely, M2 or alternatively activated, macrophages are associated with anti-inflammatory cytokine expression and are further subdivided into three types: M2a, M2b, and M2c. M2a macrophages are stimulated by IL-4 or IL-13 and described as wound healing and repair macrophages given they secrete mediators shown to contribute to extracellular matrix (ECM) deposition and remodeling [93]. M2b macrophages are instead stimulated by immune complexes, toll-like receptor activation or IL-1 receptor ligands and represent a combined M1/M2a phenotype. Finally, M2c macrophages are stimulated by IL-10 and are often referred to as regulatory macrophages with anti-inflammatory activity [94, 95]. It is important to note that M2c macrophages contribute to an environment that enhances survival as opposed to the neutralization of pathogens. Because microglia have been shown to express many of the same neuroinflammatory markers as macrophages, the neuroinflammation field extended the M1/M2 taxonomy to classify microglia. This classification system was then used to harness new neuroinflammation-targeted therapies for AD in the early 2000s.

In 1998 E.G. McGeer and P.L. McGeer introduced the concept of the autotoxic loop and subsequently the neuroinflammation hypothesis of AD. The autotoxic loop was described by McGeer and McGeer as a “vicious cycle” in which

microglia were activated as a consequence of amyloid pathology [96]. Activated microglia then said to result in the secretion cytotoxic cytokines that induced rapid neuronal death and provided cellular debris that further exacerbated the process [96]. This hypothesis was ultimately supported by the finding that cytokine levels are increased in the brains and cerebrospinal fluid (CSF) of AD patients [97]. However, a number of successive studies demonstrated the levels of these cytokines are not sufficient to or sustained enough to cause substantial neuronal damage. In fact, attempts to recreate the autotoxic loop in transgenic mouse models of AD revealed that the initiation of an inflammatory response in the brain leads to the clearance of amyloid plaques; a finding that ultimately led to one of the most extensively explored potential therapies for AD: anti-A□ immunotherapy.

In 1999, Dale Schenk and colleagues demonstrated that active immunization with $A\beta_{1-42}$ prevents plaque formation, neuritic dystrophy, and astrogliosis in 6-week-old PDAPP mice [98]. Furthermore, this study demonstrated that immunization with $A\beta_{1-42}$ reduces $A\beta$ deposition in aged, 11-month-old PDAPP mice [98]. Subsequent studies in transgenic mice, aged beagles, and nonhuman primates indicated that active immunization with $A\beta_{1-42}$ improves cognition in addition to reducing $A\beta$ deposition [99-102]. The first anti-$A\beta$ immunotherapy trial, AN-1792, was initiated as a result of these findings. AN-1792 consisted of a synthetic, full-length $A\beta_{1-42}$ peptide formulated in the QS-21 adjuvant [103]. Although no adverse events were reported in Phase 1, 6% of the 372 trial participants in Phase 2a developed aseptic meningoencephalitis [104]. Though affected participants responded well to treatment with corticosteroids, the risk was

deemed too high and the vaccine was ultimately discontinued. As previously discussed, it wasn't until the first participant of the AN-1792 trial died that a beneficial effect of the vaccine was observed. The failure of this active immunization trial ultimately encouraged scientists to explore passive immunization strategies.

In 2003, Wilcock et al. demonstrated that bilateral intracranial injection of an anti-$A\beta_{1-42}$ monoclonal antibody dramatically reduced the $A\beta$ load in mice [105]. This study showed that diffuse $A\beta$ levels were significantly reduced by 24 hours post-injection, but it wasn't until 72 hours post-injection that compact plaque deposition was reduced [105]. This early reduction in $A\beta$ load was shown to occur in the absence of the microglial activation markers CD45 and MHC-II, whereas reduction of compact plaques was shown to occur in association with microglial activation [105]. This temporal association of compact amyloid reduction with microglial activation suggested that microglial activation is crucial for the clearance of compact, fibrillogenic amyloid deposits. The authors deduced that between 24 and 72 hours activated microglia near amyloid deposits likely phagocytose opsonized amyloid via $Fc\gamma$- or complement-mediated mechanisms [105, 106]. In 2004, this same group demonstrated that weekly intraperitoneal injections of an anti-$A\beta_{1-42}$ monoclonal antibody reversed learning and memory deficits in aged, APP-transgenic mice [107]. Although dramatic reductions in amyloid deposition were observed, this study also found a significant increase in vascular amyloid deposition and the number of microhemorrhages in the brain following immunization; Granted, it may be noted that cognitive benefits persisted in the

presence of these cerebrovascular pathologies [107]. Soon after, Pfeifer et al. demonstrated that spontaneous microhemorrhages were significantly increased in APP23 mice following 5 months of passive immunization [108], and DeMattos et al. showed the same phenomenon in PDAPP mice [109]. Further studies into the appearance of microhemorrhages revealed a time-dependent increase in vascular amyloid deposition and the number of microhemorrhages, as well as an association of the microhemorrhages with these vascular deposits [109-111].

Despite the observance of cerebrovascular pathologies in association with passive immunization of transgenic mice, successes in amyloid clearance and improved cognition spurred a number of clinical trials. The most promising antibody to enter clinical trials was bapineuzumab. Bapineuzumab is a humanized monoclonal IgG1 antibody that targets the N-terminal region of Aβ and is thought to activate microglial phagocytosis and cytokine production [112]. In the Phase 1 trial, participants received a single dose of 0.5, 1.5 or 5 mg/kg of bapineuzumab [112]. Notably, while the Phase 1 trial was not designed to measure effects on cognition, participants underwent cognitive testing before receiving their assigned dose and again 16 weeks later, allowing for the determination that bapineuzumab improved MMSE scores in those randomized to the 0.5 and 1.5 mg/kg groups [112]. Despite the fact that 3 of the 10 participants receiving 5 mg/kg of bapineuzumab developed vasogenic edema [112], the antibody progressed to a Phase 2 clinical trial. The Phase 2 trial included 234 participants with mild-to-moderate AD randomized to bapineuzumab or placebo in one of four dose cohorts: 0.15, 0.5, 1 or 2 mg/kg [113]. Participants received an infusion of their assigned

dose every 13 weeks for a total of 6 infusions and underwent final assessments at week 78 [113]. Unfortunately, no significant differences were observed in the primary efficacy analysis and 9.7% of bapineuzumab treated patients developed reversible vasogenic edema [113]. It may be noted that vasogenic edema was more frequent in ApoE4 carriers and those randomized to higher dose cohorts. Despite disappointing Phase 2 outcomes, a Phase 3 program was initiated. Importantly, because Phase 2 post-hoc exploratory efficacy by ApoE4 carrier status suggested a treatment response in noncarriers [114], the Phase 3 program consisted of separate clinical trials for E4 carriers and noncarriers [115]. Unfortunately, bapineuzumab failed to demonstrate therapeutic efficacy in both the carrier and noncarrier studies [115]. Furthermore, vasogenic edema was observed in 11.4% of participants heterozygous for E4, 27.3% of participants homozygous for E4, 14.2% of noncarriers randomized to 2.0 mg/kg, 9.4% of noncarriers randomized to 1.0 mg/kg, and 4.2% of participants randomized to 0.5 mg/kg of bapineuzumab [115].

The magnetic resonance imaging (MRI) abnormalities observed in the bapineuzumab trials, vasogenic edema and microhemorrhages, have since been associated with other amyloid modifying therapies. As a result, these abnormalities are now collectively referred to as amyloid-related imaging abnormalities, or ARIA [116]. ARIA-E refers to MRI signal alterations thought to represent vasogenic edema, while ARIA-H refers to alterations believed to be attributable to microhemorrhage and/or hemosiderosis [116]. ARIA-E is typically observed as a transient hyperintensity on FLAIR imaging and, at the cellular level, is thought to

represent an increase in extracellular fluid volume due to enhanced permeability of the brain capillaries [116]. By contrast, ARIA-H manifests as a low-intensity signal on T2* MRI or susceptibility-weighted imaging (SWI) and is thought to represent iron deposits indicative of a small leakage of blood from a vessel into the adjacent parenchyma (microhemorrhage) or subarachnoid space (superficial siderosis) [116]. To date, there is limited information regarding the relationship between ARIA-E and ARIA-H, however, their relation to dose in the bapineuzumab trials suggests ARIA may arise due to enhanced clearance of parenchymal amyloid [41, 44]. Hypotheses suggest the rapid movement of amyloid from the parenchyma into the perivascular space creates a drainage backup resulting in excess fluid shifts and vasogenic edema. Hypotheses also suggest that extraction of amyloid from the vasculature might result in enhanced permeability and fragility of brain capillaries. Assuming vessel wall integrity is sufficiently compromised, this proposed mechanism could explain the increased incidence of microhemorrhages following the administration of amyloid-modifying therapies.

The aforementioned hypotheses relate to those proposed for the mechanism by which anti-Aβ antibodies clear amyloid from the brain. The first hypothesis centers on the traditional role of an antibody to opsonize antigens and induce phagocytosis and complement activation [117]. More specifically, this hypothesis suggests that anti-Aβ antibodies bind to Aβ, after which the Fc portion of the antibody binds the Fcγ-receptor (FcγR) on microglia thereby inducing phagocytosis of amyloid. As previously discussed, experimental models of AD and observations from clinical trials have provided evidence that FcγR-induced

phagocytosis is largely responsible for amyloid clearance following immunotherapy [118]. Granted, due to the adverse events that accompany immunotherapy, a number of Aβ antibodies with Fc modifications have been developed and are currently in trials. An alternative hypothesis, known as the "peripheral sink" mechanism, negates the assumption that anti-Aβ antibodies cross the BBB [119]. This mechanism instead proposes that antibodies clear Aβ from the blood, in turn generating a concentration gradient that favors exportation of Aβ from the brain into the blood [119]. A third proposed mechanism suggests that anti-Aβ antibodies modify the secondary structure of Aβ monomers making them less prone to aggregate into oligomeric or fibrillogenic forms [120]. Irrespective of their differences, it is unlikely that these three mechanisms are mutually exclusive. Rather, antibodies may use each of these mechanisms to varying degrees, and utilization likely depends on the specific binding sites and isotype of each antibody [118, 121].

Holistic interpretation of these data yields only one conclusion: it remains unclear whether microglial function in AD is beneficial but insufficient, whether microglia simply lose their efficacy, or whether microglia become detrimental throughout the course of disease progression. It is likely that analyzing bulk cell populations based on a subset of surface markers has contributed to conflicting reports regarding the role of microglia in AD. The recent advent of single-cell genomics has enabled unbiased characterization of immune cell types and states, in turn permitting the identification of new markers, pathways, and regulatory factors. A landmark study published by Keren-Shaul et al. in 2017 used single-cell

genomics to identify a new microglia phenotype associated with restricting neuroinflammation [122]. This study identified a subset of microglia that express both microglial genes (Cst3 and Hexb) and a unique signature of genes associated with lipid metabolism and phagocytosis (ApoE, Lpl, and Cst7) [122]. Notably, microglia possessing this phenotypic signature were observed in only in 5xFAD mice and therefore were defined as disease-associated microglia (DAM). Additionally, this study revealed that DAM are spatially associated with amyloid pathology and display an enhanced phagocytic capacity. In fact, genes expressed by DAM throughout disease progression revealed elevated lipid metabolism pathways as well as enhanced phagocytic genes, corresponding to the need for plaque clearance [122]. Interestingly, DAM were found to be regulated by the immunoreceptor TREM2 and its associated adaptor protein DAP12. TREM2 and DAP12 are known to form a signaling complex that may enhance phagocytosis and participate in the suppression of the inflammatory response by repressing microglia-mediated cytokine production [123]. Finally, activation of DAM was shown to occur via two sequential, but distinct phases. The first phase was shown to be TREM2-independent whereas the second phase involving the induction of lipid metabolism and phagocytic pathways (via increased expression of Lpl, Cst7, and CD9) requires TREM2 [122]. Importantly, the transition from homeostatic to fully activated DAM does not occur in the absence of TREM2, which ultimately supports the observation that the absence of TREM2 in late, but not early, AD exacerbates pathology [122, 123]. Therefore, it is possible the genes expressed by DAM are necessary to enhance phagocytosis and clear amyloid, but that

activation of DAM may occur relatively late in the disease. Genes expressed by homeostatic microglia, stage 1 DAM (TREM2-independent) and stage 2 DAM (TREM2-dependent) are outlined in Figure 1.3.

TREM2

Triggering receptor expressed on myeloid cells-2 (TREM2) is a single-pass transmembrane protein expressed in cells of myeloid origin such as bone marrow and monocyte-derived macrophages and osteoclasts. Importantly, TREM2 is also expressed in the brain exclusively by microglia. Support for this claim arises from several in vitro studies showing primary cultured microglia express TREM2 as well as numerous in vivo studies demonstrating TREM2 expression in mouse microglia [124-132]. To date, TREM2 has been proposed to bind a variety of ligands including lipids, lipoproteins, and ligands associated with damage- or pathogen-related molecular patterns [133]. Lipids have been shown to activate TREM2 signaling both as components of a cellular membrane and as components of a lipoprotein complex [134]. More specifically, studies have shown that both lipidated and non-lipidated APOE binds the extracellular region of TREM2 in vitro and that TREM2 appears to have no preference in APOE isoform [135-137]. Moreover, Yeh et al. showed that TREM2 also associates with other lipidated apolipoproteins, specifically APOA1, APOB, and APOJ [137]. Additional ligands for TREM2 include high-density lipoprotein (HDL), low-density lipoprotein (LDL), heparin sulfate proteoglycans and other negatively charged lipids [137-141].

Because TREM2 has a short cytoplasmic tail, it requires aid from its associated intracellular adaptor protein (DAP12) to mediate its signaling functions. Ligand binding to TREM2 results in the phosphorylation of DAP12 and subsequent recruitment of spleen tyrosine kinase (SYK) [142, 143]. SYK activation, in turn, activates a number of signaling cascades that ultimately induce Ca^{2+} mobilization, regulate phagocytosis, inhibit inflammatory signaling and promote cell survival (Figure 1.2) [142, 143].

Much of what we know about the genetics of TREM2 can be attributed to an autosomal recessive form of early-onset dementia known as Nasu-Hakola Disease (NHD). NHD is characterized clinically by bone cysts and fractures, neuropsychiatric symptoms, and importantly, presenile dementia [144-146]. Moreover, patients suffering NHD also experience axonal degeneration, white matter damage, and cortical atrophy accompanied by microglia and astrocyte activation [147-149]. Paloneva and colleagues were the first to link TREM2 variants with NHD [150], and it has since been verified that homozygous expression of TREM2 variants causes NHD. TREM2 variants have recently been identified as risk factors for LOAD, and are now known to confer similar risk for LOAD as one copy of ApoE4 [151-153].

In 2013, two genome-wide association studies (GWAS) revealed that heterozygous expression of the TREM2 R47H and D87N variants were significantly associated with LOAD risk [154, 155]. Numerous studies have since replicated the association of these TREM2 variants with LOAD [156-161], one of which validated the R47H variant in neuropathologically confirmed cases [162].

Additional TREM2 variants (R62H, L211P, T96K, and H157Y) have also been consistently shown to enhance LOAD risk [163-165]. Unlike variants causative of NHD which reduce TREM2 expression on the cell surface, LOAD-associated variants of TREM2 have been shown to impair the efficiency of TREM2 signaling, influence ligand affinity, and diminish phagocytic capacity.

In 2016, two groups independently demonstrated that cells expressing the TREM2 variants R47H and R62H displayed impaired TREM2 signaling [138, 166]. Multiple groups also showed that the R47H, R62H, and D87N variants display decreased binding affinity between ApoE and TREM2 [135, 137, 141]. Furthermore, the R47H and R62H variants have been shown to exhibit decreased binding affinity between TREM2 and proteoglycans of the cell surface, whereas the T96K variant was shown to enhance this affinity [141]. The rarity of the T96K variant makes it difficult for scientists to determine its impact on AD risk, however, the ability of TREM2 variants to enhance or impair function suggests altered TREM2 homeostasis has neurodegenerative consequences [134]. In 2016 Kober et al. suggested potential structure-function mechanisms for the differing effects of LOAD-associated TREM2 variants [141]. This work established that the R47H and R62H variants are located within the extracellular, basic region of TREM2 likely important for its association with negatively charged ligands [141]. Variants within this basic region are predicted to decrease the binding affinity of TREM2 for a number of ligands. Interesting, the T96K variant was identified as being adjacent to this basic region and is therefore predicted to extend the site of the basic patch, subsequently enhancing ligand binding to TREM2 [141]. Expression of R47H in

Hek293 cells was shown to modestly decrease phagocytic capacity [167], and microglia from TREM2 knock-out mice have been shown to exhibit reduced uptake of APOJ, LDL, and $A\beta_{1-42}$ [137]. Importantly, despite their structural diversity, almost all of the TREM2 variants identified have been suggested to confer loss of function through different mechanisms.

To date, several laboratories have assessed whether partial or complete loss of TREM2 function contributes to Aβ deposition or Aβ-associated microglial activation and phagocytosis. Notably, studies have consistently shown that TREM2 deficiency results in a strong reduction in Aβ-associated microgliosis, possibly due to an impaired transition of homeostatic microglia to DAM (Figure 1.3). While this supports the notion that loss of TREM2 function is detrimental, there is no evidence that TREM2 gain of function would be beneficial.

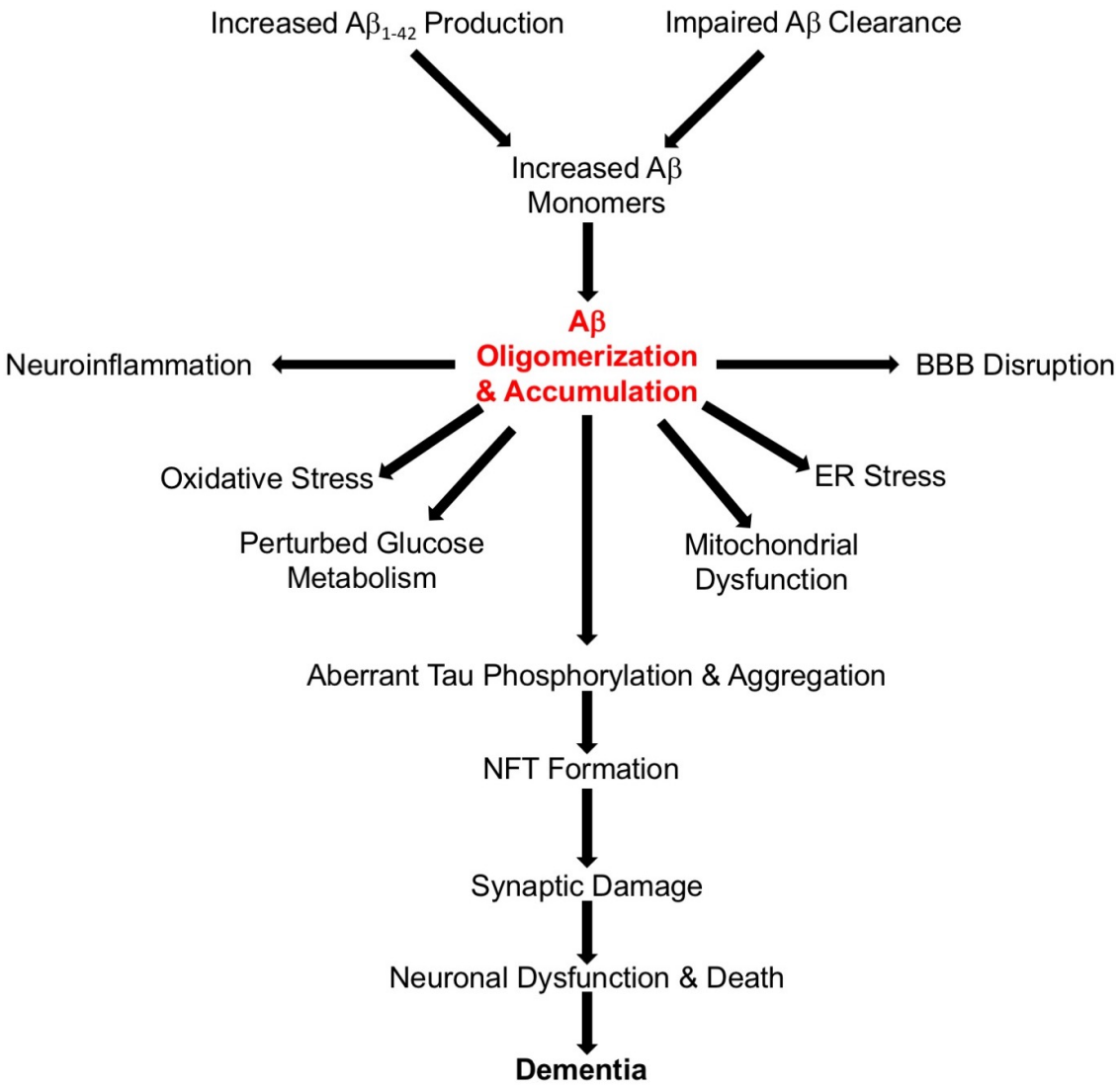

Figure 1.1: Amyloid Cascade Hypothesis.

The amyloid cascade hypothesis suggests that alterations in Aβ metabolism lead to the oligomerization and deposition of Aβ. Aβ induced toxicity is then hypothesized to result in a number of cellular disturbances, subsequent hyperphosphorylation of tau, synaptic dysfunction, and neuronal death.

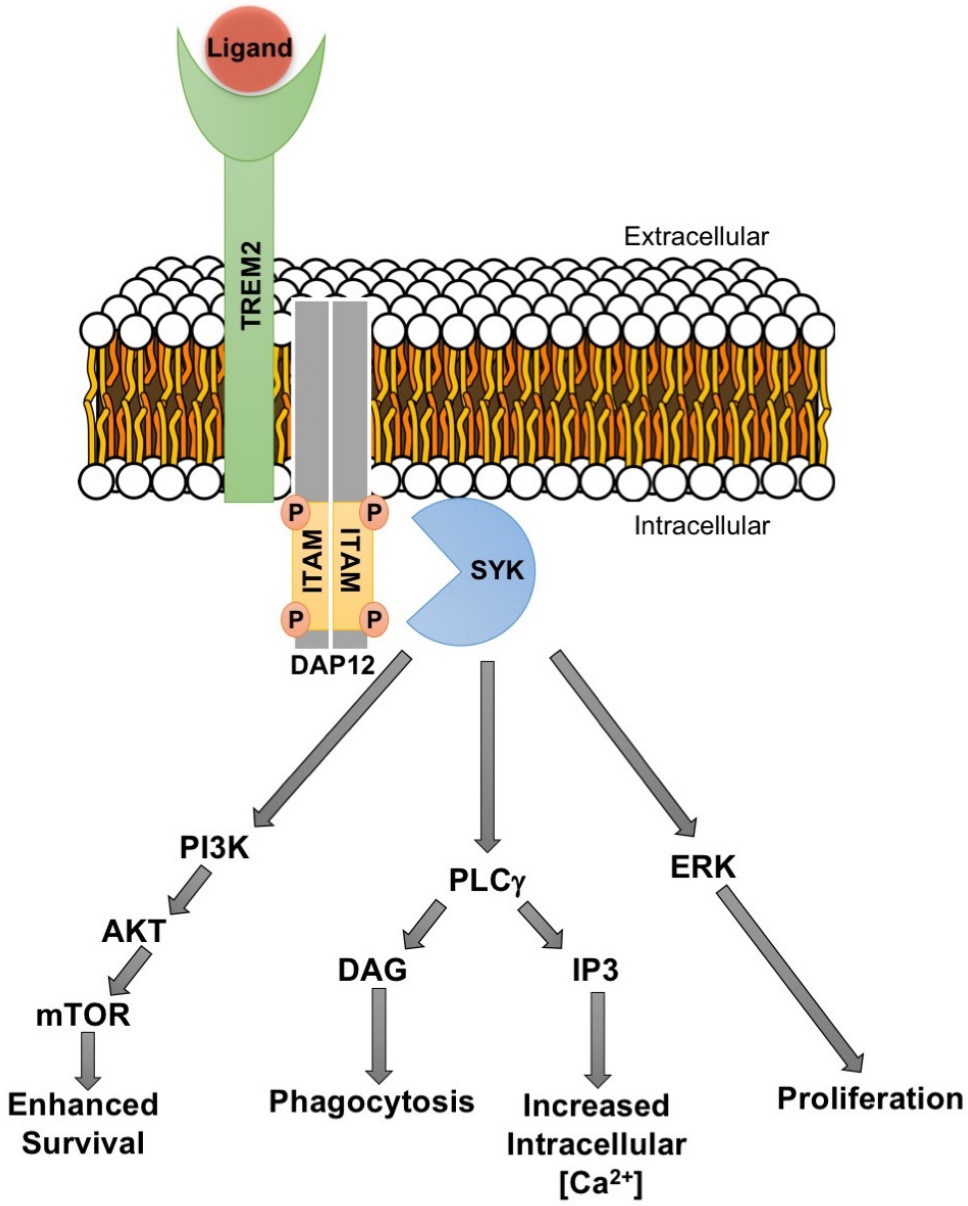

Figure 1.2: TREM2 Signaling Cascade.

Upon ligand binding to TREM2, tyrosine residues on the immunoreceptor tyrosine-based activation motif (ITAM) region of DAP12 are phosphorylated and SYK is recruited. Activation of SYK initiates a number of signaling cascades that ultimately enhance the survival, proliferation, and phagocytic capacity of microglia.

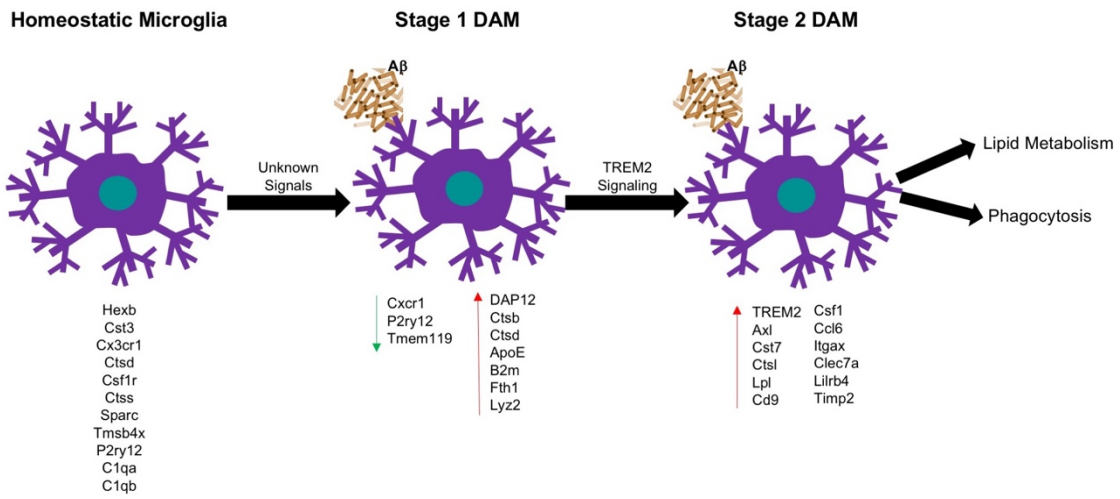

Figure 1.3: Gene Expression in DAM Microglia.

In the presence of Aβ, homeostatic microglia transition into stage 1 DAM via TREM2-independent mechanisms. Conversely, the transition from stage 1 to stage 2 DAM requires the presence of TREM2. Key genes expressed in each stage are listed. Red arrows indicate the up-regulation of genes in the specific stage, whereas green arrows represent the down-regulation.

Chapter 2

TREM2 activation recruits microglia, ameliorates amyloid deposition, and improves cognition in a model of amyloid deposition.

Brittani R. Price[a,1], Tiffany L. Sudduth[a,1], Erica M. Weekman[a], Danielle Hawthorne[a], Abigail Woolums[a], Arnon Rosenthal[b], Donna M. Wilcock[a,2]

[a]: University of Kentucky, Sanders-Brown Center on Aging, College of Medicine, Department of Physiology, Lexington, KY 40536 USA

[b]: Alector, LLC, 151 Oyster Point Blvd, Suite 300, South San Francisco, CA 94080 USA

Author Contributions

BRP performed the histological, biochemical, and behavioral studies, and also contributed to the writing of the manuscript, TLS collected data and maintained the mice, EMW performed dosing, DH and AW performed image analysis and collated data, AR conceived of the antibody and provided the 5XFAD mice, DMW supervised the execution of the studies, designed the studies, and contributed to the writing of the manuscript.

Abstract

Triggering receptor expressed on myeloid cells-2 (TREM2) is a lipid and lipoprotein binding receptor expressed by activated innate immune cells. Homozygous TREM2 loss of function mutations cause early onset progressive

presenile dementia while heterozygous, function-reducing point mutations triple the risk of Alzheimer's disease (AD). This is due in part to a reduction in microglia survival, proliferation, chemotaxis and phagocytic activity. Although human genetic findings support the notion that loss of TREM2 function exacerbates neurodegeneration, it is not clear whether activation of TREM2 in a disease state would result in therapeutic benefits. Here we show that chronic activation of TREM2, in the 5XFAD mouse model of AD, leads to reversal of AD gene expression signature, recruitment of microglia, decreased amyloid deposition, and improvement in spatial learning and novel object recognition memory. These findings indicate that TREM2 activators may be effective for the treatment of AD and possibly other neurodegenerative disorders.

Significance Statement

TREM2 is a receptor expressed on myeloid cells including microglia and monocytes. Mutations in TREM2, while rare, have been shown to significantly increase an individual's risk for developing AD. Much of the literature supports the hypothesis that the TREM2 mutation increases AD risk through a loss-of-function of the receptor. Based on this hypothesis, we have chosen to explore therapeutic targeting of TREM2 as a treatment for AD with the goal of agonizing TREM2 and activating its signaling. An antibody, AL-002a, agonizes TREM2 and results in clustering of microglia around plaques, clearance of amyloid plaques, and improved cognition. These data suggest targeting TREM2 is a feasible therapeutic approach for the treatment of AD.

Introduction

The triggering receptor expressed on myeloid cells 2 (TREM2) is a single transmembrane receptor expressed on the surface of microglia, and other myeloid cells, that binds damaged DNA, amyloid beta (Aβ), lipids, glycolipids, lipoproteins and apolipoproteins including ApoE and clusterin/ApoJ [123, 135-137]. Ligand binding leads to TREM2 co-clustering with the immunoreceptor tyrosine-based activation motif (ITAM) containing transmembrane protein TYROBP/DAP12 and to tyrosine phosphorylation of DAP12 by Src family kinases. Phosphorylated DAP12 in turn recruits tyrosine kinase Syk leading to activation of downstream signaling events, including intracellular Ca^{2+}, flux [143], activation of extracellular signal-regulated kinases (ERK) and of phosphoinositide 3-kinase (PI3K) [168], and nuclear translocation of the transcription factor Nuclear Factor of Activated T cells (NFAT) [123]. The resulting changes in gene expression and post transcriptional modifications induce an increased cellular response to colony stimulating factor [169], actin reorganization [143], process extension [170], cytokine release [171, 172], survival [173, 174], proliferation [169], migration [175] and phagocytosis [176] in TREM2 expressing dendritic cells (DC) [172], tissue macrophages [177], osteoclasts [178] and microglia [179]. People with homozygous loss of function mutations in TREM2 [180] invariably develop polycystic lipomembranous osteodysplasia with sclerosing leukoencephalopathy (PLOSL), also known as Nasu-Hakola disease (NHD), which manifests as early onset presenile dementia with frequent bone cysts [181], or as frontotemporal dementia (FTD) [154] with seizures and corpus callosum atrophy. Heterozygous TREM2 point mutations,

which reduce either ligand binding [137] or cell surface expression [167], are associated with a reduction in the number of microglia surrounding amyloid plaques, microglial inability to compact beta-amyloid deposits and form a barrier between plaques and neurons [170], an increase in the number of phospho- tau positive, dystrophic neurites [182] as well as increased tau in cerebrospinal fluid [183]**.** Heterozygous mutations also double the rate of brain atrophy [182, 184], triple the risk of AD [151, 155] and decrease the age of AD onset by 3-6 years [185].

TREM2 homozygous (TREM2-/-) or heterozygous (TREM2+/-) deficient wildtype (WT) or AD mice also display multiple microglia pathologies, including increased apoptotic cell death, reduced number of microglia, inability to coalesce around and compact beta amyloid plaques [186]**,** nonreactive cell morphology, abnormal AD gene expression signature [187], age dependent inability to reduce total Aβ plaque load [188] and an inability to support Aβ antibody-mediated beta amyloid plaque clearance [189]. TREM2 *(-/-)* microglia fail to fully activate into phagocytic*,* disease-associated microglia and to express the associated gene signature in AD mice [122]. Although, human genetics indicate that loss of TREM2 function is detrimental, there is no evidence that TREM2 gain of function would be beneficial. TREM2 pathology, like beta amyloid pathology [190], may begin decades before clinical findings, rendering intervention in diagnosed AD patients ineffective. Likewise, activation of TREM2 may result in indiscriminate and harmful stimulation of microglia and other innate immune cells. To determine the viability of TREM2 activation as a therapeutic strategy, we sought to identify and

characterize an agonistic TREM2 antibody and test its efficacy and mechanism of action in an aggressive mouse model of AD.

Materials and Methods

Animals. 5XFAD transgenic mice overexpressing the K670N/M671L (Swedish), I716V (Florida), and V717I (London) mutations in human APP (695), as well as M146L and L286V mutations in human PS1 (28-30) [61] were aged to 3.5 months at Taconic and transferred to University of Kentucky. The study was approved by the University of Kentucky Institutional Animal Care and Use Committee and conformed to the National Institutes of Health Guide for the Care and Use of Animals in Research. All studies were performed blinded. Alector provided the antibodies coded, and the mice were also coded and randomized into each group. Only upon completion of the data analysis were the groups unblinded.

Murine macrophages. Murine bone marrow precursor cells from TREM2-KO and TREM2-WT (Alector colony) were obtained by flushing tibial and femoral marrow cells with cold PBS containing 2% FBS. Red blood cells were lysed using ACK lysing buffer, washed twice with 2% FBS/PBS and re-suspended in complete media (RPMI, 10% FBS, Pen/Strep, L-glutamine, non-essential amino acid) with 50ng/mL murine M-CSF (m-MCSF) to differentiate macrophages for 6 days. For FACS analysis of AL-002abinding to BMM's, cells were washed in FACS buffer (PBS + 2% FBS) and incubated with either AL-002a, rat anti-TREM2 (R&D Systems) as a positive control, or murine IgG1 isotype (BD Biosciences) as a negative control in FACS buffer for one hour on ice. Cells were washed thrice in

FACS buffer and spun. Goat anti-mouse APC conjugated secondary antibody was added (BD Biosciences, 1:100) in FACS buffer and cells were incubated on ice for 30 minutes. Cells were again washed as before, re-suspended in FACS buffer and analyzed on a BD Canto Flow Cytometer.

Biochemistry. Before stimulation, BMM were starved for 4h in 1% serum RPMI. 5 × 10^6 cells for Syk immunoprecipitation or 15 × 10^6 cells for TREM2 immunoprecipitation were then incubated in ice for 15 min with 1μg of antibody for 1 ×10^6 cells. Cells were then washed and incubated at 37°C for the indicated period of time in the presence of goat anti-human IgG or goat-anti mouse IgG (1.5μg for 1 ×10^6 cells). After stimulation, cells were lysed with lysis buffer (1% v/v NP-40%, 50 Mm Tris-HCl (pH 8.0), 150 mM NaCl, 1 mM EDTA, 1.5 mM $MgCl_2$, 10% glycerol, plus protease and phosphatase inhibitors) and immunoprecipitated with anti-Syk antibody (N-19, Santa Cruz). For receptor immunoprecipitation cells were lysed with 1% n-Dodecyl-β-D-Maltoside and immunoprecipiated with anti-TREM2 (R&D system) or isotype control. Precipitated proteins were fractionated by SDS-PAGE, transferred to PVDF membranes and probed with anti-phosphotyrosine Ab (4G10, Millipore) and anti-Dap12 antibody (Cell Signaling). To confirm that all substrates were adequately immunoprecipitated, immunoblots were reprobed with anti-Syk antibody (Abcam, for BMM). Because anti-TREM2 antibody does not detect TREM2 in immunoblotting, each cell lysate used for TREM2 immunoprecipitations contained equal amount of proteins with a control antibody (anti-actin, Santa Cruz).

Intracranial Administration. Twenty-four 5-month old male 5XFAD mice were assigned to one of two injection groups: MOPC (control antibody; mIgG1 isotype; Bioxcell), or AL-002a (mIgG1isotype; Alector). On the day of surgery mice were weighed, anesthetized with isoflurane, and placed in a stereotaxic apparatus (51733D digital dual manipulator mouse stereotaxic frame; Stoelting). A mid-sagittal incision was made to expose the cranium and four burr holes were drilled with a dental drill mounted in the stereotaxic frame over the frontal cortex and hippocampus to the following coordinates: frontal cortex, anteroposterior, +2.0 mm, lateral ± 2.0 mm; hippocampus, anteroposterior - 2.7 mm; lateral, ± 2.5 mm, all taken from bregma. A 26-gauge needle attached to a 10 mL Hamilton syringe containing the solution to be injected was lowered 3.0 mm ventral to bregma, and a 2□L injection was made over a 2 min period. Antibodies were diluted to a final concentration of 5 mg/kg in 1X PBS. The incision was cleaned and closed with surgical staples. Buprenophine hydrochloride diluted to 0.015 mg/mL was intraperitoneally injected immediately post-surgery at 0.1 mg/kg dose per body weight. Animals received subsequent doses every 12 hours until sacrifice. Tissue was harvested 72 hours post injection.

Systemic administration. The two antibodies (MOPC; mIgG1 isotype; Alector, LLC, or AL-002a; mIgG1isotype; Alector, LLC) were diluted to a final concentration of 5mg/mL in 1XPBS. Twenty-four 5XFAD (N=12 per antibody group) and 15 wildtype mice (N=8 in AL-002agroup and N=7 in MOPC group) aged 4 months received AL-

002a, or MOPC control antibody at a dose of 50 mg/kg/week administered intraperitoneally for 14 weeks. Mice were tested in our behavioral paradigms during the 2 weeks prior to sacrifice. Mice were euthanized and tissue was harvested 24 hours after the last injection.

Tissue processing. Mice were perfused intracardially with 25mL of normal saline. Brains were rapidly removed and bisected in the mid-sagittal plane. The left half was immersion fixed in freshly prepared 4% paraformaldehyde for 24 hours. The right half was dissected into cerebral cortex (anterior and posterior), hippocampus, striatum, and cerebellum. The dissected pieces were flash frozen in liquid nitrogen, and stored at -80°C. The left hemibrain was passed through a series of 10, 20, and 30% sucrose solutions as cryoprotection and 25μm frozen horizontal sections were collected using a sliding microtome and stored floating in PBS containing sodium azide at 4°C. Sections were collected sequentially for the intracranial study and serially for the intraperitoneal study.

Histology and immunohistochemistry. For the intracranial study, six sections spaced 300μm spanning the estimated injection site were initially mounted and stained by mouse IgG to identify the injection site. For all subsequent histology and immunohistochemistry on the intracranial study, six sections spanning the injection site, spaced ~100 μm apart, were selected and analyzed. For the systemic administration study, serial horizontal sections spaced 600μm apart were selected for histology and immunohistochemistry. Sections were mounted onto

slides and stained for Congo red as described previously. Free-floating immunohistochemistry for CD11b (rat monoclonal; AbD Serotec) and Aβ (rabbit polyclonal Aβ1–16; Invitrogen). Briefly, sections were quenched for endogenous peroxidase, blocked and permeabilized. They were then incubated overnight in primary antibody at 4°C (Aβ 1:3000, CD11b 1:1000). After washing, sections were incubated for 2 hours in the appropriate biotinylated secondary antibody (goat anti-rabbit IgG for Aβ, goat anti-rat for CD11b, all 1:3000; Vector Laboratories, Burlingame, CA, USA). Sections were then washed and incubated for 1 hour in ABC. DAB with (CD11b) and without (Aβ) nickel was used for color development. Stained sections were mounted, air dried overnight, dehydrated, and coverslipped in DPX (Electron Microscopy Sciences, Hatfield, PA, USA). Immunohistochemical analysis was performed by measuring percent area occupied by positive stain using the Nikon Elements BR image analysis system (Melville, NY, USA) as described previously (32).

Microglial clustering around plaques: We performed double label of sections to detect plaques and microglia using CD11b immunohistochemistry counter-stained with Congo red. Using a macro developed in our image analysis software, eight plaques of a defined size per section were identified by the software in each of the frontal cortex and hippocampus. A ring was projected around the perimeter of the plaque that was 2 cell bodies wide (15μm). The blinded analyst then clicked on each CD11b-positive cell body within the perimeter to determine the numbers of microglia surrounding that plaque. Between six and eight sections per mouse were

analyzed in this way. Mean number of microglia per plaque were calculated for each animal before being analyzed statistically as described below.

Quantitative real-time reverse transcription (RT)-PCR. RNA was extracted from left hippocampus using the EZNA RNA II Purification System (Omega Bio-Tek) according to the manufacturer's instructions. RNA was quantified using the BioSpec Nano spectrophotometer (Shimadzu) and cDNA was reverse transcribed using the cDNA High Capacity kit (Applied Biosystems) according to the manufacturer's instructions. Real-time RT-PCR was performed using the 384-well microfluidic card custom TaqMan assays containing TaqMan Gene Expression probes for our genes of interest (Applied Biosystems, Invitrogen). All gene expression data were normalized to 18S rRNA expression. Fold change was determined using the $^{\Delta\Delta}$Ct method.

Radial Arm Water Maze. After 12 weeks of treatment, mice were subject to a two-day radial arm water maze (RAWM) paradigm, as previously described (33). On day one, 15 trials were run in two blocks of 6 followed by the last three trials. A cohort of 4 mice was run sequentially for each block (i.e., each of 4 mice undergo trial one, then the same mice undergo trial two, etc.). After each block, a second cohort of mice was run, permitting an extended rest period before mice were exposed to the next block trials (extra wait time was added to the end of the block with three trials to make the rest period similar throughout the behavior). The goal arm was different for each mouse in a cohort to minimize odor cues. The start arm

was varied for each trial, with the goal arm remaining constant for a given individual for both days. For the first 11 trials, the platform was alternately visible then hidden (hidden for the last 4 of 15 trials). On day two, the mice were run in exactly the same manner as day one except that the platform remained hidden for all 15 trials. The number of errors (incorrect arm entries) was measured in a one-minute time frame. As standard practice, mice failing to make an arm choice in 15 seconds are assigned one error. In order to minimize the influence of individual trial variability, each mouse's errors for 3 consecutive trials were averaged producing 5 data points (termed “blocks”) for each day, which were then analyzed statistically by ANOVA using the JMP statistical analysis program (SAS).

Novel Object Recognition. Following the RAWM, the novel object recognition task was performed. During the habituation phase, each mouse was gently placed into a square box (50 × 50 × 15 cm, length × width × height) for 30 min per day for 1 day without any objects. During the training phase, two identical objects, A1 and A2, were placed parallel to and near one wall of the square box. Each mouse was placed singly in the box and allowed to explore the objects for 5 min. Exploratory behavior was defined as directing the nose at the object at a distance of less than 2 cm and/or touching the object with the nose. The mouse was then returned to its home cage with a 1 h inter-trial interval. Both objects were replaced; one being a familiar object (A1) and the other a novel object (B). The mouse was returned to the box and allowed to explore the objects for 5 min during the test phase. Novel and familiar objects were alternated between the left and right positions to reduce

potential bias toward a particular location. The objects and the box were cleaned with ethanol (10%) after each individual trial to eliminate olfactory cues. The exploration time (s) for each object in the trials was recorded. The preferential index (PI) was calculated as [time spent exploring novel object/total exploration time].

Analysis. Data are presented as mean± SEM. Statistical analysis was performed using the JMP statistical analysis program (SAS). Statistical significance was assigned where the *p* value was lower than 0.05. One-way ANOVA and two-way ANOVA were used, where appropriate, to detect treatment differences and differences within treatment groups along the time course. Student's *t* Test was used for post-hoc comparisons. Mice were genotyped for the retinal degeneration (rd) mutation postmortem. We found that there were six total mice homozygous for the rd mutation. Five of these were wildtype mice, and one was a 5XFAD in the AL-002a group. These mice were included for histological analysis but excluded for the radial arm water maze and novel object recognition data analysis.

Results

AL-002a is a mouse IgG1 antibody that has been generated to recognize the extracellular portion of the TREM2 receptor. AL-002aspecifically recognizes TREM2 on WT bone marrow derived macrophages (BMM), while binding is reduced to isotype control levels in cells derived from TREM2 KO mice (Figure 2.1A). In vitro, AL-002a activates the TREM2 signaling pathway. Treatment of peripheral bone marrow derived macrophages (BMM) with AL-002a resulted in

DAP12 and Syk phosphorylation, indicating activation of the TREM2 signaling pathway. Importantly, when these studies were repeated using BMM from TREM2-/- mice, there was no DAP12 or Syk response, indicating specific action through TREM2 (Figure 2.1B and 2.1C).

Intracranial Administration of AL-002a

To determine the effects of AL-002a in the brain, we performed stereotaxic surgery to inject 2μl of 5mg/mL AL-002a or the isotype control antibody, MOPC, into the frontal cortex and hippocampus bilaterally (N=12 / antibody). In previous studies working with anti-Aβ antibodies, a time-course revealed the optimal time-point to examine the brain post-injection is 72 hours. Using that study as our guide, mice survived for 72 hours and, upon euthanasia, the right hippocampus was flash frozen and RNA was extracted to perform gene expression analysis. The left hemisphere was immersion fixed in paraformaldehyde and processed for histology. Since we hypothesized that TREM2 activation would modulate the immune response in the brain, we used RNA extracted from the hippocampus to perform real-time RT-PCR for inflammatory genes. The data are shown as a fold change from the 5XFAD mice receiving control IgG (Figure 2.2A). We found at 72 hours there was a significant increase in both pro-inflammatory (IL1β, TNFα, CCL3, CCL5, CCR2, CXCL10, Gata3, Rorc) and anti-inflammatory (YM1, CD86) mediators as a result of AL-002a treatment compared to mice injected with control antibody. To determine microglial activation, we performed immunohistochemistry for CD11b, which labels both activated and resting microglia. Activated microglia express greater levels of CD11b and cover a greater area due to the enlarged cell

bodies and thickened processes associated with activation. We found a significant increase in CD11b immunoreactivity in 5XFAD and WT mice treated with a TREM2 antibody compared to the control treated mice, suggestive of microglial activation in the regions injected with AL-002a compared to the same regions injected with control antibody (Figure 2.2B).

Deposition of Aβ occurs as both diffuse and compact plaques with the vast majority of Aβ deposited being diffuse. Immunohistochemistry for total Aβ, which detects both compact and diffuse deposits, in 5XFAD transgenic mice receiving control antibody showed a typical staining pattern for mice of this age (Figure 2.2C) [61]. Mice receiving the AL-002a antibody showed significant reductions in total Aβ immunohistochemistry in both the frontal cortex and hippocampus compared to mice receiving control antibody. In the frontal cortex, Aβ deposition was reduced by 50% and in the hippocampus Aβ deposition was reduced by 35-40% (Figure 2.2C). The histological dye Congo red labels only compact amyloid deposits and stains approximately 5% of the material stained by immunohistochemistry for total Aβ. As shown in Figure 2.2D, the distribution of Congophillic deposits resembles that observed for total Aβ. Mice receiving the AL-002a antibody showed significant reductions in compact amyloid deposits in both the frontal cortex and hippocampus compared to those mice receiving the control antibody (Figure 2.2D).

Systemic Administration of AL-002a

Given the positive outcomes of our stereotaxic studies above, we moved to perform a chronic, systemic administration study. Twenty-four male 5XFAD and fifteen wildtype mice aged 4 months received AL-002a (N=12 5XFAD, N=8 WT) or

control antibody (N=12 5XFAD, N=7 WT) at a dose of 50 mg/kg/week administered intraperitoneally for 14 weeks. Mice were tested in our behavioral paradigms during the 2 weeks prior to sacrifice. The radial-arm water maze (RAWM) is a behavioral test that reliably detects spatial learning and memory deficits in aged transgenic mice [68]. 5XFAD transgenic mice were tested after 12 weeks of treatment with AL-002a or MOPC (control antibody). Included in the task were age-matched non-transgenic littermate mice treated with AL-002a or control antibody (these mice were grouped due to no significant difference between the two treatments in the non-transgenic mice). We found that the 5XFAD transgenic mice receiving control antibody were significantly impaired when compared with the non-transgenic mice (Figure 2.3A). However, 5XFAD transgenic mice treated with AL-002a performed significantly better than control treated 5XFAD transgenic mice (Figure 2.3A). The AL-002a-treated 5XFAD mice were indistinguishable from the WT mice at the end of the second day of testing, averaging less than one error, our criterion for stable acquisition of this task (Figure 2.3A). In examining the AL-002a effect at the end of the second day of testing, we found that there was a significant reduction in the number of errors in the 5XFAD mice receiving AL-002a compared to 5XFAD receiving control antibody (Figure 2.3B).

One week after completion of the RAWM, the novel object recognition (NOR) task was performed to investigate recognition memory [191]. We found that 5XFAD transgenic mice treated with the control antibody spent significantly more time on the familiar object compared to the 5XFAD mice treated with AL-002a (Figure 2.3C). Additionally, AL-002a treated 5XFAD transgenic mice exhibited

significantly increased explorative behavior as compared to the control antibody treated 5XFAD transgenic mice (Figure 2.3C).

Immunohistochemistry detecting total Aβ, both compact and diffuse deposits, in the 5XFAD transgenic mice treated with control antibody showed a typical staining pattern for mice of this age (Figure 2.4D) [61]. The 5XFAD mice treated with AL-002a showed significant reductions in total Aβ immunohistochemistry in both the frontal cortex and hippocampus compared to control treatment (Figure 2.3D). In the frontal cortex, Aβ deposition was reduced by 40% and in the hippocampus Aβ deposition was reduced by 35% (Figure 2.3D). The distribution of Congophillic deposits resemble that observed for total Aβ (Figure 2.3E). The 5XFAD mice treated with AL-002a showed significant reductions in compact amyloid deposits in only the hippocampus with no significant change in the frontal cortex (Figure 2.3E).

To characterize the neuroinflammatory response to AL-002a, we isolated RNA from the right hippocampus and performed real-time RT-PCR for genes relatively specific for inflammatory and anti-inflammatory properties. The data in Figure 2.4A are shown as a fold change from the 5XFAD mice treated with the control antibody. We found after 14 weeks of treatment there was a significant increase in both pro-inflammatory (IL1β, TNFα, CCL2, CXCL10, Gata3, Rorc) and anti-inflammatory phenotypic markers (YM1 and IL1Rn) compared to control treated mice (Figure 2.4B). Immunohistochemistry detecting CD11b indicated a significant increase in microglial staining in 5XFAD mice treated with AL-002a compared to the 5XFAD mice treated with control antibody (Figure 2.4B). During

image processing, it was noted that there appeared to be more microglia associated with plaques in some mice as compared to others. Using an analysis method developed for this purpose, we calculated the mean number of microglial cells per plaque for each animal. We found significantly increased numbers of microglia associated with plaques in mice treated with AL-002a compared to mice treated with control antibody. The increase was approximately double the number of microglia in the frontal cortex and triple the number of microglia in the hippocampus per plaque.

Discussion

Therapeutic approaches to the treatment of AD continue to focus on the major pathological hallmarks of the disease: amyloid plaques and neurofibrillary tangles [192-194]. These two pathologies remain the requirements for diagnosis of AD. However, the explosion of genetic data has suggested that risk for sporadic AD is driven by several distinct pathways such as neuroinflammation, membrane turnover and storage, and lipid metabolism [195]. Of particular importance was the description that a mutation in the TREM2 gene significantly increases an individual's risk of developing AD [151, 155]. While this mutation has low penetrance in the population, those who carry the TREM2 R47H loss of function mutation have a 4.5-fold increased risk of developing AD compared to those without the mutation. Our hypothesis in the current study was that targeting TREM2 with an antibody, thereby activating the receptor, would increase TREM2 function leading to immune modulation, clearance of amyloid deposition, and

improved cognition without the need to directly target the Aβ protein itself. To test this hypothesis, the antibody developed by Alector, AL-002a, was found to activate TREM2 signaling in vitro and activate immune responses in vivo, whether injected intracranially or systemically. AL-002a also activated microglial cells, increased clustering of microglia around the amyloid plaques, and ultimately resulted in reduced amyloid deposition and improved cognition (cognition was only examined in the systemic administration study).

It is not unusual to find an association between microglial activation and amyloid reductions. As far back as 2000, lipopolysaccharide (LPS), the prototypical immune activator, was found to activate microglia and reduce amyloid deposition [196]. Anti-Aβ antibodies also activate microglia and reduce amyloid deposition [105, 107]. It is interesting to compare and contrast the findings of AL-002a to an anti-Aβ antibody treatment approach currently in clinical trials. We have previously shown that anti-Aβ immunotherapy activates microglia [106, 107, 197], and alters neuroinflammatory gene expression [198], but we find a unique inflammatory signature with AL-002a as opposed to the anti-Aβ antibody. AL-002a increased both pro-inflammatory and anti-inflammatory / repair gene expression, while anti-Aβ antibodies have only been shown to increase pro-inflammatory gene expression and, in some cases, decrease the anti-inflammatory gene expression. It is possible that the increase in gene expression by AL-002a represents a more homeostatic neuroinflammatory response with a more limited capacity to induce surrounding tissue damage while also ameliorating the amyloid deposition.

It is intriguing that we found immune-associated genes being expressed in different ways depending on whether AL-002a is administered intracranially or systemically. Following intracranial administration of AL-002a, we found almost every gene measured was increased compared to the age-matched 5XFAD mice receiving intracranial injection of control antibody. This likely reflects the acute response to the antibody and activation of TREM2. In contrast, following fourteen weeks of systemic administration, the chemokines CCL3, CCL5 and CCR2 were not significantly increased but IL1β and IL1Rn were significantly increased with systemic administration. Of note, activation of several genes by the AL-002a antibody indicate a novel mechanism of action relative to immunotherapy targeting Aβ. CCR2 is a chemokine receptor expressed on microglia thought to mediate the accumulation of phagocytes at sites of inflammation [199]. CCL2 and CCL5 are chemokines that have been shown to increase the chemotaxis of microglia toward amyloid deposits [200]. The increased CCL2 and CCL5 expression, along with the increased CCR2 expression could be responsible, in part at least, to the increased clustering of microglia around the amyloid deposits seen in our systemic administration study. We also found increases in two key genes that are associated with T-cell differentiation into Th17 cells; Gata3 and Rorc [201]. While increased expression of IL1β and TNFα are sometimes associated with tissue damage and neurodegeneration, in some settings, the increase in these pro-inflammatory cytokines accompanies clearance of pathological proteins such as amyloid deposits [202, 203]. Anti-Aβ antibodies have been shown to increase these cytokines [198], as has genetic deletion of IL-10 [204] and injection of LPS

[196, 205]. Additionally, reductions in these cytokines has been associated with worse cognitive outcomes and exacerbation of amyloid deposition as observed when IL10 is over-expressed [206], or when lithium is administered to mice, which enhances IL-10 signaling [207]. It is our hypothesis that the enhanced expression of inflammatory genes in the current setting is balanced by the YM1, IL1Rn, and CD86 expression, thereby limiting the capacity for tissue damage. Future studies will further examine this hypothesis.

By using two distinct behavioral paradigms in the current study, we are confident in concluding that AL-002a significantly enhances cognition, or at the very least, prevents progression of cognitive decline, in the 5XFAD mouse model. The two-day radial arm water maze task was designed to test both working memory (the day 1 learning) and long-term spatial memory (day 1 to day 2 retention). The novel object recognition task, as used in the current study, is a useful task to assess short-term memory. Both tasks have been shown to be heavily hippocampal dependent, but also have aspects of cortical involvement [208, 209]. In contrast to the radial arm water maze, the novel object recognition does not rely on motivation or reward, but simply on the innate exploratory behavior of a mouse. We found robust improvements in cognition with AL-002a systemic administration as detected in either the radial arm water maze task or the novel object recognition task.

In summary, we show here that the therapeutic targeting of TREM2 using a TREM2-activating antibody leads to activation of microglia, recruitment of microglia to amyloid plaques, reduced amyloid deposition, and ultimately,

improved cognition. TREM2 deficient microglia fail to fully activate into phagocytic, disease-associated microglia and to express the associated gene signature in AD mice. Likewise, TREM2 deficient microglia fail to clear myelin debris. Our data support a critical role for TREM2 in microglial phagocytosis with increased microglial clustering at amyloid plaques and reductions in amyloid deposition using a TREM2-activating approach. We predict that activation of TREM2 through the use of antibodies like AL-002a will prove to be a novel, innovative therapeutic approach to the treatment of AD that will lack the adverse events observed with direct binding of Aβ in the brain by anti-Aβ antibodies.

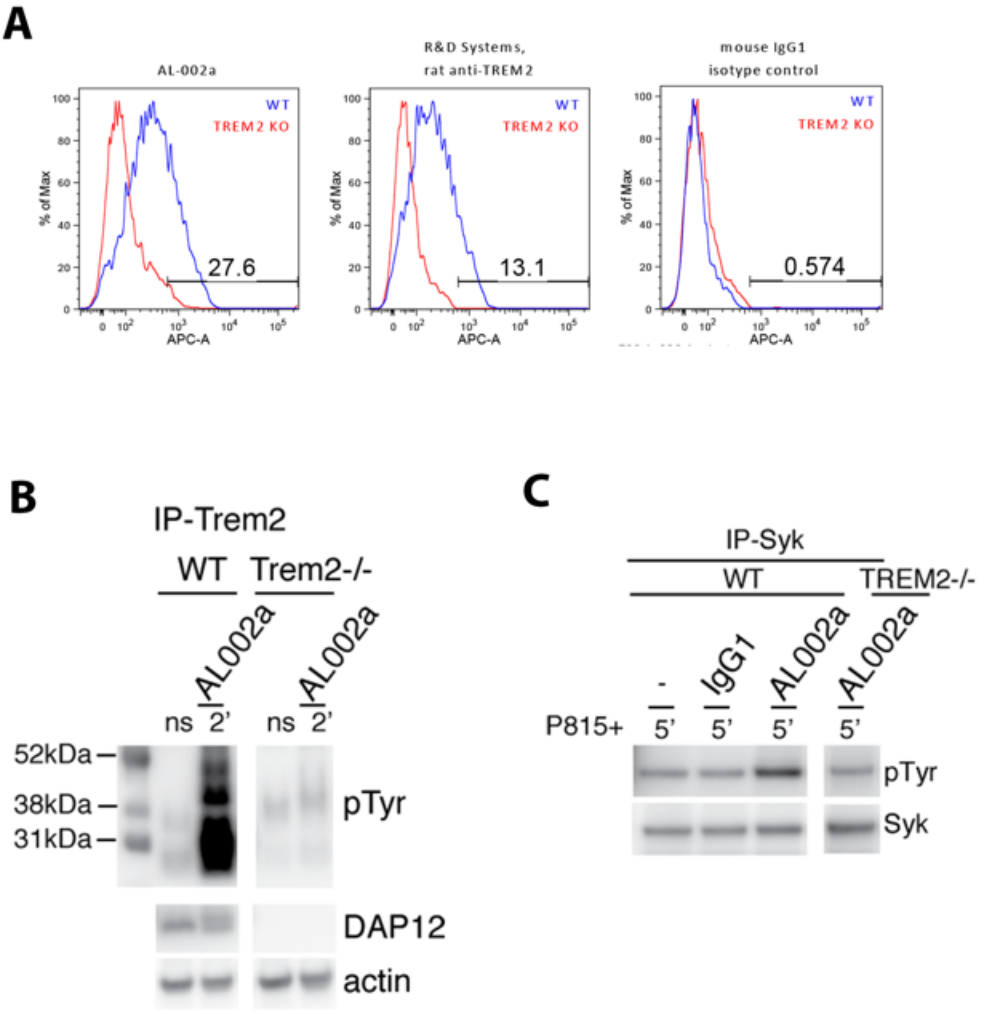

Figure 2.1: AL-002a promoted TREM2-dependent DAP12 and Syk phosphorylation. Panel A shows that AL-002a binds to BMM derived from WT, but not TREM2 KO mice, as measured by FACS. A rat anti-TREM2 antibody from R&D Systems was used as a positive binding control and an isotype msIgG1 antibody as a negative control. Panel B: Following AL-002a stimulation, WT or Trem2-/- BMM were lysed and immunoprecipitated with TREM2 antibody. Protein was loaded on a SDS gel in unreduced conditions. Membranes were first blotted with anti-phosphotyrosine antibody and later stripped and blotted again

with anti-Dap12 antibody and anti-actin. Panel C: After AL-002a stimulation, WT or TREM2-/- BMM were lysed and immunoprecipitated with Syk antibody. Membranes were first blotted with anti-phosphotyrosine antibody and later stripped and blotted again with anti-Syk antibody.

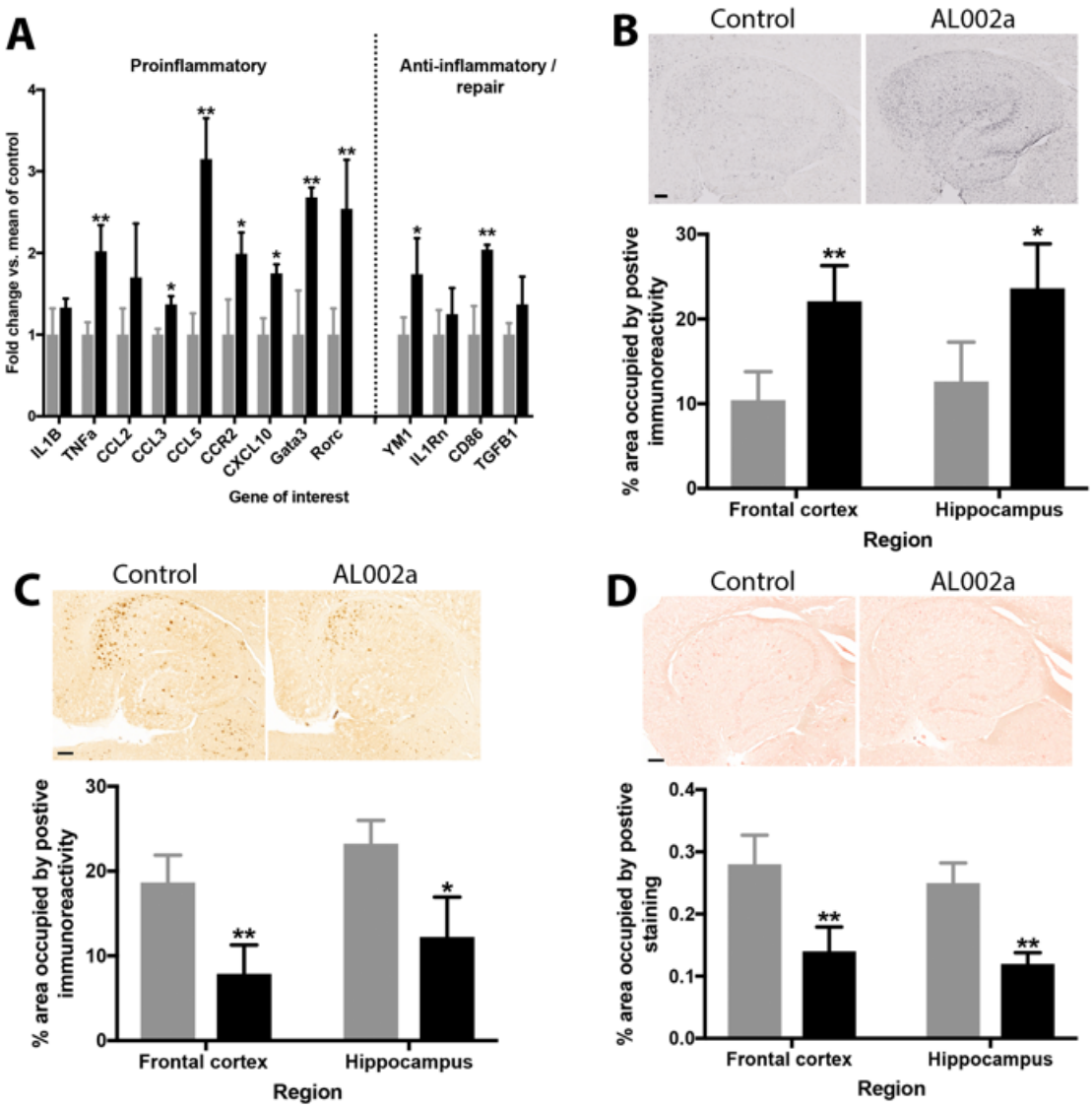

Figure 2.2: Intracranial injection of AL-002a activates microglia and ameliorates amyloid deposition in 5XFAD mice. Panel A shows the RT-PCR data obtained from the right hippocampus of the injected mice. All data are shown as fold-change relative to the mean of the control antibody-injected mice. Data were analyzed using single, one-way ANOVA measures for each gene of interest, using a Bonferroni correction for multiple comparisons. Panel B shows the microglial activation (CD11b) in the hippocampus (images shown) and frontal

cortex following intracranial injection of control antibody or AL-002a. Panel C shows the total Aβ deposition in the hippocampus (images shown) and frontal cortex following intracranial injection of control antibody or AL-002a. Panel D shows Congo red labeling of compact amyloid deposits in the hippocampus (images shown) and frontal cortex following intracranial injection of control antibody or AL-002a. For all graphs, black bars represent AL-002a while grey bars represent control antibody. * indicates $P<0.05$, ** indicates $P<0.01$. For images in B, C and D, magnification = 40X, scale bars shown = 120μm.

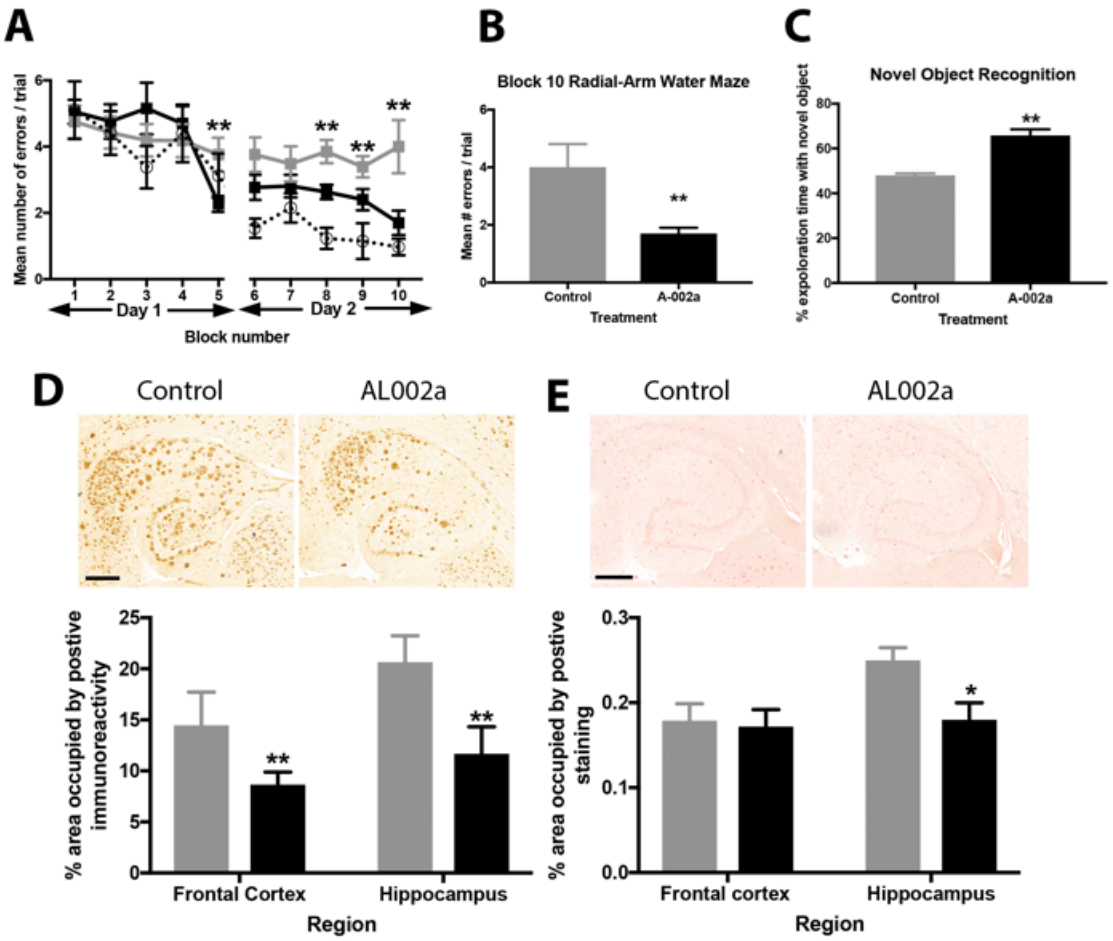

Figure 2.3: Systemic administration of AL-002a improves learning and memory and lowers amyloid deposition in 5XFAD mice. Panel A shows the radial-arm water maze data. Blocks 1-5 are day 1, blocks 6-10 are day 2. The black line is the learning curve of the 5XFAD mice receiving AL-002a, the grey line is the learning curve of the 5XFAD mice receiving control antibody, and the dashed line is the learning curve of the non-transgenic littermates receiving control or AL-002a (data was pooled due to lack of difference between the two treatment groups). Panel B shows a bar graph to illustrate the difference in number of errors made for the final block of trials (block 10). Panel C shows the bar graph for the novel object recognition data, where % exploration time with

novel object is shown. 50% exploration time would represent chance. Panel D shows the total Aβ deposition in the hippocampus (images shown) and frontal cortex of control antibody or AL-002a. Panel E shows Congo red labeling of compact amyloid deposits in the hippocampus (images shown) and frontal cortex of control antibody or AL-002a. For all graphs, black bars are AL-002a, and grey bars are control antibody. * indicates $P<0.05$, ** indicates $P<0.01$. For images in B, C and D, magnification = 40X, scale bars shown = 120μm.

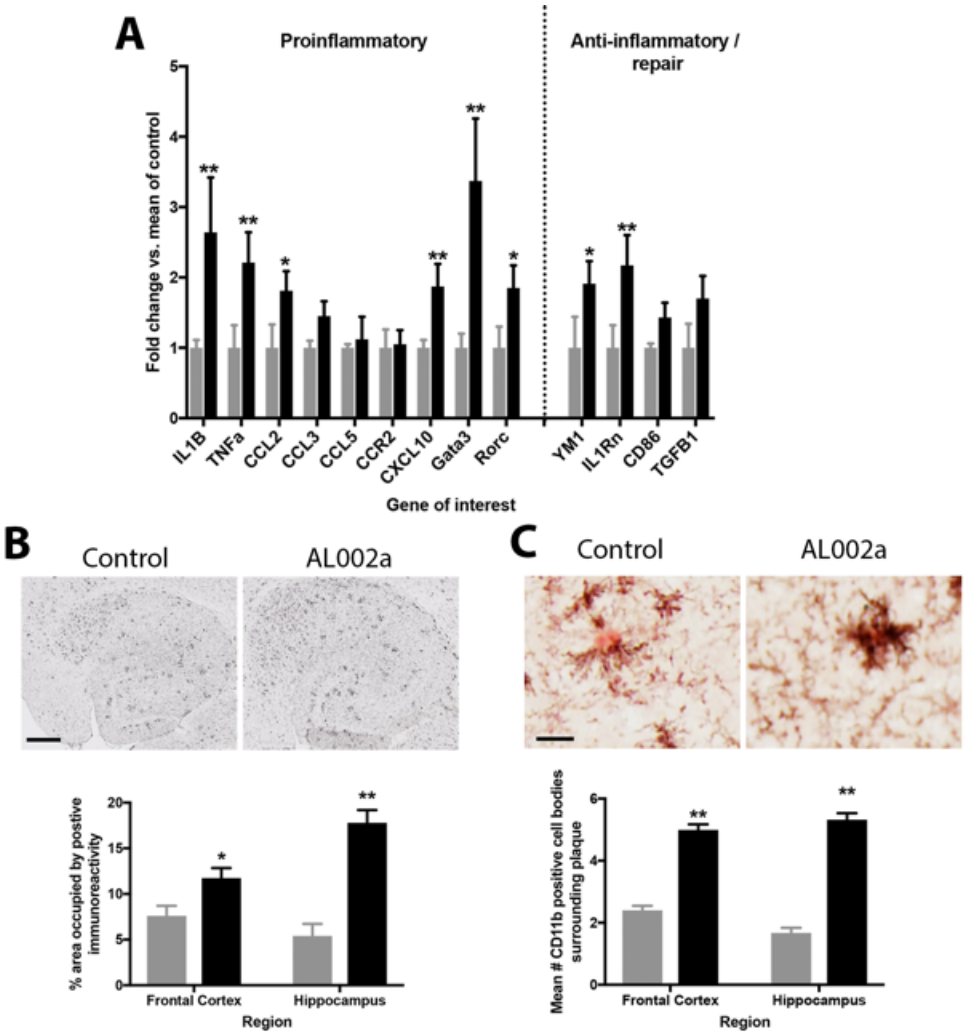

Figure 2.4: Neuroinflammatory changes are apparent following AL-002a treatment. Panel A shows RT-PCR data obtained from the right hippocampus. All data are shown as fold-change relative to the mean of the control antibody treated mice. Data were analyzed using single, one-way ANOVA measures for each gene of interest, using a Bonferroni correction for multiple comparisons. Panel B shows the microglial activation (CD11b) in the hippocampus (images shown) and frontal cortex of control antibody or AL-002a. Magnification = 40X, scale bar shown = 120μm. Panel C shows the microglial clustering around an amyloid plaque. Magnification = 400X, scale bar shown = 12.5μm. For all graphs,

black bars are AL-002a, and grey bars are control antibody. * indicates $P<0.05$, ** indicates $P<0.01$.

Chapter 3

Intracranial co-administration of TREM2 agonizing and anti-Aβ antibodies does not further augment amyloid clearance in the 5XFAD model of AD despite unique neuroinflammatory responses.

Abstract

Alzheimer's disease (AD) is the most common form of dementia, accounting for roughly 60% of dementia cases. To date, therapeutic approaches to the treatment of AD continue to focus on the major pathological hallmarks of the disease: extracellular amyloid plaques comprised of the Aβ peptide and intracellular neurofibrillary tangles comprised of hyperphosphorylated tau protein. One of the most extensively characterized therapeutics for AD is anti-Aβ immunotherapy, which uses antibodies against Aβ to promote its clearance from the brain via microglial Fcγ-receptor (FcγR)-mediated phagocytosis. Numerous studies have confirmed the ability of anti-Aβ immunotherapy to clear Aβ and improve cognition in transgenic mouse models of AD. Loss-of-function mutations in the microglial TREM2 receptor have been shown to increase an individual's risk for late-onset, sporadic AD. We recently demonstrated administration of a TREM2-agonizing antibody, AL-002a, leads to immune modulation, enhanced microglial clustering around amyloid plaques, reduced amyloid deposition, and improved cognition in the 5XFAD model of AD. Based on these data, we hypothesized that acutely engaging microglia through two receptor mechanisms (FcγR and TREM2) would further enhance Aβ clearance from the

brains of 5XFAD mice. Here we show that dual engagement of these microglial receptors does not further augment Aβ clearance, but also show that AL-002a appears to have similar efficacy as the well-characterized N-terminal anti-Aβ antibody. We also found some unique patterns of Aβ reductions, notably, only anti-Aβ alone increased insoluble Aβ40, the Aβ species associated with cerebral amyloid angiopathy. Collectively, the data indicate that AL-002a is as efficacious as anti-Aβ and may not induce the vascular accumulation of amyloid that has been observed following treatment with some anti-Aβ antibodies.

Introduction

Alzheimer's disease (AD) is the most common form of dementia and is characterized pathologically by amyloid plaques consisting of aggregated Aβ peptide, neurofibrillary tangles comprised of hyperphosphorylated tau protein, and evident neuronal loss [3, 8, 9]. To date, the main theoretical construct underlying AD progression is the amyloid cascade hypothesis. This hypothesis posits that neurofibrillary tangle formation, neurodegeneration, and dementia are the downstream consequences of Aβ deposition and toxicity [12, 13]. Overwhelming support for the amyloid cascade hypothesis has encouraged therapeutic targeting of Aβ, resulting in both active and passive Aβ immunization strategies. Active immunization strategies consist of vaccination with the full-length $A\beta_{1-42}$ peptide to induce the formation of anti-Aβ antibodies, whereas passive immunization strategies utilize monoclonal antibodies against Aβ. Both strategies have demonstrated efficacy in clearing Aβ from the brain and improving cognition in

transgenic models of AD [98, 106, 107, 109, 117, 119]. Proposed mechanisms of action of anti-Aβ antibodies include the sequestration of circulating Aβ resulting in an increased net efflux of Aβ from the brain into the plasma [119], disaggregation and solubilization of Aβ [120], and microglial recruitment followed by Fcγ receptor (FcγR)-mediated phagocytosis [105, 117].

As the brain's resident macrophages, microglia possess a wide variety of receptors that allow them to identify and internalize pathogens. Under physiological conditions, microglia exhibit a ramified morphology and actively survey their environment for pathological substrates. Conversely, in the presence of a pathological substrate, microglia transform into fully immunocompetent cells and become activated. In the midst of this transition, microglia acquire proliferative, secretory, phagocytic, and antigen-presenting cell properties. These functional changes are accompanied by morphological changes during which microglia retract their ramifications and acquire a round, amoeboid shape. Activated microglia are ultimately recruited by chemotactic signals to the affected region where they phagocytose the identified pathogen. The enhanced phagocytic capacity exhibited by activated microglia is due largely in part to their upregulation of the following surface receptors: CR3, MHC I, MHC II, CD45, CD68, and FcγR1 [210].

Fcγ receptors (FcγRs) bind the constant domain (Fc) of immunoglobins (Ig) and are among the best characterized phagocytic receptors. The FcγR1 is comprised of three chains: the α chain, which is important for ligand recognition, and the β and γ chains which are necessary for intracellular signaling. Binding of

the FcγR1 to an opsonized antigen activates the FcγR1. Activation of the FcγR1 results in phosphorylation of tyrosine residues on the immunoreceptor tyrosine-based activation motif (ITAM) region of the γ chain by SRC kinase [211]. Phosphorylation of the γ chain induces the recruitment of spleen tyrosine kinase (SYK), and subsequent activation of PLCγ and DAG, thereby enhancing phagocytosis [211] (Figure 3.1). Activation of microglia has been shown to occur with the evolution of amyloid plaques from diffuse to compact [212] and numerous studies have demonstrated the ability of microglia to phagocytose $A\beta_{1-42}$ [53, 213-215]. The role of FcγRs in microglia of healthy and AD brains was first suggested by Peress et al. [216] and microglia are now hypothesized to eliminate amyloid deposits by coating them with opsonins (anti-Aβ antibodies) and phagocytosing the opsonized Aβ via FcγRs. This hypothesis is supported by data from an ex vivo assay demonstrating that anti-Aβ F(ab')2 fragments, which lack the Fc domain, fail to activate microglia and are less efficient in reducing fibrillar amyloid [106].

Recently, the importance of another microglial cell surface receptor has been revealed. Triggering receptor expressed on myeloid cells-2 (TREM2) is a transmembrane protein expressed exclusively in the brain by microglia [124-132]. Importantly, TREM2 binds a variety of ligands including Aβ. Because TREM2 has a short cytoplasmic tail, it requires aid from its associated intracellular adaptor protein (DAP12) to mediate its signaling functions, however, downstream of DAP12, TREM2 shares the same intracellular signaling pathway to promote phagocytosis. As shown in Figure 3.1, ligand binding to TREM2 results in the phosphorylation of tyrosine residues on the ITAM region of DAP12 by SRC and

subsequent recruitment of SYK. SYK activation, in turn, activates PLCγ and DAG, thereby enhancing phagocytosis. In 2013, two genome-wide association studies (GWAS) found that heterozygous expression of the TREM2 variants R47H and D87N was significantly associated with increased risk for late-onset AD [154, 155]. Numerous studies have since replicated the association of these TREM2 variants with AD, demonstrating that these variants impair TREM2 signaling [138, 166], influence ligand binding affinity [135, 137, 141], and diminish phagocytic capacity [137, 167]. To date, several laboratories have assessed whether partial or complete loss of TREM2 function contributes to Aβ deposition or Aβ-associated microglial activation and phagocytosis. Notably, studies have consistently shown that TREM2 deficiency results in a strong reduction in Aβ-associated microgliosis, further supporting the notion that the loss of TREM2 function is detrimental in the AD brain. Our lab recently demonstrated administration of a TREM2 agonizing antibody, AL-002a, modulated the immune response, enhanced microglial clustering around amyloid plaques, reduced amyloid deposition, and improved cognition in the 5XFAD model of AD.

In the current study, we tested the hypothesis that acutely engaging microglia through both the TREM2 and Fcγ receptor mechanisms would act in an additive way to enhance Aβ clearance from the brains of transgenic mice. To test this hypothesis, we used 5XFAD mice, which express five familial-AD-associated mutations (3 APP mutations and 2 PS1 mutations) and rapidly develop severe amyloid pathology [61]. Using this model, we administered one of six antibody sets: AL-002a, anti-Aβ, a combination of the two, or one of three isotype-matched

experimental controls. We found that dual engagement of these microglial receptors does not further augment Aβ clearance, but AL-002a appears to have similar efficacy as the well-characterized N-terminal anti-Aβ antibody.

Materials and Methods

Study Design: This study was designed to test the hypothesis that acutely engaging microglia through two receptor mechanisms (FcγR and TREM2) will enhance amyloid clearance in the 5XFAD transgenic mouse model of AD. Sample size for the studies performed was calculated based on the sample size required to see a 30% reduction in brain Aβ levels. Our endpoints were determined ahead of the initiation of study and were based on disease-relevant outcomes hypothesized to be affected by TREM2 and FcγR agonism. Mice were randomized into groups using a random number generator. All studies were blinded. Antibodies were received numbered 1-6 with no other identifying information. Unblinding occurred only after all primary endpoint data were collected. We selected the 72-hour time-point to harvest tissue based on a published time-course of acute anti-Aβ antibody injection that revealed the optimal timepoint to examine the brain post-injection is 72 hours [105]. More specifically, this study found that by 4 hours post-injection there is broad distribution of the antibody and by 24 hours there is a reduction in diffuse Aβ deposits near both injection sites. However, this reduction in diffuse amyloid was shown to occur in the absence of significant microglial activation as assessed by the known microglial activation markers CD45 and MHC II. Conversely, by 72 hours post-injection parallel reductions in compact, fibrillar

amyloid deposits and increased microglial activation were observed, supporting a causal role for microglial activation in the clearance of compact amyloid.

Animals. 5XFAD transgenic mice overexpressing the K670N/M671L (Swedish), I716V (Florida), and V717I (London) mutations in human APP (695), as well as the M146L and L286V mutations in human PS1 [61] were aged to 3.5 months at Taconic and transferred to the University of Kentucky. The study was approved by the University of Kentucky Institutional Animal Care and Use Committee and conformed to the National Institutes of Health Guide for the Care and Use of Animals in Research. All studies were performed blinded. Alector provided the antibodies coded 1-6 and the mice were also coded and randomized to one of six groups. Only upon completion of the data analysis were the groups unblinded. Only male mice were used in the current study as the 5XFAD mice have been shown to have sex-dependent differences in amyloid deposition [61, 217]. Additionally, it is worth noting that wildtype (WT) littermates were included to check for an abnormal, off target, inflammatory response following treatment with an assigned antibody. Having confirmed there were no inappropriate immune responses in WT mice, we focused on the comparisons of the different antibody groups within the 5XFAD genotype.

Intracranial Administration: Five-month old male 5XFAD mice and male wildtype littermates were assigned to one of six injection groups: AL-002a (IgG1 isotype; Alector) N= 14 5XFAD, N= 6 WT; IgG1 (mouse IgG1 kappa monoclonal; MOPC;

control antibody for AL-002a; Alector) N= 14 5XFAD, N= 5 WT; anti-Aβ (IgG2a isotype; Alector) N= 14 5XFAD, N= 7 WT; IgG2a (mouse IgG2a kappa monoclonal; MOPC; control antibody for anti-Aβ; Alector) N= 13 5XFAD, N= 7 WT; AL-002a + anti-Aβ (Alector) N= 13 5XFAD, N= 5 WT; IgG1 + IgG2a (Alector) N= 13 5XFAD, N= 6 WT. The uneven group numbers reflect the death of some animals during or immediately following stereotactic surgery. The n numbers provided reflect only those animals that completed the study. Animals that died prior to the completion of the study were not included in post-mortem statistical analyses. Notably, deaths appeared to be unrelated to treatment with any specific antibody. It is worth noting that the anti-Aβ antibody used here is most similar to Aducanumab, an IgG2a isotype that has been shown to selectively bind insoluble fibrillar and soluble oligomeric Aβ aggregates at the extreme amino terminus ($A\beta_{3-7}$) [218]. On the day of surgery mice were weighed, anesthetized with isoflurane, and placed in a stereotaxic apparatus (51733D digital dual manipulator mouse stereotaxic frame; Stoelting). A mid-sagittal incision was made to expose the cranium and four burr holes were drilled with a dental drill mounted in the stereotaxic frame over the frontal cortex and hippocampus to the following coordinates: frontal cortex, anteroposterior, +2.0 mm, lateral ± 2.0 mm; hippocampus, anteroposterior -2.7 mm; lateral ± 2.5 mm, all taken from bregma. A 26-guage needle attached to a 10 mL Hamilton syringe containing the solution to be injected was lowered 3.0 mm ventral to bregma, and a 2 μL injection was made over a 2-minute period. The AL-002a and IgG2a antibodies were diluted to a final concentration of 5 mg/kg in 1X PBS. The anti-Aβ and IgG1 antibodies were diluted to a final concentration of 2

mg/kg in 1X PBS. The incision was cleaned and closed with surgical staples. Buprenophine hydrochloride diluted to 0.015 mg/mL was intraperitoneally injected immediately post-surgery at 0.1 mg/kg dose per body weight. Animals received subsequent doses every 12 hours until sacrifice. Tissue was harvested 72 hours post injection.

Tissue Processing: Mice were perfused intracardially with 25mL of normal saline. Brains were rapidly removed and bisected in the mid-sagittal plane. The left half was immersion fixed in freshly prepared 4% paraformaldehyde for 24 hours. The right half was dissected into cerebral cortex (anterior and posterior), hippocampus, striatum, thalamus, and cerebellum. The dissected pieces were flash frozen in liquid nitrogen and stored at -80°C. The left hemibrain was passed through a series of 10, 20, and 30% sucrose solutions as cryoprotection, 24 hours each, and 25μm frozen horizontal sections were collected using a sliding microtome and stored floating in PBS containing sodium azide at 4°C. Sections were collected sequentially.

Histology and Immunohistochemistry: Six sections spaced 300μm spanning the estimated injection site were mounted and stained by mouse IgG to identify the injection site. For all subsequent histology and immunohistochemistry, six sections spanning the injection site, spaced ~100 μm apart, were selected and analyzed. Sections were mounted onto slides and stained for Congo red as previously described [109, 219]. Free-floating immunohistochemistry for Aβ (4G8; biotinylated

mouse monoclonal Aβ17-24; Biolegend, San Diego, CA, USA) was performed. Briefly, sections were quenched for endogenous peroxidase, blocked and permeabilized. They were then incubated overnight in primary antibody at 4°C (1:3000). Sections were then washed and incubated for 1 hour in ABC. DAB was used for color development. Stained sections were mounted, air dried overnight, dehydrated, and coverslipped in DPX (Electron Microscopy Sciences, Hatfield, PA, USA). Immunohistochemical analysis was performed by measuring the percent area occupied by positive immunostain using the Nikon Elements BR image analysis system (Melville, NY, USA) as previously described.

Aβ Multiplex ELISA: Biochemical analysis of Aβ levels was performed using the commercially available V-PLEX Aβ Peptide Panel 1 (6E10) Kit (MSD, Rockville, MD, USA). Briefly, soluble protein was extracted from the right frontal cortex using MPER lysis buffer (Thermo Fisher Scientific, Waltham, MA, USA) with complete protease and phosphatase inhibitor (Pierce Biotechnology, Waltham, MA, USA). Following centrifugation, the resulting supernatant and pellet were separated. The supernatant was labeled the "soluble" extract, whereas the pellet was homogenized in 70% formic acid. The homogenized pellet was then subject to centrifugation and neutralization with 1M Tris-HCL and ultimately labeled the "insoluble" extract. Protein concentrations were determined using the BCA protein assay kit (Pierce Biotechnology, Waltham, MA, USA). The Meso-Scale Discovery (MSD) multiplex ELISA system was then used to measure $A\beta_{1-38}$, $A\beta_{1-40}$, and $A\beta_{1-}$

$_{42}$ levels in both the soluble and insoluble extracts. It may be noted that in both the soluble and insoluble extracts $A\beta_{1-38}$ levels were below the detectable range.

Inflammation Multiplex ELISA: Biochemical analysis of 10 proinflammatory cytokines (IFN-g, TNFa, KC/GRO, IL1-β, IL-2, IL-4, IL-5, IL-6, IL-10, and IL-12p70) was performed using the commercially available V-PLEX Proinflammatory Panel 1 Mouse Kit (MSD, Rockville, MD, USA). Soluble protein was extracted from the right frontal cortex using MPER lysis buffer (Thermo Fisher Scientific, Waltham, MA, USA) with complete protease and phosphatase inhibitor (Pierce Biotechnology, Waltham, MA, USA). Protein concentrations were determined using the BCA protein assay kit (Pierce Biotechnology, Waltham, MA, USA). The Meso-Scale Discovery (MSD) multiplex system was then used to measure levels of the aforementioned cytokines.

Analysis: Data are presented as mean ± SEM. Statistical analysis was performed using JMP statistical analysis program (SAS Institute). Outlying data points were identified using Grubb's Test. As a result, two data points were excluded from the 4G8 immunostain statistical analysis. No other data points were excluded. One-way ANOVA and two-way factorial ANOVA were used, where appropriate, to detect treatment differences and differences within treatment groups. Student's *t* Test was used for post-hoc comparisons. Statistical significance was assigned where the *p* value was lower than 0.05.

Results

Total Aβ immunohistochemistry was used to determine the efficacy of co-administration of AL-002a and anti-Aβ in reducing Aβ levels. In the current study we performed immunohistochemistry for total Aβ using the 4G8 antibody, which binds the middle portion of the Aβ peptide (amino acids 17-24). Considering the anti-Aβ antibody being injected binds the N terminus (1-16) of the Aβ peptide, 4G8 will avoid reduced staining due to antigen masking. Immunohistochemistry for total Aβ, which detects both diffuse and compact amyloid, in 5XFAD mice receiving a control antibody (IgG1, IgG2a, or a combination of the two) demonstrate a staining pattern consistent with those reported by ourselves and others [61]. 5XFAD mice receiving a combination of AL-002a and anti-Aβ show non-significant, but trending, reductions in Aβ immunohistochemistry in the frontal cortex and hippocampus compared to those receiving a combination of IgG1 and IgG2a control antibodies (Figure 3.2). Notably, reductions in Aβ in 5XFAD mice receiving the combination therapy (AL-002a and anti-Aβ) were no greater than those receiving only AL-002a or anti-Aβ (Figure 3.2).

Biochemical quantification of the soluble and insoluble Aβ species $A\beta_{1-38}$, $A\beta_{1-40}$, and $A\beta_{1-42}$ extracted from the right frontal cortex was also performed. It may be noted that in both the soluble and insoluble extracts, $A\beta_{1-38}$ levels were below the detectable range, which is typical of the 5XFAD mice and is the result of the PS1 mutations driving cleavage at the $A\beta_{1-42}$ peptide length, and less so at the $A\beta_{1-38}$ and $A\beta_{1-40}$ lengths [220]. No significant differences in soluble Aβ species were

observed in any of the groups, likely due to considerable variation among the individual samples (Figure 3.4). Interestingly, intracranial administration of anti-Aβ significantly increased the concentration of insoluble $A\beta_{1-40}$ and decreased that of $A\beta_{1-42}$ compared to administration of the relevant isotype control (IgG2a) (Figure 3.3). Concentrations of insoluble Aβ species were not significantly affected by co-administration of AL-002a and anti-Aβ, or AL-002a alone (Figure 3.3).

As discussed, there is a large body of evidence supporting a causal role for microglial activation in the clearance of amyloid, especially compact amyloid. Moreover, one of the proposed mechanisms for anti-Aβ immunotherapy's reduction of Aβ involves activation of microglia leading to phagocytosis (Figure 3.1). However, in addition to triggering phagocytosis, activation of microglia results in their production of proinflammatory cytokines, which have been implicated in both neurodegeneration and neuroprotection. Here we used a sensitive sandwich ELISA platform to characterize the expression of well-known proinflammatory proteins in the right frontal cortex of treated 5XFAD mice (Figures 3.5 & 3.6). We found that intracranial co-administration of AL-002a and anti-Aβ only significantly increases the expression of KC/GRO, also known as CXCL1 (Figure 3.5). Conversely, treatment with AL-002a increases the expression of both TNFα and IL-1β (Figure 3.5).

Discussion

Recent GWAS studies have suggested the risk for sporadic AD is driven by a number of distinct pathways including neuroinflammation, a response regulated

primarily by microglia and astrocytes. Microglial activation is characterized by changes in microglial morphology and function. Morphologically, activation of microglia involves a transition from their characteristic, homeostatic ramified morphology to an amoeboid pathology. Activated microglia also acquire proliferative, secretory, phagocytic, and antigen-presenting cell properties and are ultimately recruited by chemotactic signals to sites of pathology where they phagocytose the identified pathogen. Therapeutic approaches to the treatment of AD continue to focus on one of the major pathological hallmarks of AD, amyloid plaques, and in doing so take advantage of microglial activation. Both active and passive Aβ immunization strategies have demonstrated efficacy in reducing brain Aβ load and improving cognition in animal models of AD [98, 101, 102, 105, 107, 117, 119]. One proposed mechanism of action of anti-Aβ antibodies is microglial Fcγ receptor-mediated phagocytosis [107, 117]. Surface expression of FcγR is upregulated when microglia become activated and activation of this receptor induces phagocytosis through downstream activation of PLCγ (Figure 3.1).

Recently, loss of function mutations in another microglia surface immunoreceptor, TREM2, have been shown to increase an individual's risk for late-onset AD [154, 155]. This enhanced risk is believed to arise in part from reduced phagocytic capacity of a non-functional TREM2 receptor. Similar to the signaling cascade observed with FcγR-mediated phagocytosis, binding of a ligand to TREM2 normally induces phagocytosis through downstream activation of PLCγ (Figure 3.1). Our lab has previously shown a TREM2 agonizing antibody developed by Alector, AL-002a, activates TREM2 signaling in vitro and in vivo

whether injected intracranially or intraperitoneally. We also demonstrated the efficacy of AL-002a in activating microglia, enhancing the number of microglia clustered around plaques, reducing amyloid deposition, and improving cognition in the 5XFAD model of AD. These results are discussed in depth in chapter 1. Because anti-Aβ and TREM2 immunotherapy induce phagocytosis via FcγR-mediated and TREM2-mediated phagocytosis, respectively, our hypothesis in the current study was that dual engagement of microglia through each of these receptor mechanisms would additively augment amyloid clearance in the 5XFAD model of AD.

Ultimately, the anti-Aβ and AL-002a antibodies developed by Alector were shown to reduce amyloid deposition, though dual engagement of microglial phagocytosis was no more efficacious than engagement of FcγR or TREM2 alone (Figures 3.2 & 3.3). 5-month-old 5XFAD mice display significant amyloid pathology in the frontal cortex and hippocampus [61]. Receptor saturation refers to the state in which all receptors are effectively occupied at a given time. It is possible that the abundance of Aβ in the brains of 5XFAD mice leads to saturation of both the FcγR and TREM2 surface immune receptors. Thus, we hypothesize the lack of additive amyloid clearance is due to the fact that individual microglia can only be stimulated to phagocytose so much of a given pathogen. The significantly increased insoluble $A\beta_{1\text{-}40}$ is notable because this species is associated with cerebral amyloid angiopathy (CAA) in humans, and CAA has been shown to be increased with anti-Aβ antibody treatment [221].

Acute co-administration of anti-Aβ and AL-002a does not appear to induce significant production of neurotoxic, proinflammatory cytokines (Figures 3.5 & 3.6). Rather, co-administering anti-Aβ and TREM2 only upregulates the expression of KC/GRO, otherwise known as CXCL1, when compared to treatment with anti-Aβ alone (Figure 3.5). The upregulation of CXCL1 as a result of acute combination therapy is interesting. CXCL1 has been shown to be expressed by macrophages and act as a chemoattractant for leukocyte recruitment [222]. This is interesting given that ample literature supports the notion that two different types of microglia exist in the brain, resident microglia and those derived from bone-marrow-derived (BMD) macrophages [223-227]. Studies also suggest that a limited number of BMD macrophages are recruited into the normal adult brain after which they differentiate into functional parenchymal microglia. Moreover, data from transgenic models suggest that BMD macrophages are consistently recruited to sites of amyloid pathology [228-231]. Importantly, BMD macrophages have been shown to exhibit higher levels of proteins necessary for antigen presentation and are therefore hypothesized to be more efficient at preventing the formation of or eliminating Aβ [232-234]. In 2013, Zhang et al. assessed transcriptional differences between BMD macrophages of AD patients and aged-matched controls to identify the determinants allowing transmigration of these cells across the blood-brain-barrier (BBB) [235]. This study found that BMD macrophages from AD patients overexpress CXCL1, which interacts with CXC chemokine receptor 2 (CXCR2) to facilitate transendothelial migration through endothelial tight junctions [235]. Another study found that expression of CXCR2, the only receptor identified for

CXCL1, is strongly upregulated in neuritic plaques [236]. Collectively, these data suggest that acute co-administration of anti-Aβ and AL-002a may encourage infiltration of bone marrow-derived macrophages from the blood into the brain parenchyma. Additionally, we found that acute administration of AL-002a, but not anti-Aβ, increases levels of the pro-inflammatory cytokines TNFα and IL-1β. This is interesting given that amyloid modifying therapies such as anti-Aβ are known to induce the expression of TNFα and IL-1β. It is likely that modulation of the immune response following treatment with AL-002a operates on a different time course and that by 72 hours post-injection, anti-Aβ has already induced and resolved increased levels of TNFα and IL-1β. However, we cannot be certain of this explanation given that the aforementioned published time-course of acute anti-Aβ antibody injection did not address the expression of specific cytokines.

Numerous studies indicate microglial phagocytosis is defective in the AD brain. Our data ultimately supports the microglial dysfunction hypothesis of AD which states that microglia become senescent [237] and that senescence profoundly impacts the ability of microglia to phagocytose Aβ, further indicating phagocytosis is defective as opposed to pathologically activated. Overall, our data demonstrate efficacy of both the anti-Aβ and AL-002a antibodies in clearing Aβ from the brains of 5XFAD mice and reveal that this clearance may in part be due to the infiltration of peripheral monocytes. Subsequent studies comparing the actions of these antibodies when administered chronically will be discussed in chapter 4.

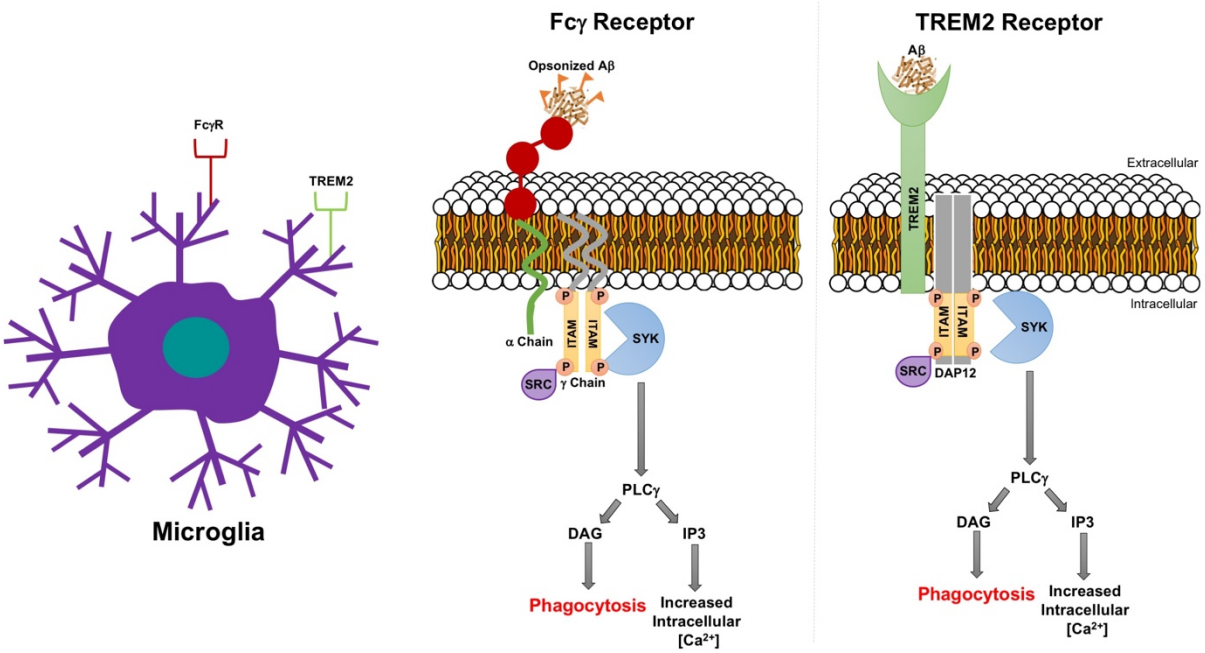

Figure 3.1: Engagement of both the microglial Fcγ and TREM2 surface immunoreceptors induces receptor-mediated phagocytosis. Binding of the α chain of the FcγR to opsonized Aβ (Aβ coated with anti-Aβ antibodies and therefore tagged for destruction) results in phosphorylation of the ITAM region of the FcγR γ chain by SRC kinase. This phosphorylation subsequently recruits SYK, whose activation induces the activation of PLCγ, DAG, and IP_3, thereby promoting phagocytosis. Similarly, binding of the Aβ peptide to the TREM2 receptor results in phosphorylation of the ITAM region of its associated intracellular adaptor protein, DAP12, by SRC. This phosphorylation also induces the recruitment of SYK and subsequent activation of PLCγ, DAG, and IP_3, resulting in phagocytosis.

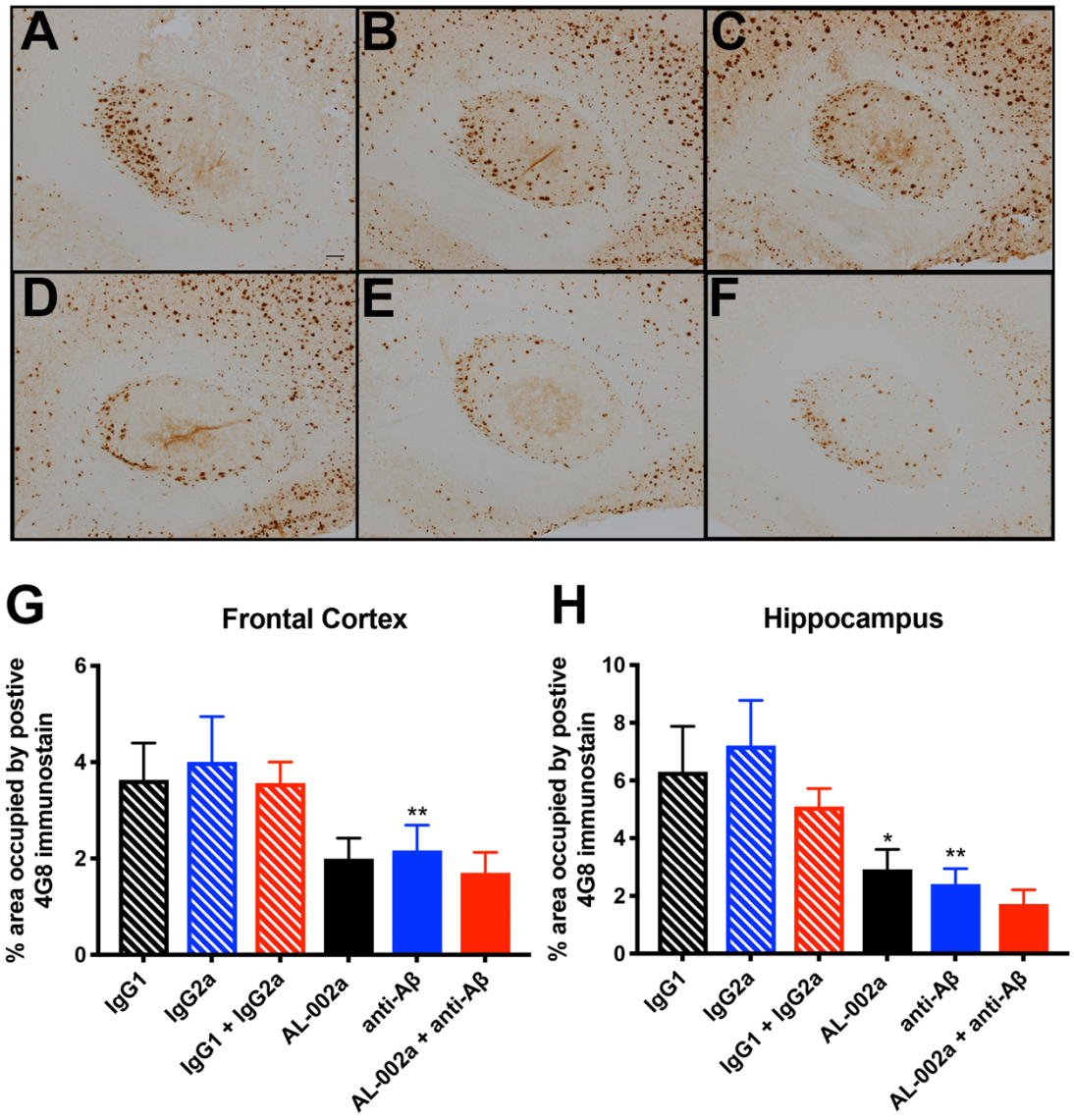

Figure 3.2: Intracranial co-administration of TREM2 agonizing and anti-Aβ antibodies does not lead to additive reductions in Aβ load. Representative images of Aβ staining in the hippocampus of 5XFAD mice injected with IgG1 (A), with IgG2a (B), with both IgG1 and IgG2a antibodies (C), AL-002a (D), with anti-Aβ (E), and with both AL-002a and anti-Aβ antibodies (F) are shown. Scale Bar: (A) 100 μM. Quantification of percentage positive immunostain in the frontal cortex

(G) and hippocampus (H). *p<0.05, **p<0.01, compared with 5XFAD injected with the relevant control antibody. It is worth noting that, with respect to the hippocampus, the *p* value for 5XFAD mice injected with both AL-002a and anti-Aβ compared to those injected with both IgG1 and IgG2a was 0.0508.

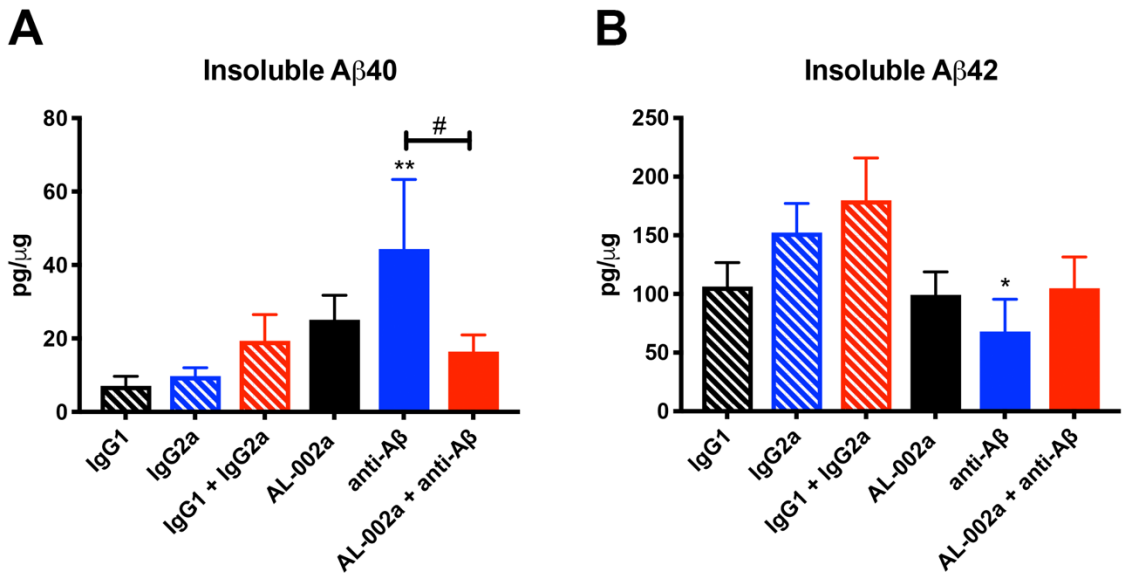

Figure 3.3: Biochemical quantification reveals intracranial co-administration of AL-002a and anti-Aβ does not additively reduce insoluble $A\beta_{1\text{-}40}$ or $A\beta_{1\text{-}42}$. Data are represented as mean ± SEM. *p<0.05, **p<0.01, compared with 5XFAD injected with the relevant control antibody. #p<0.05, compared with 5XFAD injected with a different experimental antibody. It is worth noting that, with respect to insoluble $A\beta_{1\text{-}42}$, the *p* value for 5XFAD mice injected with both AL-002a and anti-Aβ compared to those injected with both IgG1 and IgG2a was 0.0506.

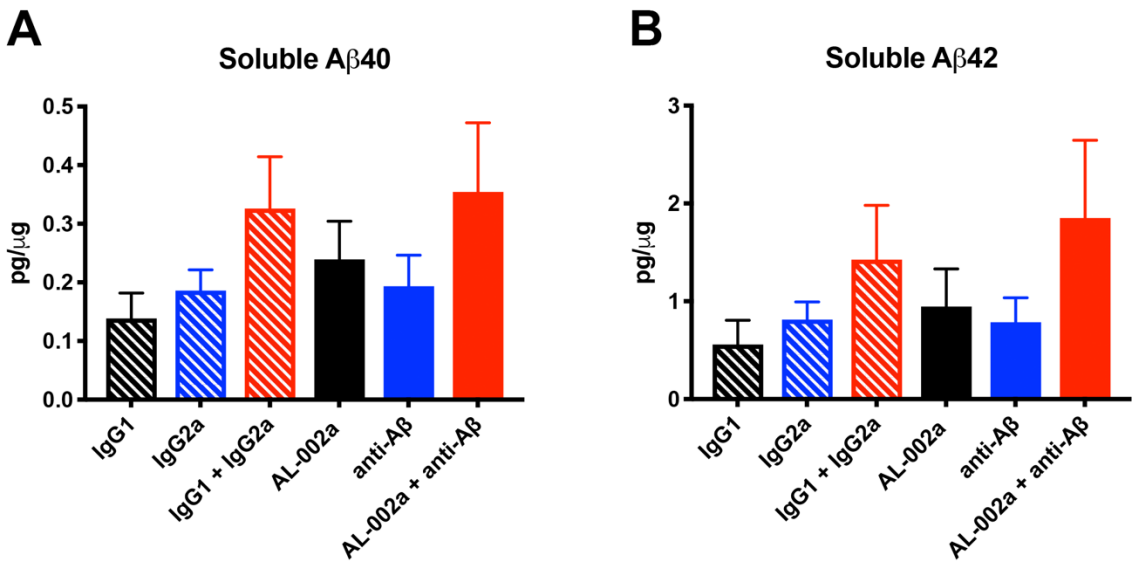

Figure 3.4: Biochemical quantification reveals intracranial co-administration of AL-002a and anti-Aβ does not additively reduce soluble $A\beta_{1-40}$ or $A\beta_{1-42}$. Data are represented as mean ± SEM. *p<0.05, **p<0.01, compared with 5XFAD injected with the relevant control antibody.

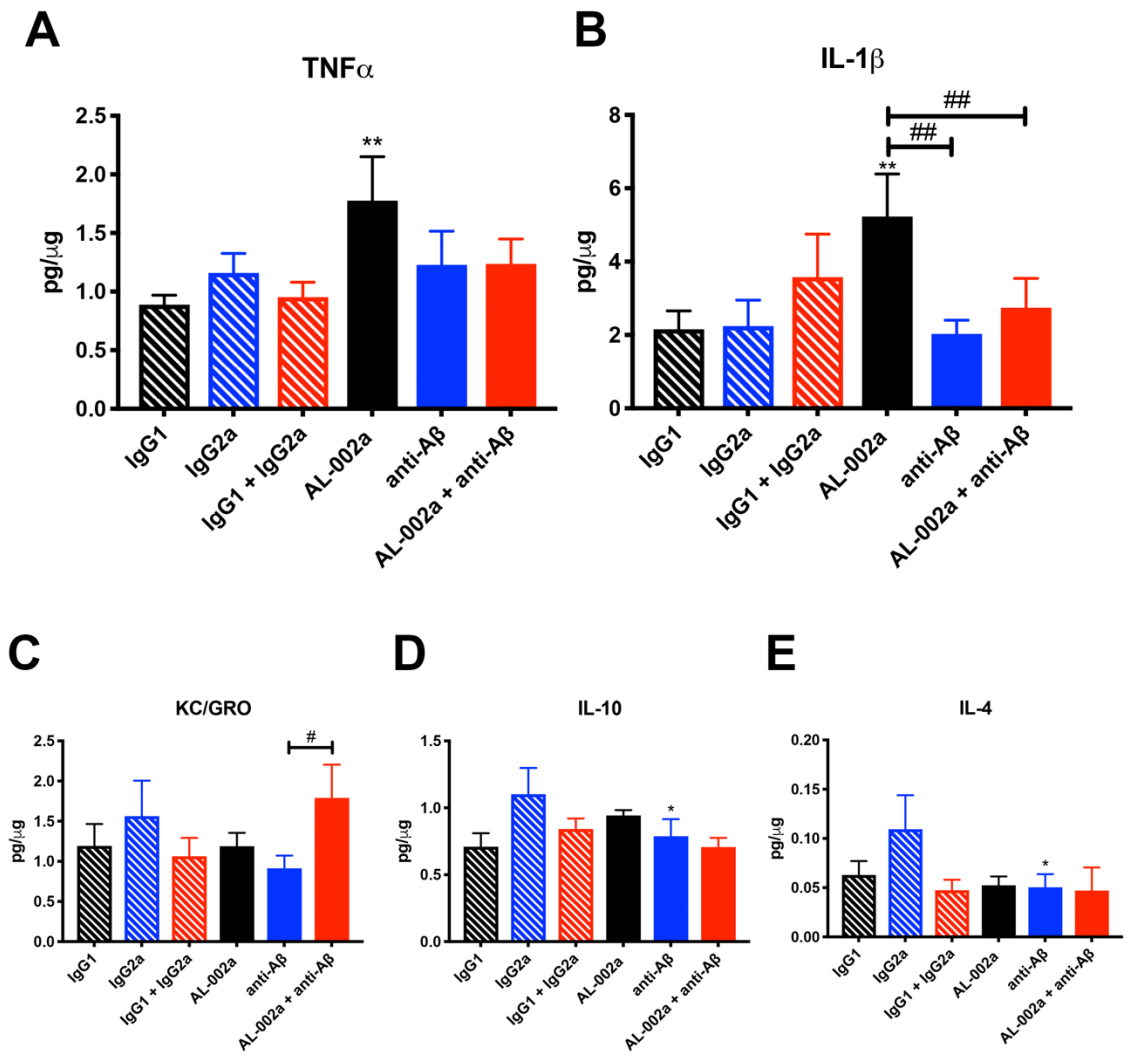

Figure 3.5: Pro-inflammatory cytokines whose expression were significantly influenced by antibody treatment. Data are represented as mean ± SEM. *p<0.05, **p<0.01, compared with 5XFAD injected with the relevant control antibody. #p<0.05, ##p<0.01, compared with 5XFAD injected with a different experimental antibody.

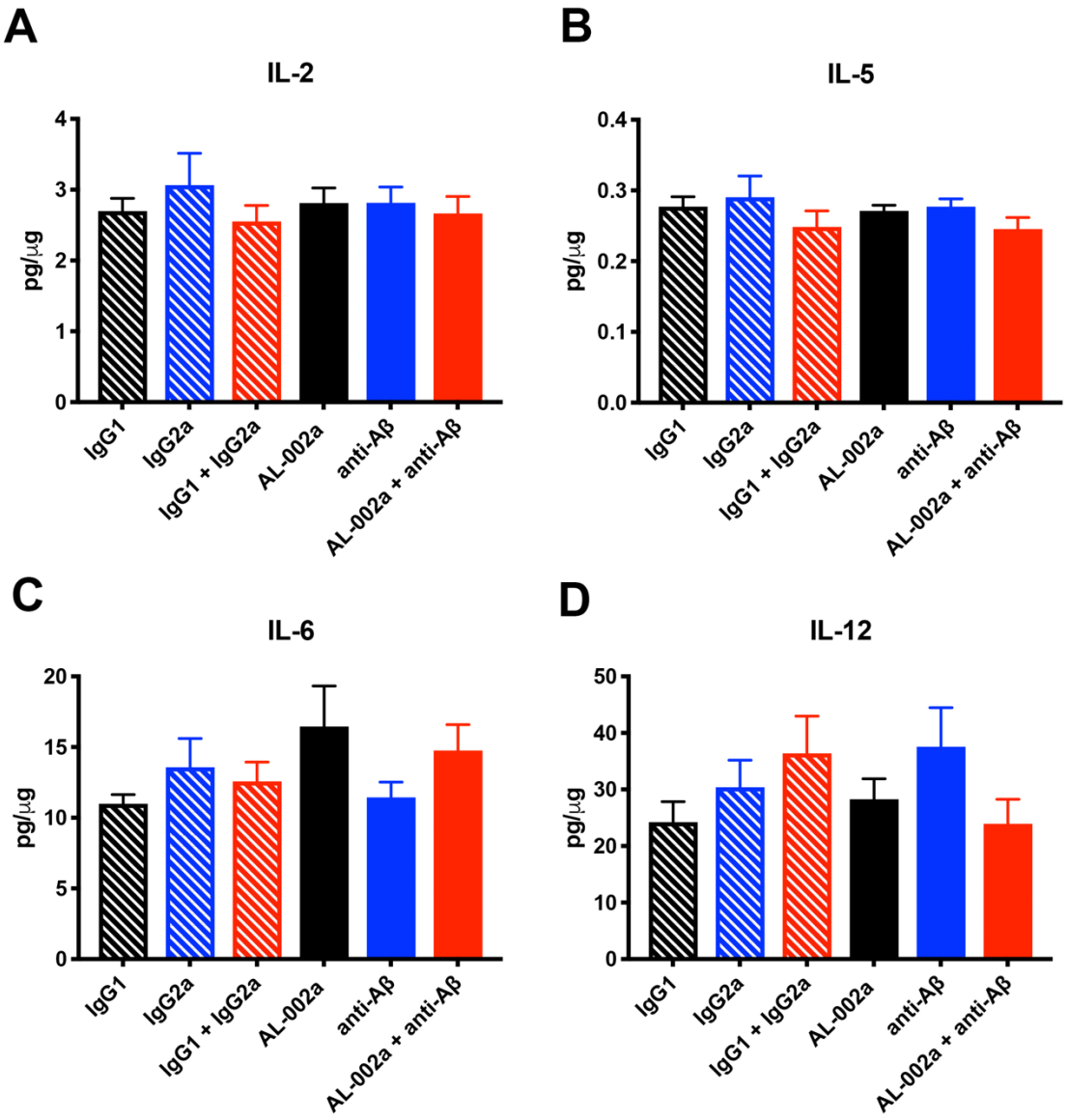

Figure 3.6: Pro-inflammatory cytokines whose expression was not significantly influenced by antibody treatment. Data are represented as mean ± SEM.

Chapter 4

Agonism of TREM2 by an activating antibody ameliorates cerebrovascular adverse events normally associated with anti-Aβ immunotherapy.

Abstract:

Despite significant mouse model data demonstrating both pathological and cognitive efficacy of anti-Aβ immunotherapy, clinical trials continue to fail to meet primary endpoints for efficacy. Dosage for anti-Aβ immunotherapy is limited in order to minimize the occurrence of cerebrovascular adverse events, namely microhemorrhages and vasogenic edema. As a result of the Aβ-targeted immunotherapy failures, identifying alternate therapeutic strategies is of paramount importance, and targeting neuroinflammation through TREM2 is such an approach. Though our previous work demonstrated acute administration of a combination of TREM2-agonizing (AL-002a) and anti-Aβ antibodies did not additively reduce Aβ deposition, it suggested that AL-002a has similar efficacy to a well characterized anti-Aβ antibody in reducing Aβ deposition in the brains of 5XFAD mice. Chronic, systemic administration is more clinically relevant, and so we tested the hypothesis that systemic co-administration of AL-002a, a TREM2 agonizing antibody, and an N-terminal anti-Aβ antibody, would additively augment Aβ clearance from the brains of 5XFAD mice. Though we demonstrate that systemic co-administration does not additively reduce Aβ deposition, we show that AL-002a is as efficacious as an anti-Aβ antibody in preventing the deposition of newly-generated Aβ when administered systemically. Notably, the reduction in Aβ

following treatment with the anti-Aβ antibody was associated with an increase in the incidence of microhemorrhage whereas reduction of Aβ by AL-002a was significant in the absence of cerebrovascular pathology. Moreover, combined treatment using AL-002a and an anti-Aβ antibody also showed reduced Aβ deposition in the absence of cerebrovascular adverse events. Our data therefore ultimately demonstrate that agonization of TREM2 may be a promising new immunotherapy for the treatment of late-onset AD.

Introduction:

Alzheimer's disease (AD) is the most common form of dementia and is characterized by three pathological hallmarks: 1) extracellular amyloid plaques consisting of aggregated Aβ peptide, 2) neurofibrillary tangles comprised of hyperphosphorylated tau protein, and 3) neuronal loss [3, 8, 9]. The main theoretical construct underlying AD progression is the amyloid cascade hypothesis, which posits that neurofibrillary tangle formation, neurodegeneration, and dementia are downstream consequences of Aβ deposition and toxicity [12, 13]. Overwhelming support for the amyloid cascade hypothesis continues to encourage therapeutic targeting of the Aβ peptide. One of the most extensively characterized therapeutics for AD is anti-Aβ immunotherapy, which uses antibodies against Aβ to promote its clearance from the brain via microglial Fcγ-receptor (FcγR)-mediated phagocytosis [105, 117]. Despite significant mouse model data demonstrating pathological and cognitive efficacy of anti-Aβ immunotherapy, virtually all clinical trials of Alzheimer's drugs fail. Furthermore,

MRI signal alterations, thought to represent vasogenic edema and cerebral microhemorrhages, have been associated with a number of Aβ-targeted immunotherapies, thereby necessitating the need for novel AD therapeutic targets [114, 116].

Recent GWAS studies have identified the importance of the microglial surface immunoreceptor TREM2 [154, 155], which appears to be the most significant immune-associated gene influencing AD risk. To date, several laboratories have assessed whether partial or complete loss of TREM2 function contributes to Aβ deposition. Their efforts have consistently shown that TREM2 deficiency results in a strong reduction in Aβ-associated microgliosis, ultimately supporting the notion that loss of function of TREM2 is detrimental to the AD brain. Previous work from our lab has shown that administration of a TREM2 agonizing antibody, AL-002a, modulated the immune response, enhanced microglial clustering around amyloid plaques, reduced amyloid deposition, and improved cognition in the 5XFAD model of AD.

Recently, our lab has shown that acute engagement of both the Fcγ and TREM2 microglial receptors through anti-Aβ and TREM2-agonizing antibodies does not further augment Aβ clearance. However, we also demonstrated that the TREM2 agonizing antibody AL-002a appears to have similar efficacy in the reduction of Aβ deposition as the well-characterized anti-N-terminal Aβ antibody. Considering replication of these data in a systemic study could have significant clinical implications moving forward, we tested the hypothesis that systemic co-administration of AL-002a and an anti-Aβ antibody would additively augment Aβ

clearance from the brains of 5XFAD mice. Notably, previous work from our lab also demonstrated that the anti-Aβ antibody, but not AL-002a, increases levels of insoluble $A\beta_{1-40}$, the Aβ species associated with cerebral amyloid angiopathy [238, 239], in turn suggesting that AL-002a does not induce the vascular accumulation of amyloid commonly observed with Aβ immunotherapy. Based on these data, we also hypothesized that agonism of TREM2 would reduce the incidence of cerebrovascular adverse events typically associated with anti-Aβ immunotherapy.

To test these hypotheses, we used 5XFAD mice, which express five familial-AD-associated mutations (3 APP mutations and 2 PS1 mutations) and rapidly develop severe amyloid pathology [61]. Using this model, we administered one of six antibody sets: AL002a, anti-Aβ, a combination of the two, or one of three isotype-matched experimental controls. Similar to our results from the acute study, we found that chronic engagement of the Fcγ and TREM2 microglial receptors does not further augment Aβ clearance. Importantly, biochemical quantification of soluble and insoluble Aβ species indicate that AL-002a is as efficacious in preventing additional Aβ deposition as a well-characterized N-terminal anti-Aβ antibody. Notably, treatment with the anti-Aβ antibody was shown to significantly increase the incidence of microhemorrhage whereas reduction of Aβ by AL-002a was shown to occur in the absence of cerebrovascular pathology.

Material and Methods:

Study Design: This study was designed to test two hypotheses: 1) that systemic co-administration of AL-002a and an anti-Aβ antibody will further enhance amyloid

clearance in the 5XFAD transgenic mouse model of AD, and 2) that agonism of TREM2 via AL-002a will reduce the incidence of cerebrovascular adverse events typically associated with anti-Aβ immunotherapy. Sample size for the studies performed was determined by statistical power analyses with behavior as the primary outcome for power calculations due to it being the most variable outcome. Our endpoints were determined ahead of the initiation of study and were based on disease-relevant outcomes hypothesized to be affected by TREM2 and FcγR agonism. Mice were randomized into groups using a random number generator. All studies were blinded. Antibodies were received numbered 1-6 with no other identifying information. Unblinding occurred only after all primary endpoint data were collected.

Animals. 5XFAD transgenic mice overexpressing the K670N/M671L (Swedish), I716V (Florida), and V717I (London) mutations in human APP (695), as well as the M146L and L286V mutations in human PS1 [61] were aged to 3.5 months at Taconic and transferred to the University of Kentucky. The study was approved by the University of Kentucky Institutional Animal Care and Use Committee and conformed to the National Institutes of Health Guide for the Care and Use of Animals in Research. All studies were performed blinded. Alector provided the antibodies coded and the mice were also coded and randomized to one of six groups. Only upon completion of the data analysis were the groups unblinded. Only male mice were used in the current study as the 5XFAD mice have been shown to have sex-dependent differences in amyloid deposition [61, 217].

Systemic Administration: Four-month-old male 5XFAD and male wildtype littermates were assigned to one of six antibody groups: 1) AL-002a (IgG1 isotype; Alector) N=15 5XFAD, N=9 WT; 2) N-terminal anti-Aβ (IgG2a isotype; Alector) N= 17 5XFAD, N= 9 WT; 3) AL-002a + anti-Aβ, N =17 5XFAD, N= 12 WT; 4) IgG1 (mouse IgG1 kappa monoclonal; MOPC; control antibody for AL-002a) N= 15 5XFAD, N= 10 WT; 5), IgG2a (mouse IgG2a kappa monoclonal; MOPC; control antibody for anti-Aβ) N= 17 5XFAD, N= 10 WT; or 6) IgG1 + IgG2a, N= 17 5XFAD, N= 11 WT. The uneven group numbers reflect the death of some animals throughout the course of treatment or following behavior testing. The n numbers provided reflect only those animals that completed the study. Animals that died prior to the completion of the study were not included in post-mortem statistical analyses. Notably, deaths appeared to be unrelated to treatment with any specific antibody. It is worth noting that the anti-Aβ antibody used here is most similar to Aducanumab, an IgG2a isotype that has been shown to selectively bind insoluble fibrillar and soluble oligomeric Aβ aggregates at the extreme amino terminus ($A\beta_{3-7}$) [218]. AL-002a and its isotype control were administered at a dose of 50mg/kg/week. The anti-Aβ antibody and its isotype control were administered at a dose of 10mg/kg/week. Where mice were receiving combination, they received the same dosage of each antibody at the same interval. Mice were subject to multiple behavior paradigms during the two weeks prior to sacrifice (i.e. week 12). Mice were euthanized and tissue was harvested 24 hours after the final injection.

Tissue Processing: Mice were perfused intracardially with 25mL of normal saline. Brains were rapidly removed and bisected in the mid-sagittal plane. The left half was immersion fixed in freshly prepared 4% paraformaldehyde for 24 hours. The right half was dissected into cerebral cortex (anterior and posterior), hippocampus, striatum, thalamus, and cerebellum. The dissected pieces were flash frozen in liquid nitrogen and stored at -80°C. The left hemibrain was passed through a series of 10, 20, and 30% sucrose solutions as cryoprotection, 24 hours each, and 25μm frozen horizontal sections were collected using a sliding microtome and stored floating in PBS containing sodium azide at 4°C. Sections were collected sequentially.

Histology and Immunohistochemistry: Eight serial horizontal sections spaced 1200 μm apart were selected for free-floating immunohistochemistry for Aβ (biotinylated mouse monoclonal Aβ17-24; Biolegend, San Diego, CA, USA), IBA1 (rabbit polyclonal; Wako, Richmond, VA, USA) and CD45 (rat monoclonal; Biolegend, San Diego, CA, USA). Briefly, sections were quenched for endogenous peroxidase, blocked and permeabilized. They were then incubated overnight in primary antibody at 4°C (Aβ 1:3000; IBA1 1:1000, CD45 1:3000). After washing, sections were incubated for 2 hours in the appropriate biotinylated secondary antibody (goat anti-rabbit IgG for IBA1, goat anti-rat IgG for CD45 at 1:3000 and 1:5000, respectively). Sections were then washed and incubated for 1 hour in ABC. DAB with (IBA1, CD45) and without (Aβ) nickel was used for color development. Stained sections were mounted, air dried overnight, dehydrated, and coverslipped

in DPX (Electron Microscopy Sciences, Hatfield, PA, USA). Immunohistochemical analysis was performed by measuring the percent area occupied by positive immunostain using the Nikon Elements BR image analysis system (Melville, NY, USA) as previously described. Additionally, eight serial horizontal sections spaced 600 μm apart were mounted on sides and stained for Prussian blue as previously described [109]. Neutral red was used as a counterstain for Prussian blue.

Aβ Multiplex ELISA: Biochemical analysis of Aβ levels was performed using the commercially available V-PLEX Aβ Peptide Panel 1 (6E10) Kit (MSD, Rockville, MD, USA). Briefly, soluble protein was extracted from the right frontal cortex using MPER lysis buffer (Thermo Fisher Scientific, Waltham, MA, USA) with complete protease and phosphatase inhibitor (Pierce Biotechnology, Waltham, MA, USA). Following centrifugation, the resulting supernatant and pellet were separated. The supernatant was labeled the "soluble" extract, whereas the pellet was homogenized in 70% formic acid. The homogenized pellet was then subject to centrifugation and neutralization with 1M Tris-HCL and ultimately labeled the "insoluble" extract. Protein concentrations were determined using the BCA protein assay kit (Pierce Biotechnology, Waltham, MA, USA). The Meso-Scale Discovery (MSD) multiplex ELISA system was then used to measure $A\beta_{1-38}$, $A\beta_{1-40}$, and $A\beta_{1-42}$ levels in both the soluble and insoluble extracts. It may be noted that in both the soluble and insoluble extracts $A\beta_{1-38}$ levels were below the detectable range.

Inflammation Multiplex ELISA: Biochemical analysis of 10 proinflammatory cytokines (IFN-g, TNFa, KC/GRO, IL1-b, IL-2, IL-4, IL-5, IL-6, IL-10, and IL-12p70) was performed using the commercially available V-PLEX Proinflammatory Panel 1 Mouse Kit (MSD, Rockville, MD, USA). Soluble protein was extracted from the right frontal cortex using MPER lysis buffer (Thermo Fisher Scientific, Waltham, MA, USA) with complete protease and phosphatase inhibitor (Pierce Biotechnology, Waltham, MA, USA). Protein concentrations were determined using the BCA protein assay kit (Pierce Biotechnology, Waltham, MA, USA). The Meso-Scale Discovery (MSD) multiplex system was then used to measure levels of the aforementioned cytokines.

MMP ELISA: Biochemical analysis of MMP3 and MMP9 levels was performed using the commercially available Mouse Total MMP3 and Mouse Total MMP9 ELISA Kits (R&D Systems, Minneapolis, MN, USA), respectively. Soluble protein was extracted from the right frontal cortex using MPER lysis buffer (Thermo Fisher Scientific, Waltham, MA, USA) with complete protease and phosphatase inhibitor (Pierce Biotechnology, Waltham, MA, USA). Protein concentrations were determined using the BCA protein assay kit (Pierce Biotechnology, Waltham, MA, USA). The appropriate ELISA kit was then used to measure levels of MMP3 and MMP9.

Radial Arm Water Maze: After 12 weeks of treatment, mice were subject to a two-day radial arm water maze (RAWM) paradigm, as previously described [68]. On

day one, 15 trials were run in two blocks of 6 followed by the last three trials. A cohort of 4 mice was run sequentially for each block (i.e. each of 4 mice undergo trial one, then the same mice undergo trial two, etc.). After each block, a second cohort of mice was run, permitting an extended rest period before mice were exposed to the next block of trials. It should be noted that extra wait time was added to the end of the block with three trials to ensure the rest period was similar throughout testing. The goal arm was different for each mouse in a cohort to minimize odor cues. Conversely, the start arm was varied for each trial, with the goal arm remaining constant for a given individual for both days. For the first 11 trials, the platform was alternately visible then hidden (hidden for the last 4 of the first 15 trials). On day two, the mice were run in exactly the same manner as day one except that the platform remained hidden for all 15 trials. The number of errors (incorrect arm entries) were measured in a one-minute time frame. As standard practice, mice failing to make an arm choice within 15 seconds were assigned one error. In order to minimize the influence of individual trial variability, each mouse's errors for 3 consecutive trials were averaged, producing 5 data points (termed "blocks") for each day. Blocks were then analyzed statistically by repeated measures ANOVA using SAS.

Novel Object Recognition: Following the RAWM, the novel object recognition task was performed. During the habituation phase, each mouse was gently placed into a square box (50 x 50 x 15 cm, length x width x height) for 30 min without any objects. During the training phase, two identical objects, A1 and A2, were placed

parallel to and near one wall of the square box. Each mouse was placed singly in the box and allowed to explore the objects for 5 minutes. Exploratory behavior was defined as directing the nose at the object at a distance of less than 2 cm and/or touching the object with the nose. The mouse was then returned to its home cage with a 1-hour inter-trial interval. Both objects were replaced; one being a familiar object (A1) and the other a novel object (B). The mouse was returned to the box and allowed to explore the objects for 5 minutes during the test phase. Novel and familiar objects were alternated between the left and right positions to reduce potential bias toward a particular location. The objects and the box were cleaned with 10% ethanol after each individual trial to eliminate olfactory cues. The exploration time (s) for each object in the trials was recorded. The preferential index (PI) was calculated as [time spent exploring the novel object/total exploration time].

Analysis: Data are presented as mean ± SEM. Statistical analysis was performed using JMP statistical analysis program (SAS Institute). Outlying data points were identified using Grubb's Test and removed from their respective dataset. RAWM data were analyzed by repeated-measures ANOVA. For other data, one-way ANOVA and two-way factorial ANOVA were used, where appropriate, to detect treatment differences and differences within treatment groups. Student's *t* Test was used for post-hoc comparisons. Statistical significance was assigned where the *p* value was lower than 0.05.

Results:

Mice were tested in our behavioral paradigms during the two weeks prior to sacrifice. The radial arm water maze (RAWM) is a behavioral task that reliably detects spatial learning and memory deficits in aged transgenic mice [68]. 5XFAD mice were tested after 12 weeks of treatment with either AL-002a, anti-Aβ, a combination of AL-002a and anti-Aβ, or 1 of 3 isotype-matched experimental controls. Included in the task were age-matched wildtype littermate mice treated with 1 of the 6 aforementioned antibodies. We found that the 5XFAD mice receiving IgG1, IgG2a, or a combination of IgG1 and IgG2a were significantly impaired compared to 5XFAD mice receiving AL-002a, anti-Aβ, or a combination of the two (Figure 4.1A). In examining the antibody effects at the end of the second day of testing (Block 10), we found a significant reduction in the number of errors in the 5XFAD mice receiving AL-002a compared to those receiving the relevant control antibody (IgG1) (Figure 4.1B). Importantly, no significant treatment effects were observed in wildtype mice, indicating the effects of AL-002a and anti-Aβ on cognition are genotype specific.

Within the same week following completion of the RAWM, the Novel Object Recognition (NOR) task was performed to investigate short-term recognition memory [191]. We found that 5XFAD mice treated with IgG1, IgG2a, or a combination of IgG1 and IgG2a spent significantly more time exploring the familiar object compared to the 5XFAD mice treated with AL-002a, anti-Aβ, or a combination of the two (Figure 4.2A). Additionally, the 5XFAD mice treated with AL-002a, anti-Aβ, or a combination of the two exhibited significantly increased

explorative behavior as compared to control antibody treated 5XFAD mice (Figure 4.2A). Again, no significant treatment effects were observed in wildtype mice, indicating the effects of AL-002a and anti-Aβ on cognition are genotype specific.

Total Aβ immunohistochemistry was used to determine the efficacy of systemic co-administration of AL-002a and anti-Aβ in reducing Aβ levels. Because the anti-Aβ antibody being injected binds the N terminus (amino acids 1-16) of the Aβ peptide, we performed immunohistochemistry for total Aβ using the 4G8 antibody, which binds the middle portion of the Aβ peptide (amino acids 17-24). 4G8 therefore avoids potential reductions in staining due to antigen masking. In line with the results of our acute study, here we show that systemic co-administration of AL-002a and anti-Aβ does not additively reduce Aβ levels (Figure 4.3). However, in contrast to the results of our acute study, we also show that treatment with AL-002a or anti-Aβ alone does not significantly reduce Aβ levels in the hippocampus, and that only treatment with anti-Aβ significantly reduces Aβ levels in the frontal cortex. It is worth nothing these data regarding Aβ reductions following treatment with AL-002a directly contradict previous work from our lab (see Chapter 2), and that this discrepancy may be due to the fact that these studies used different anti-Aβ antibodies for immunohistochemistry. Interestingly, co-administration of the two significantly reduces Aβ levels in both the frontal cortex and hippocampus when compared to 5XFAD mice treated with the isotype-matched control. The inconsistencies observed between our acute and systemic datasets may be attributable to the fact that while antibodies can cross the BBB into the brain parenchyma, they don't do so very well. In fact, only 0.1-0.2% of

antibody is able to enter the brain [240]. The disparity in amyloid clearance observed in mice treated with AL-002a or anti-Aβ may be due to enhanced permeability of the BBB following treatment with anti-Aβ but not AL-002a. Despite these discrepancies, biochemical quantification of several Aβ species suggests both the AL-002a and anti-Aβ antibodies prevent additional deposition of newly-generated Aβ.

Biochemical quantification of the soluble and insoluble Aβ species $A\beta_{1-38}$, $A\beta_{1-40}$, and $A\beta_{1-42}$ extracted from the right frontal cortex was also performed. It may be noted that in both the soluble and insoluble extracts, $A\beta_{1-38}$ levels were below the detectable range, which is typical of the 5XFAD mice and is the result of the PS1 mutations driving cleavage at the $A\beta_{1-42}$ length, and less so at the $A\beta_{1-40}$ and $A\beta_{1-38}$ lengths [220]. We found that systemic administration of anti-Aβ significantly decreases levels of insoluble $A\beta_{1-40}$ and $A\beta_{1-42}$, whereas administration of AL-002a or a combination of AL-002a and anti-Aβ significantly reduces levels of insoluble $A\beta_{1-42}$ (Figure 4.4A). Conversely, systemic administration of AL-002a, anti-Aβ, or a combination of the two significantly increases levels of soluble $A\beta_{1-40}$, whereas only the administration of anti-Aβ significantly increases levels of soluble $A\beta_{1-42}$ (Figure 4.4B).

As previously discussed, one of the proposed mechanisms for anti-Aβ immunotherapy's reduction of Aβ involves activation of microglia. We therefore performed immunohistochemistry for IBA1, which labels both activated and resting microglia, to determine whether there was an increase in the total number of

microglia. IBA1 staining in the frontal cortex and hippocampus of 5XFAD mice revealed that treatment with AL-002a or a combination of AL-002a and anti-Aβ significantly increases the total number of microglia compared to treatment with anti-Aβ alone (Figure 4.5A).

Considering activation of microglia is thought to reflect their increased expression of proinflammatory cytokines, we used a sensitive sandwich ELISA platform to characterize the levels of well-known proinflammatory cytokines in the right frontal cortex of treated 5XFAD mice (Figures 4.6 & 4.7). Interestingly, we found that treatment with anti-Aβ significantly increases the expression of several hallmark proinflammatory cytokines, including TNFα, IL-1β, IL-12, IL-6, IL-2, and KC/GRO (CXCL1) (Figure 4.6). Conversely, treatment with AL-002a significantly increased the expression of the anti-inflammatory cytokine IL-10 (Figure 4.6). It may be noted a number of cytokines were unaffected following treatment (Figure 4.7).

Given their implication in extracellular matrix degradation, we also used a sensitive sandwich ELISA platform to characterize the levels of two matrix metalloproteinases (MMPs), MMP3 and MMP9. We found significantly increased levels of both MMP3 and MMP9 in 5XFAD mice treated with anti-Aβ (Figure 4.8). Notably, this effect was not observed among the other treatment groups. Moreover, Prussian blue histological analysis revealed a significantly increased incidence of microhemorrhage in 5XFAD mice treated with anti-Aβ, and this effect was not observed among the other treatment groups (Figure 4.9).

Discussion:

Similar to the findings of our acute study, data from this systemic study demonstrate that co-administration of AL-002a and anti-Aβ followed by subsequent dual engagement of the microglial TREM2 and Fcγ surface receptors, respectively, does not result in additive reductions in Aβ deposition. It is intriguing that systemic administration of AL-002a, anti-Aβ, or a combination of the two significantly increased levels of soluble $A\beta_{1-40}$, whereas only treatment with anti-Aβ increased levels of soluble $A\beta_{1-42}$. One of the proposed mechanisms of action of anti-Aβ immunotherapy is disaggregation and solubilization of Aβ. This mechanism was first proposed by Solomon et al., who demonstrated that antibodies raised against the N-terminal region (amino acids 1-28) of the Aβ peptide bind Aβ, leading to disaggregation and partial restoration of the peptide's solubility [120]. It is possible that treatment with AL-002a, anti-Aβ, or a combination of the two results in disaggregation of Aβ oligomers and the restoration of their solubility, which may augment Aβ efflux from the brain into the blood via low-density lipoprotein receptor related protein-1 (LRP1) or through interstitial fluid bulk-flow clearance (perivascular drainage) [241-243]. It is worth nothing that increased levels of soluble Aβ species, concomitant increases in CAA, and an increased density of cortical microhemorrhages have been reported in a number of human neuropathological studies [42-44]. Interestingly, in one study two of the nine patients assessed exhibited almost complete absence of both parenchymal amyloid plaques and CAA suggesting that, with time, Aβ is eventually cleared from the vasculature [44]. Our data are consistent with the hypothesis that Aβ

immunotherapy results in the solubilization of Aβ, but also suggest that only treatment with anti-Aβ is disaggregating and solubilizing parenchymal amyloid plaques.

By using two distinct behavioral paradigms to test learning and memory in the current study, we are confident in concluding that co-administration of AL-002a and anti-Aβ does not doubly enhance cognition in the 5XFAD model of AD. Notably, comparable to data from our acute study, data presented here indicate that AL-002a is as efficacious as anti-Aβ in the reduction of Aβ deposition and that the reduction of Aβ by AL-002a does not induce cerebrovascular pathology observed following treatment with anti-Aβ. The absence of cerebrovascular pathology following treatment with AL-002a, but not anti-Aβ, is likely due to the observed differences in immune modulation and matrix metalloprotease (MMP) expression.

It is well understood that microglia express a wide variety of pattern recognition receptors (PRRs), which trigger a series of intracellular cascades that culminate with the production of pro- and anti-inflammatory cytokines upon recognition of a particular pathogen. Thus, depending on the encountered pathologic events, microglia are able to exert a variety of effector functions, which may be either neurotoxic (pro-inflammatory) or neuroprotective (anti-inflammatory). It should be noted that the activated microglial response initially provides the environment needed for neuronal regeneration and functional recovery and is, therefore, neuroprotective. However, dysregulation of the microglial inflammatory response may lead to the uncontrolled production of

immune mediators as well as the recruitment of peripheral immune cells that induce secondary damage to intact tissue [244, 245]. Thus, immune cell activation must be tightly regulated in order to avoid bystander degeneration of otherwise healthy neurons. Biochemical quantification of a number of cytokines revealed that treatment with AL-002a significantly increases levels of the anti-inflammatory cytokine IL-10, whereas treatment with anti-Aβ significantly increases levels of TNFα, IL-1β, IL-12, and IL-6, all of which are considered to be pro-inflammatory.

The upregulation of IL-10 following treatment with AL-002a, but not anti-Aβ, is interesting considering the production of IL-10 has been described as one of the most important mechanisms evolved by immunologically competent cells to counteract damage driven by excessive inflammation [246]. This is because IL-10 binding to its receptor results in decreased cytokine gene expression as well as the downregulation of MHC II which subsequently decreases antigen presentation to T cells [247, 248]. Furthermore, IL-10 has been shown to prevent apoptosis by activating the PI3K/AKT signaling cascade, thereby enhancing the expression of anti-apoptotic factors [248]. IL-10 has also been shown to inhibit the production of pro-inflammatory cytokines by microglia [249, 250] and to act on astrocytes by potentiating their production of TGFβ [251]. Finally, IL-10 has been shown to provide trophic support to neurons and is, therefore, associated with enhanced survival [252].

In addition to discrepancies in immune modulation, our data demonstrate that treatment with anti-Aβ, but not AL-002a, induces increased expression of MMP3 and MMP9, both of which have been implicated in tight junction breakdown

and subsequent blood-brain-barrier (BBB) leakage responsible [253]. MMP9 belongs to the gelatinase family of MMPs and can therefore degrade gelatin, cytokines, and even Aβ [254, 255]. Given MMP9's variety of substrates, its expression is tightly regulated by a number of cytokines, growth factors, and other proteins. In particular, its expression is induced by the proinflammatory cytokines TNFα and IL-1β [256, 257], both of which were upregulated following treatment with anti-Aβ but not AL-002a. Due to the necessity of its tight regulation, MMP9 is secreted as a zymogen that requires cleavage by MMP3, the expression of which is also induced by pro-inflammatory cytokines, to become active [258]. Notably, MMP9 has been implicated in BBB breakdown following anti-Aβ immunotherapy. Significant increases in gene expression of MMP3 coupled with significantly decreased expression of TIMP1, the endogenous inhibitor of MMP9, were observed in AβPPSw/NOS2$^{-/-}$ mice treated with an Aβ vaccine [115]. Protein measurements confirmed these increased levels and demonstrated that robust expression of MMP9 was found to be associated with the vasculature [115]. Moreover, similar results have been reported in passively immunized AD transgenic mice and are further supported by the data shown here. Interestingly, an in vitro study using BV2 cells treated with either an anti-Aβ IgG-Aβ or anti-tau IgG-tau immune complex demonstrated increased MMP3 and MMP9, suggesting that activation of MMP9 requires the Fcγ receptor [259].

Collectively, our data suggest AL-002a and anti-Aβ function differently to reduce Aβ deposition in the brains of 5XFAD mice. It is likely that increased levels of the proinflammatory cytokines TNFα and IL-1β following treatment with anti-Aβ

are directly responsible for the observed upregulation of MMP3 and MMP9 and subsequent increased incidence of microhemorrhage. Conversely, the absence of cerebrovascular pathology in the 5XFAD mice treated with AL-002a is likely due to increased levels of IL-10. As discussed previously, IL-10 inhibits the production of proinflammatory cytokines, thereby preventing the production of MMP3 and MMP9 and, in turn, tight junction breakdown and BBB leakage. Ultimately, our data demonstrate that agonism of TREM2 by an activating antibody does not induce adverse cerebrovascular events associated with other amyloid-modifying therapies, further suggesting that agonization of TREM2 is a promising new immunotherapy for the treatment of late-onset AD.

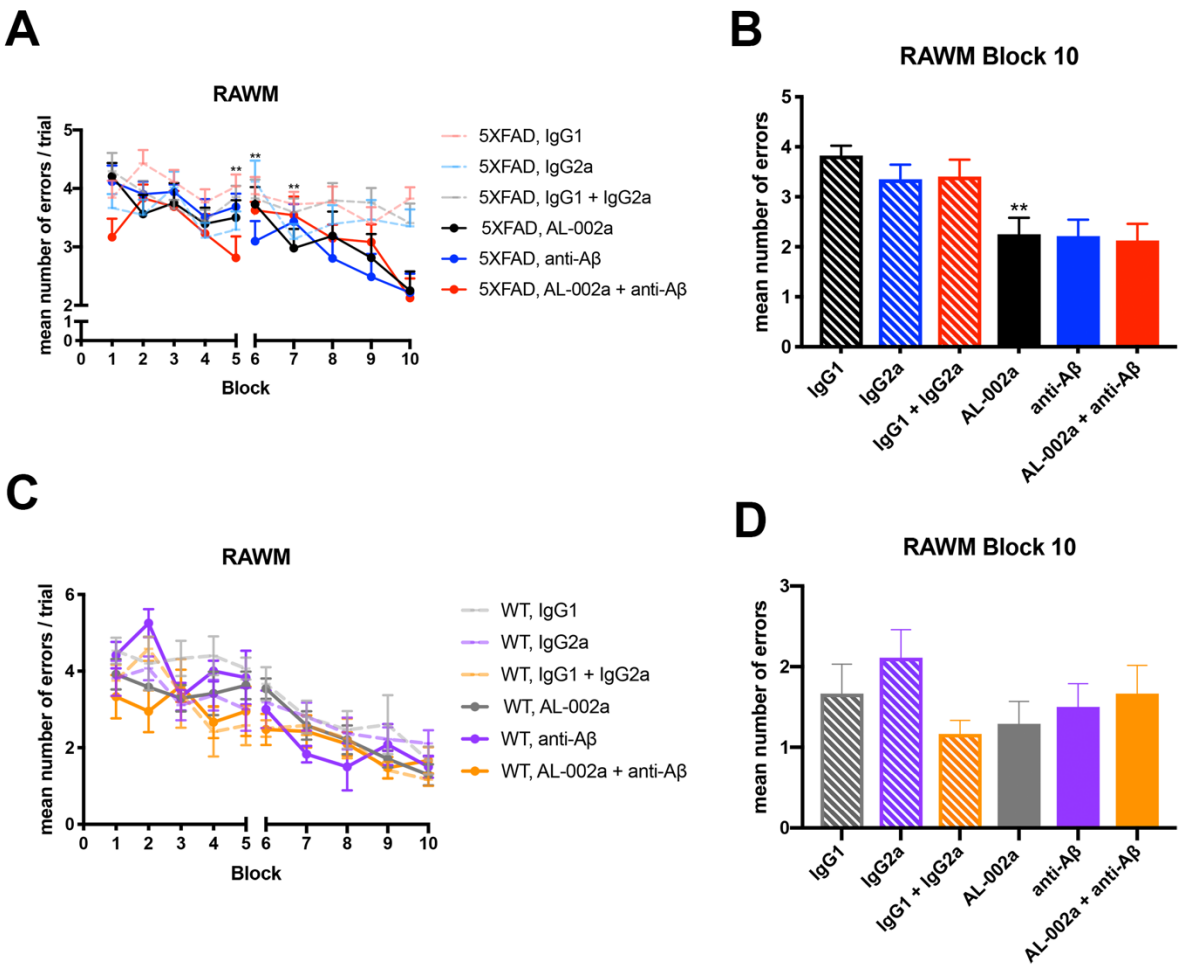

Figure 4.1: Systemic administration of AL-002a, anti-Aβ, and a combination of the two improves spatial learning and memory in 5XFAD mice, but fails to significantly effect cognition in wildtype mice. Panel A shows the radial-arm water maze data from 5XFAD mice. Blocks 1-5 are day 1, blocks 6-10 are day 2. Panel B shows a bar graph to illustrate the difference in the number of errors made for the final block of trials (block 10). Panel C shows the radial-arm water maze data from wildtype (WT) mice. Panel D shows a bar graph to illustrate the difference in the number of errors made for the final block of trials (block 10). Data

are represented as mean ± SEM. *p<0.05, **p<0.01, compared with 5XFAD injected with the relevant control antibody.

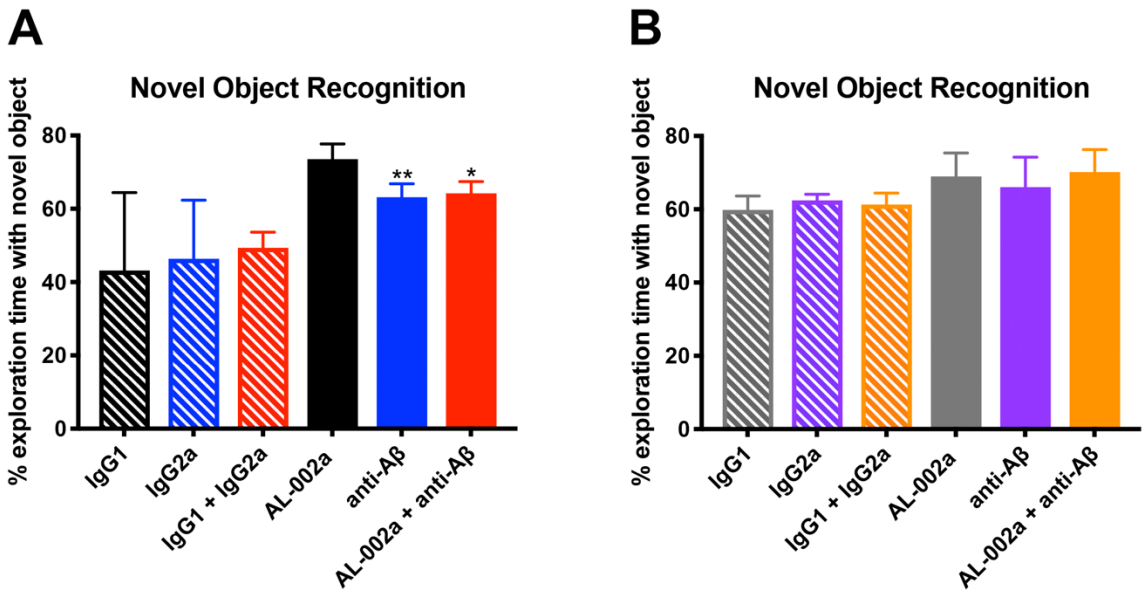

Figure 4.2: Systemic administration of AL-002a, anti-Aβ, and a combination of the two improves recognition memory in 5XFAD mice, but fails to significantly effect cognition in wildtype mice. Panel A shows the bar graph for the novel object recognition data from 5XFAD mice, where % exploration time with the novel object is shown. 50% exploration time would represent chance. Panel B shows the bar graph for the novel object recognition data from wildtype mice. Data are represented as mean ± SEM. *p<0.05, **p<0.01, compared with 5XFAD injected with the relevant control antibody.

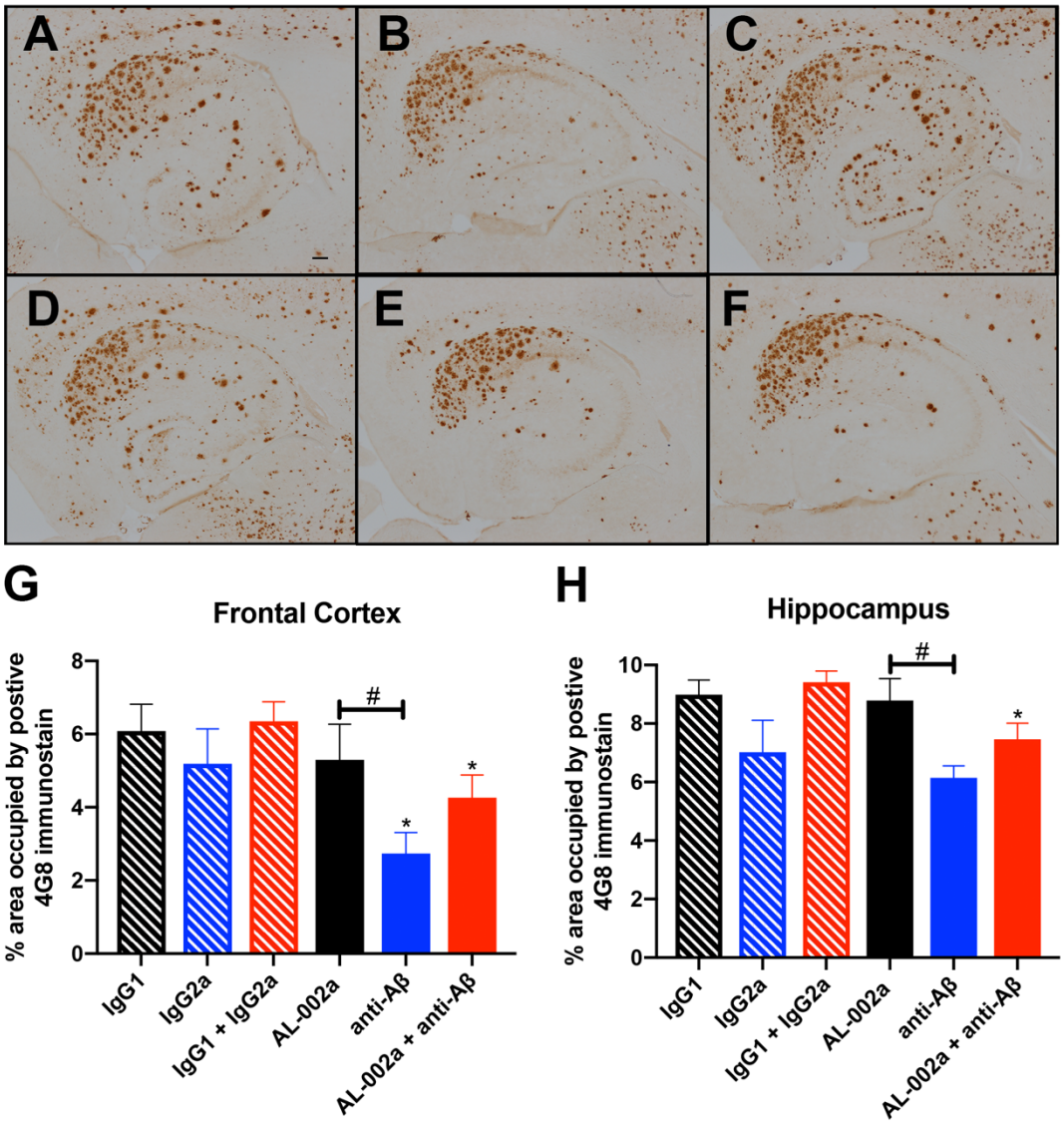

Figure 4.3: Systemic co-administration of AL-002a and anti-Aβ does not lead to additive reductions in Aβ. Representative images of Aβ staining in the hippocampus of 5XFAD mice injected with IgG1 (A), with IgG2a (B), with both IgG1 and IgG2a antibodies (C), AL-002a (D), with anti-Aβ (E), and with both AL-002a and anti-Aβ antibodies (F) are shown. Scale Bar: (A) 100 μM. Quantification of percentage positive immunostain in the frontal cortex (G) and (H) hippocampus.

*p<0.05, **p<0.01, compared with 5XFAD injected with the relevant control antibody.

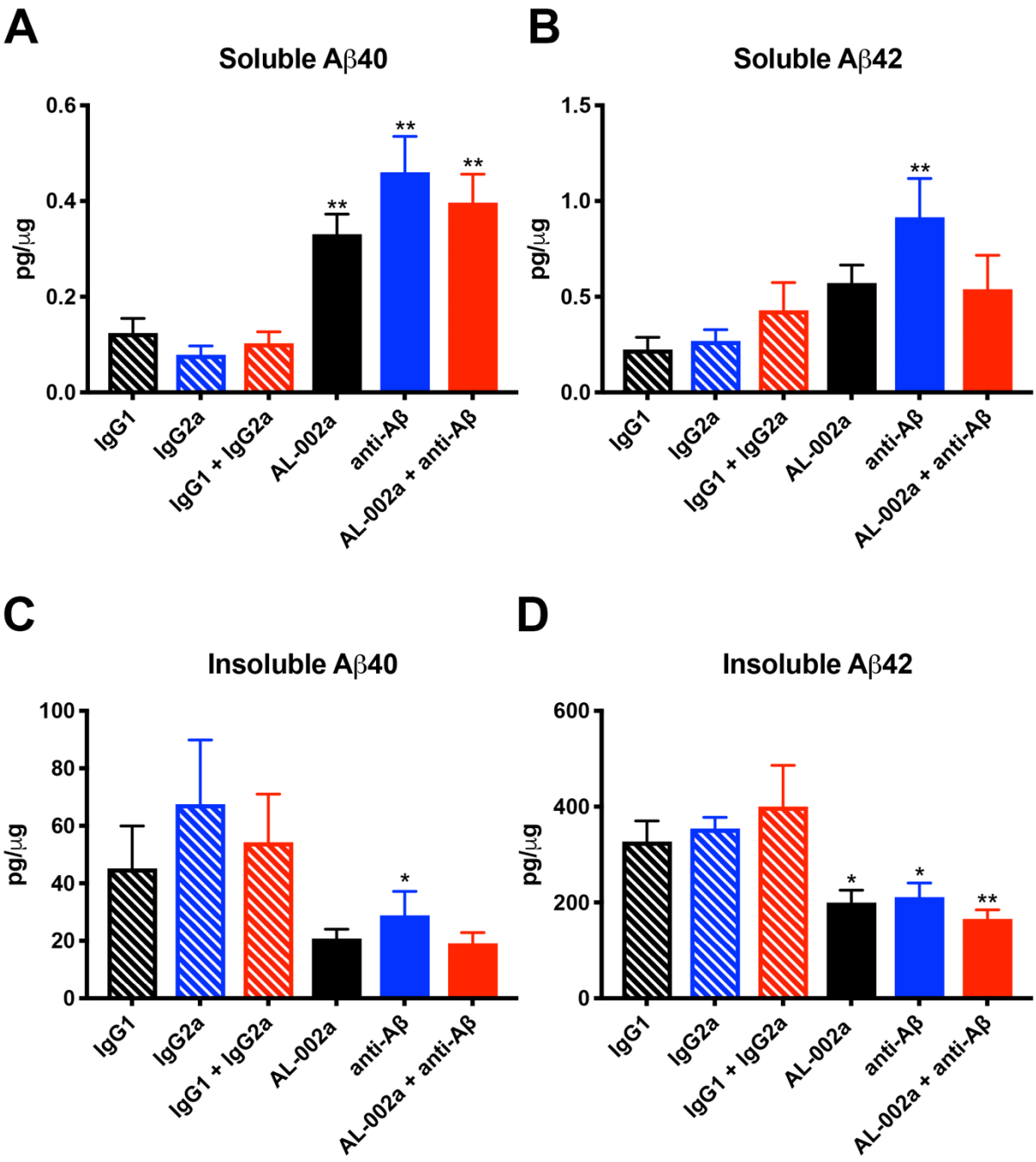

Figure 4.4: Biochemical quantification reveals systemic co-administration of AL-002a and anti-Aβ does not additively reduce soluble or insoluble Aβ species. Data are represented as mean ± SEM. *p<0.05, **p<0.01, compared with 5XFAD injected with the relevant control antibody.

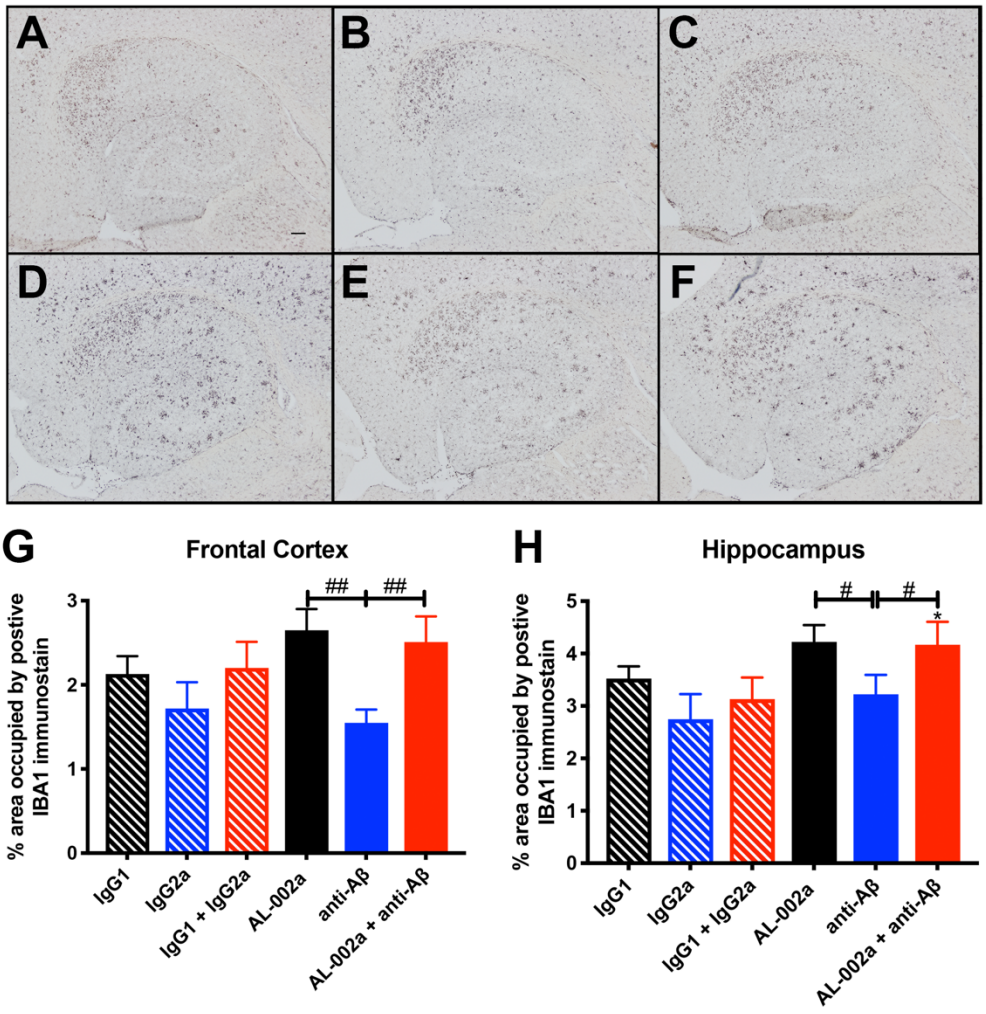

Figure 4.5: Systemic administration of AL-002a and a combination of AL-002a and anti-Aβ enhances microglial staining.

Representative images of IBA-1 staining in the hippocampus of 5XFAD mice injected with IgG1 (A), with IgG2a (B), with both IgG1 and IgG2a antibodies (C), AL-002a (D), with anti-Aβ (E), and with both AL-002a and anti-Aβ antibodies (F) are shown. Scale Bar: (A) 100 μM. Quantification of percentage positive immunostain in the frontal cortex (G) and hippocampus (H). *p<0.05, **p<0.01,

compared with 5XFAD injected with the relevant control antibody. #p<0.05, ##p<0.01, compared with 5XFAD injected with a different experimental antibody.

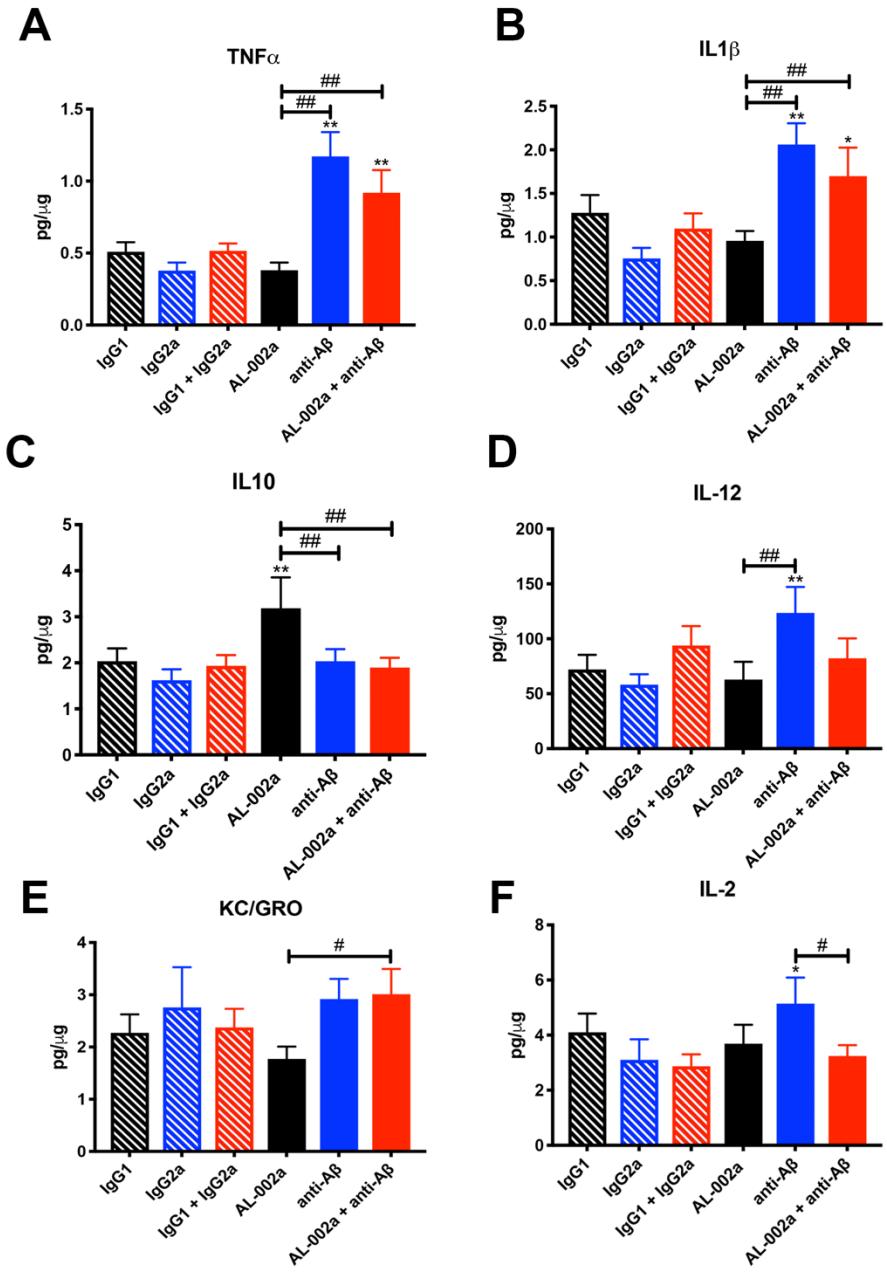

Figure 4.6: Pro-inflammatory cytokines whose expression were significantly influenced by antibody treatment. Data are represented as mean ± SEM. *p<0.05, **p<0.01, compared with 5XFAD injected with the relevant control antibody. #p<0.05, ##p<0.01, compared with 5XFAD injected with a different experimental antibody. It is worth noting that with respect to TNFα, the p value for

5XFAD mice treated with anti-Aβ compared to those treated with both AL-002a and anti-Aβ was 0.0533. With respect to KC/GRO, the p value for 5XFAD mice treated with AL002a compared to those treated with anti-Aβ was 0.0578.

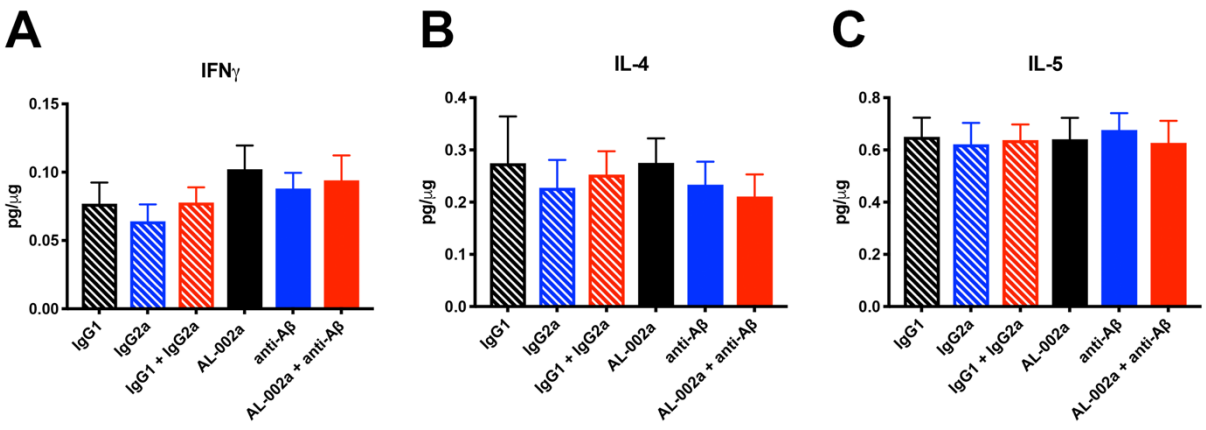

Figure 4.7: Pro-inflammatory cytokines whose expression was not significantly influenced by antibody treatment. Data are represented as mean ± SEM.

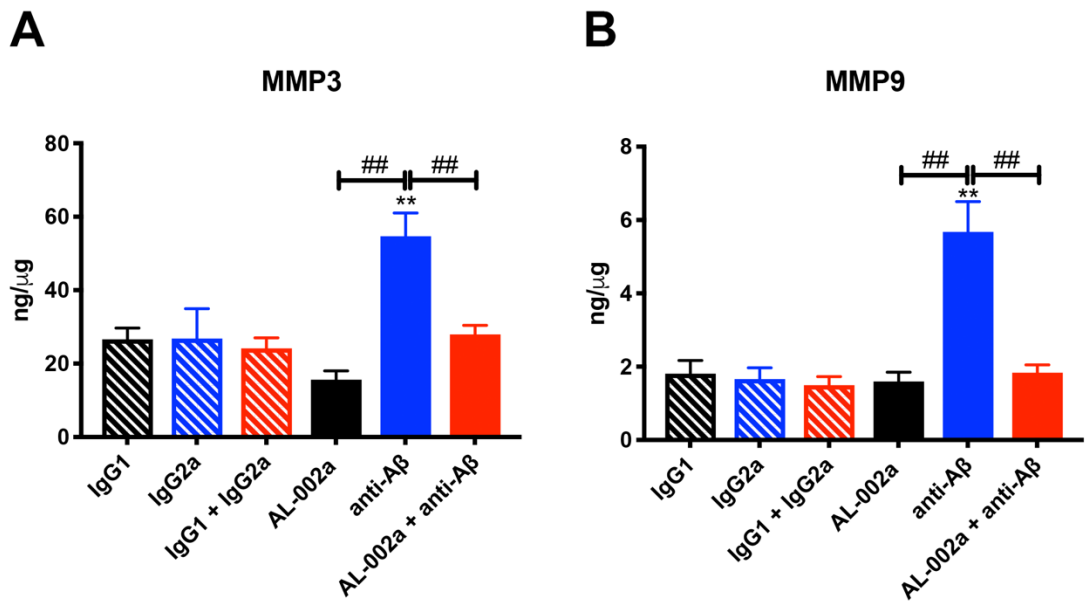

Figure 4.8: Biochemical quantification reveals that treatment with anti-Aβ increases MMP system markers. Data are represented as mean ± SEM. *p<0.05, **p<0.01, compared with 5XFAD injected with the relevant control antibody. #p<0.05, ##p<0.01, compared with 5XFAD injected with a different experimental antibody.

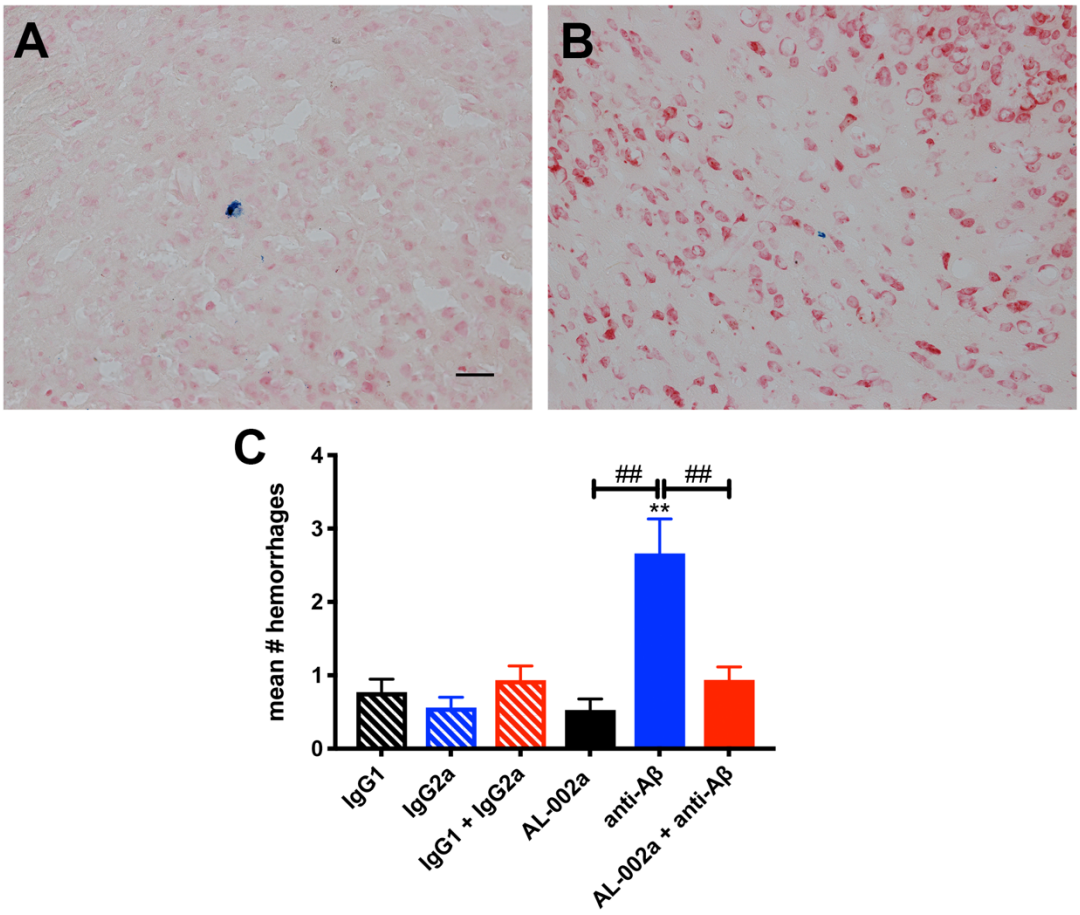

Figure 4.9: Treatment with anti-Aβ increases the incidence of Prussian blue detected microhemorrhages. Representative images of Prussian Blue staining are shown (A & B). Scale Bar: (A) 50 μM. (C) Quantification of the mean number of microhemorrhages per section. *p<0.05, **p<0.01, compared with 5XFAD injected with the relevant control antibody. #p<0.05, ##p<0.01, compared with 5XFAD injected with a different experimental antibody.

Chapter 5

Discussion

Microglia serve as the resident phagocytes of the brain where they utilize their highly motile processes to survey their environment for the presence of pathogens such as misfolded or aggregated proteins. In addition to inspecting their environment, ramified, or sometimes referred to as “resting,” microglia also provide neurotrophic factors that support tissue maintenance and simultaneously contribute to the protection and refinement of synapses [260-262]. Upon recognition of a pathogen microglia extend their processes to the injury site, later migrating to said site and initiating an immune response characterized by the secretion of numerous inflammatory mediators. It is, therefore, without question that microglia serve a number of crucial roles in the maintenance of brain homeostasis. However, in the context of neurodegeneration, inflammation is viewed as a double-edged sword given the actions of microglia have been deemed both neuroprotective and neurotoxic. Opposing opinions likely arise from the fact that acute inflammation protects against invading pathogens and promotes healing, whereas chronically sustained inflammation can induce serious damage to the host’s own tissue. Opposing views are more likely attributed to the fact that, depending on the disease stage and transgenic model, microglia exhibit different roles, thereby inducing different effects.

In the context of Alzheimer’s disease (AD) specifically, numerous studies have indicated that microglia recognize and surround amyloid plaques [263-266]. Furthermore, inefficient clearance of Aβ, one of the three hallmark pathologies of

AD, has been identified as a major pathogenic pathway in both early- and late-onset AD (EOAD and LOAD, respectively) [267, 268]. Studies have shown that Aβ deposition results in the activation of microglia and the subsequent production of cytokines and neurotoxins that, when chronically sustained, induce bystander damage to otherwise healthy neurons. Conversely, microglia have also been shown to express a variety of surface receptors that promote the clearance and phagocytosis of Aβ, and thereby restrict senile plaque formation [232, 269-271]. In addition to phagocytosing Aβ, studies have demonstrated that microglia secrete proteolytic enzymes (insulin-degrading enzyme (IDE), neprilysin, matrix metalloproteinase 9 (MMP9), and plasminogen) that degrade Aβ, which further suggests microglia serve neuroprotective roles in the AD brain [255, 272]. Support for the hypothesis that compromised microglial function contributes to AD pathogenesis comes from rare mutations in TREM2 that confer significantly increased risk for LOAD.

Triggering receptor expressed on myeloid cells-2 (TREM2) is highly expressed by microglia and has been shown to mediate phagocytic clearance of Aβ, amongst other pathogens. In 2013, two genome-wide association studies (GWAS) revealed that heterozygous expression of the TREM2 R47H and D87N variants were significantly associated with LOAD risk [154, 155]. To date, numerous studies have since replicated the association of these and other TREM2 variants with LOAD [156-161, 163-165]. LOAD-associated variants of TREM2 have been shown to impair the efficiency of TREM2 signaling, influence ligand affinity, and diminish phagocytic capacity. Studies have also assessed whether

partial or complete loss of TREM2 function contributes to Aβ deposition or Aβ -associated microglial activation and phagocytosis, and consistently show that TREM2 deficiency results in a strong reduction in Aβ-associated microgliosis. Ultimately, human genetics along with biochemical studies assessing the functional consequences of TREM2 variants agree that loss of TREM2 function is detrimental for the AD brain; Our data supports this conclusion. We have shown that agonization of TREM2 using an activating antibody, AL-002a, modulates the immune response by increasing gene expression levels of both pro- and anti-inflammatory cytokines and chemokines (discussed in detail in Chapter 2). Our data also demonstrate that systemic treatment with AL-002a significantly enhances the number of microglia clustered around congophillic amyloid plaques (discussed in detail in Chapter 2). Most importantly, our data demonstrate the efficacy of AL-002a in reducing amyloid deposition and subsequently improving cognition in the 5XFAD model of AD (discussed in detail in Chapter 2).

Data supporting the role for microglia in Aβ clearance is undoubtedly compelling. Yet, these data raise an interesting question: Why does Aβ continue to accumulate and drive the progression of AD pathology despite paralleled microglia recruitment in humans? Several possible explanations have been suggested, of which two will be discussed here. One possible explanation for this well-described phenomenon is that microglia simply become overwhelmed by enhanced amyloidogenic processing and are unable to clear Aβ at the same pace it is being generated. Another possible explanation is that, as AD pathology continues to progress, the phenotype of accumulating microglia changes resulting

in the loss of Aβ-clearing capabilities. Though numerous studies support both of these explanations, one in particular makes them cohesive. In 2008, Hickman et al. demonstrated that as APP/PS1 mice age their microglia become dysfunctional [267]. In this study, microglia that exhibited a significant decrease in their expression of homeostatic Aβ-binding receptors and Aβ degrading enzymes were deemed dysfunctional [267]. Interestingly, these dysfunctional microglia were found to retain their ability to produce pro-inflammatory cytokines, which have been shown to down-regulate expression of Aβ phagocytic receptors on microglia [267].

This finding brings us back to the differential roles of acute and chronically sustained neuroinflammation; When microglia recognize a pathogen under homeostatic conditions the subsequent response quickly resolves pathology, providing an immediate benefit to the surrounding tissue. By contrast, in AD, the ongoing generation of pathogenic Aβ species and the positive feedback loops between neuroinflammation and amyloidogenic processing prevent cessation of inflammation [271]. Chronically sustained inflammation, in turn, results in additional accumulation of Aβ (likely due to the down-regulation of Aβ phagocytic receptors by pro-inflammatory cytokines) and neuronal debris (likely intensified by bystander damage of otherwise healthy neurons) which in turn may further activate factors that maintain a chronic, non-resolving inflammatory response [267]. Thus, it is hypothesized that the sustained exposure to Aβ and pro-inflammatory cytokines and chemokines is responsible for the persistent functional impairment of microglial cells observed near sites of amyloid pathology [273, 274]. Additional support for this hypothesis arises from studies of the autophagy protein Beclin-1.

Beclin-1 is downregulated in in brains of AD patients and its reduction is said to interfere with efficient phagocytosis due to deficient CD36 and TREM2 receptor recycling [275].

Importantly, microglia are not the only immune cells secreting pro-inflammatory cytokines. Rather, several studies have shown that Aβ deposition induces the recruitment of circulating monocytes to the brain parenchyma [228-231]. Bone-marrow-derived (BMD) macrophages, which originate essentially from infiltrated pro-inflammatory monocytes, exhibit elevated levels of proteins necessary for antigen presentation and are, therefore, proposed to be more efficient at preventing or eliminating Aβ [232-234]. The precise contribution of BMD macrophages in AD remains unclear to date, though several studies have implicated a spatial association between BMD macrophages and senile amyloid plaques [232].

In addition to peripheral immune cells, components of the complement cascade can aid in exacerbating the immune response. The complement cascade is a well-characterized part of the innate immune system that promotes inflammation to enhance the ability of phagocytes to clear pathogens [276]. In the central nervous system (CNS), neurons, astrocytes, oligodendrocytes, and microglia express complement receptors [276]. Moreover, microglia and astrocytes can synthesize complement components and this synthesis can be modulated by various pro-inflammatory cytokines as well as the binding of Aβ to toll-like receptors (TLRs) on the surface of microglia [277-281]. Thus, in AD, the accumulation of Aβ induces complement activation which can be further

exacerbated by a disturbed balance between complement activators and regulators, which is also seen in AD [79, 282-284]. The latter becomes increasingly problematic throughout AD progression considering there is a naturally limited neuronal expression of complement regulators, which likely underlies the susceptibility of neurons to complement activation [276].

Astrocytes are yet another mediator of neuroinflammation in AD. In post-mortem human tissue as well as AD mouse models both activated microglia and hypertrophic reactive astrocytes accumulate around senile plaques [285, 286]. Similar to microglia, astrocytes become activated, or reactive, in response to a variety of CNS pathologies. Upon exposure to a pathogen such as Aβ, astrocytes upregulate their expression of GFAP, their cellular processes hypertrophy, and they release cytokines, interleukins, nitric oxide, and other potentially neurotoxic molecules [287]. The work of Ben Barres and colleagues recently used transcriptome analysis to identify two distinct reactive states of astrocytes: A1 and A2. Akin to the polarization of activated macrophages to a pro-inflammatory M1 or anti-inflammatory M2 phenotype, A1 astrocytes upregulate a number of proinflammatory genes (e.g., complement cascade genes such as those encoding C1q) that have been previously shown to be destructive to synapses. Conversely, A2 astrocytes upregulate neurotrophic factors which promote the survival and growth of neurons [288]. Although the reactive profiles of astrocytes are only beginning to be characterized, it is widely accepted that different types of reactive astrocytes are induced by different types of injury.

In the context of AD, in addition to other human neurodegenerative diseases, A1 astrocytes are the most abundant [288]. Interestingly, the work of Ben Barres and colleagues has also recently demonstrated that activated, pro-inflammatory microglia are responsible for the induction of this neurotoxic A1 phenotype [289]. As previously discussed, microglia can secrete a variety of cytokines including IL-1α, TNFα, and C1q. Ben Barres and colleagues found that secretion of the aforementioned cytokines is both necessary and sufficient to induce the A1 reactive astrocyte profile and that A1 astrocytes fail to promote neuronal survival, outgrowth, synaptogenesis, and phagocytosis, instead gaining neurotoxic functions that ultimately induce the death of neurons and mature oligodendrocytes [289]. This potentially neurotoxic role of a subset of astrocytes is further supported by a study in which AAV-driven suppression of calcineurin/nuclear factor of activated T cells (NFAT) signaling reduced astrogliosis, decreased Aβ deposition, and improved cognition in the APP/PS1 model of AD [290].

Taken together, these data suggest that the deposition of Aβ activates microglia, inducing an acute neuroinflammatory response designed to clear Aβ but that, over time, microglia become overwhelmed by the accelerated pathogenic production of Aβ and simply cannot clear it at the same pace it is being generated. Data further suggest this inability of microglia to clear Aβ arises due to chronically sustained inflammation, which does not result solely from microglia. Rather, binding of Aβ to TLRs on microglia induces the complement cascade, in turn, producing C1q and further exacerbating the production and secretion of

proinflammatory mediators such as IL-1α and TNFα which, together with C1q, induce the A1 reactive astrocyte phenotype. Studies suggest the consistent production and secretion of proinflammatory mediators ultimately induces the down-regulation of Aβ phagocytic receptors on microglia.

Granted, chronically sustained neuroinflammation is also problematic from the standpoint of vascular integrity. Expression of matrix metalloproteinases 3 and 9 (MMP3 and MMP9, respectively) can be influenced by the presence of proinflammatory cytokines. Matrix metalloproteinases (MMPs) are a family of enzymes collectively responsible for extracellular matrix degradation and turnover. MMP9 belongs to the gelatinase family of MMPs and can therefore degrade gelatin, cytokines, and even Aβ [254, 255]. Given its variety of substrates, MMP9's expression is tightly regulated by a number of cytokines, growth factors, and other proteins. In particular, MMP9 expression is induced by the proinflammatory cytokines TNFα and IL-1β [256, 257]. Due to the necessity of its tight regulation, MMP9 is secreted as a zymogen (proMMP9) that requires cleavage by MMP3, the expression of which is also induced by pro-inflammatory cytokines, to become active [258]. Interestingly, recent evidence suggests that vascular amyloid contributes to enhanced MMP9 expression [254]. Isolated rat brain microvessels exposed to increasing concentrations of A$\beta_{1\text{-}40}$, the Aβ species associated with cerebral amyloid angiopathy (CAA), exhibited increased MMP9 expression and decreased expression of the tight junction proteins claudin-1 and claudin-5 [291]. Similarly, microvessels isolated from Tg2576 AD transgenic mice displayed increased MMP9, decreased claudin-1 and claudin-5, and increased permeability

[292]. Several additional studies have further implicated MMP9 in tight junction degradation, blood-brain-barrier (BBB) breakdown, and subsequent disruption of the neurovascular unit. These implications are ultimately supported by the presence of MMP9 in hemorrhagic areas [254].

The neurovascular unit is comprised of neurons, astrocytes, pericytes, endothelial cells, oligodendrocytes, and microglia (Figure 5.1). It functions to regulate local cerebral blood flow (CBF), BBB permeability, and neurovascular remodeling [293, 294]. The roles of endothelial cells and astrocytes in maintaining the integrity of the neurovascular unit are of particular importance here. Endothelial cells line the cerebral vasculature forming the BBB, tight junctions of which express specific transporters and thereby limit the passage of substrates between cells [295]. Astrocytes aid in supporting and protecting neurons by maintaining homeostatic concentrations of specific ions and neurotransmitters and also regulate CBF by directly interacting with endothelial cells through their specialized end-feet processes [295]. The cerebrovasculature of the brain is almost completely ensheathed by astrocytic processes called astrocytic end-feet. The astrocytic end-foot is a specialized unit that functions to maintain ionic and osmotic homeostasis of the brain and does so through the expression of specific channels [296, 297]. End-feet enriched channels include aquaporin 4 (AQP4), the inwardly rectifying K+ channel Kir4.1, and the Ca2+-dependent K+ channel MaxiK, or BK [298, 299]. The astrocytic end-foot is anchored to the vascular basement membrane via the α-β dystroglycan complex [300, 301].

An essential function of the astrocytes surrounding neurons of the neurovascular unit is to maintain the neuronal resting membrane potential (RMP) by controlling the extracellular potassium concentration, a process referred to as potassium siphoning or buffering [302]. Following an action potential, astrocytes take up excess K^+ ions via their Kir4.1 channels and move these ions through their connexin 43-containing gap junctions into the circulation using the astrocytic end-feet [303, 304]. Recall that ionic movement across cell membranes is commonly coupled to the movement of water and the maintenance of osmotic equilibrium and that most water movement into and out of the cells occurs via water channels known as aquaporins [305]. The AQP4 channel is expressed by astrocytes in the neurovascular unit and is highly polarized to the end-foot membrane [306]. Notably, dislocalization of AQP4 from the astrocytic end-feet is associated with potassium clearance deficits in transgenic mice [306]. Studies also suggest that astroglial-mediated interstitial fluid bulk flow through AQP4 facilitates the transport of Aβ across the BBB into the blood, ultimately clearing it from the brain [307, 308]. Thus, AQP4 appears to play two equally important roles. Importantly, the Kir4.1, AQP4, and BK channels share a common anchoring protein known as Dp71 which complexes with α-syntrophin to form the end-foot anchoring complex [306]. MMP9 has been shown to be a major degrading enzyme of the dystroglycans [309], suggesting that activation of MMP9 degrades the dystrophin-dystroglycan complex anchoring the end-foot to the basement membrane of the vasculature. This degradation in turn is can lead to dislocalization of AQP4, Kir4.1 and BK from the vasculature, thereby impairing potassium homeostasis and neurovascular

coupling [306, 310]. Thus, chronic secretion of pro-inflammatory cytokines, in particular TNFα and IL-1β, not only induces the down-regulation of Aβ phagocytic receptors on microglia, but enhances the expression of MMP9 which can negatively impact the vasculature and simultaneously induce bystander damage to otherwise healthy neurons.

The work presented in chapters 3 and 4 demonstrates that neither acute nor systemic co-administration of the anti-Aβ and AL-002a antibodies additively reduces Aβ deposition. However, it also shows that AL-002a has similar efficacy as an N-terminal targeted anti-Aβ antibody in the reducing Aβ deposition when administered intracranially and preventing the additional deposition of Aβ when administered systemically. Notably, treatment with the anti-Aβ antibody was shown to significantly increase the incidence of microhemorrhage whereas reduction of Aβ by AL-002a was shown to occur in the absence of cerebrovascular pathology. The absence of cerebrovascular pathology following treatment with AL-002a, but not the anti-Aβ antibody, is likely due to the observed differences in immune modulation and MMP9 expression.

Biochemical quantification of a number of cytokines revealed that treatment with AL-002a significantly increases levels of the anti-inflammatory cytokine IL-10, whereas treatment with the anti-Aβ antibody significantly increases levels of TNFα, IL-1β, IL-12, IL-6, IL-2, and KC/GRO (CXCL1), all of which are considered to be pro-inflammatory. In addition to discrepancies in immune modulation, our data demonstrate that treatment with the anti-Aβ antibody, but not AL-002a, induces increased expression of MMP3 and MMP9. Our data thereby suggest AL-002a and

the anti-Aβ antibody function differently to reduce Aβ deposition in the brains of 5XFAD mice (Figure 2). It is likely that increased levels of the proinflammatory cytokines TNFα and IL-1β following treatment with the anti-Aβ antibody are directly responsible for the observed upregulation of MMP3 and MMP9 and subsequent increased incidence of microhemorrhage. Our data, therefore, have important implications for AD clinical trials.

Despite significant mouse model data demonstrating both pathological and cognitive efficacy of anti-Aβ immunotherapy, clinical trials continue to fail to meet primary endpoints for efficacy. Moreover, a number of trials reported occurrences of cerebrovascular adverse events characterized by treatment-related abnormalities on brain imaging. Amyloid related imaging abnormalities (ARIA) were first identified in the Bapineuzumab trial and have since been verified by a number of subsequent anti-Aβ immunotherapy trials [112-114]. ARIA come in two flavors: 1) ARIA-E, thought to represent vasogenic edema, and 2) ARIA-H, thought to represent microhemorrhages.

ARIA-E is observed as an increased, hyperintense MR signal on FLAIR sequences [116] and is typically a transient phenomenon. ARIA-E is said to be transient due to its reversible nature; It resolves either spontaneously following the cessation of anti-Aβ immunotherapy treatment or with steroid treatment [116]. On a cellular level, ARIA-E is hypothesized to represent increased extracellular fluid volume that arises due to the increased permeability of capillary endothelial cells to serum proteins [116]. Granted, given there is no histopathological correlate for ARIA-E, it is difficult to be certain that ARIA-E is in fact related to underlying

vasogenic edema. Notably, CAA is another condition presenting neuroimaging features similar to ARIA associated with anti-Aβ immunotherapy [116, 311, 312]. CAA related inflammation is hypothesized to arise from an inflammatory response to the vascular amyloid deposits. Following its resolution either spontaneously or with steroid treatment, CAA imaging findings also reverse [116]. ARIA-E and CAA also have a shared association with ApoE4 carrier status [313]; ApoE4 carriers have been shown to exhibit increased vascular amyloid deposition, and the Phase 2 Bapineuzumab trial revealed ApoE4+ participants had a significantly increased incidence of ARIA-E [113]. Thus, there is a likely association of the inflammatory response to vascular amyloid and the incidence of ARIA-E. Interestingly, treatment with both the anti-Aβ and AL-002a antibodies, as well as a combination of the two, was shown to increase soluble $A\beta_{1\text{-}40}$ levels, the Aβ species comprising vascular amyloid in CAA (discussed in detail in chapter 4). It is possible that treatment with these antibodies results in the disaggregation of Aβ oligomers and the restoration of their solubility [120], which may augment Aβ efflux from the brain through perivascular drainage pathways or via low-density lipoprotein receptor related protein-1 (LRP1) [242, 243]. However, this could potentially contribute to ARIA-E considering the mobilization of Aβ to perivascular drainage pathways that are impaired could induce transient paradoxical increases in vascular amyloid deposition following anti-Aβ immunotherapy [114]. In fact, this concept has been demonstrated in a number of human neuropathological studies [42-44]. It will, therefore, be important to assess the presence of ARIA-E in future studies with AL-002a. Granted, given that treatment with AL-002a did not induce

microhemorrhages, we remain hopeful that FLAIR imaging will show the absence of ARIA-E following AL-002a treatment.

ARIA-H manifests as a low-intensity signal on T2* MRI or susceptibility-weighted imaging (SWI) and is thought to represent iron deposits indicative of a small leakage of blood from a vessel into the adjacent brain parenchyma (microhemorrhage) or subarachnoid space (superficial siderosis) [112]. In AD, microhemorrhages are attributed to leakage of blood from damaged vessels, particularly those with enhanced amyloid deposition (i.e. CAA) [314]. The aforementioned inflammatory response to vascular amyloid is hypothesized to weaken the vessel wall, increasing the risk of hemorrhagic events into the adjacent parenchyma and forming a microhemorrhage [116]. It should be noted that the prevalence of microhemorrhage is significantly increased in individuals with cardiovascular risk factors [315] and that the greater number of microhemorrhages at baseline confers greater risk of subsequent microhemorrhages [316].

To date, there is limited information regarding the relationship between ARIA-E and ARIA-H, however, their relation to dose in the bapineuzumab trials suggests ARIA may arise due to enhanced clearance of parenchymal amyloid from the brain parenchyma into the vasculature [112, 113]. Hypotheses suggest the rapid movement of amyloid from the parenchyma into the perivascular space creates a drainage backup resulting in excess fluid shifts and vasogenic edema and that extraction of amyloid from the vasculature results in enhanced permeability and fragility of brain capillaries [116]. Assuming vessel wall integrity is sufficiently compromised, this proposed mechanism could explain the increased

incidence of microhemorrhages following the administration of amyloid-modifying therapies.

Notably, cerebrovascular adverse events have not only been problematic for passive immunization strategies, but active immunization strategies as well. In 1999, Schenk and colleagues demonstrated that active peripheral immunization with the full-length $A\beta_{1-42}$ peptide led to the prevention of plaque formation and the removal of existing plaques in a transgenic mouse model [98]. In 2000, Morgan et al. verified that the removal of existing plaques resulted in enhanced cognition [100]. Together, these studies inspired the first clinical trial of $A\beta$ immunization in Alzheimer's disease. This trial involved 80 patients with mild to moderate AD, 64 of which received active immunization with synthetic $A\beta_{1-42}$ (AN1792). Though the AN1792 trial was ultimately stopped due to 6% of participants developing acute meningoencephalitis [104], post-mortem studies from AN1792 participants confirmed that plaque removal occurred in those that received AN1792 [42, 43]. However, this plaque removal was found to have little to no effect on cognitive outcome measures [42, 43]. Interestingly, a consistent feature of the published post-mortem AN1792 cases was the persistence of vascular amyloid despite the reduction in parenchymal amyloid [44].

As stated, our data show the AL-002a and anti-$A\beta$ antibody modulate the immune response differently in order to reduce $A\beta$ deposition in the brains of 5XFAD mice. It is likely that increased levels of the proinflammatory cytokines $TNF\alpha$ and IL-1β following treatment with the anti-$A\beta$ antibody are directly responsible for the observed upregulation of MMP3 and MMP9 and subsequent

increased incidence of microhemorrhage. An in vitro study using BV2 cells treated with either an anti-Aβ IgG-Aβ or anti-tau IgG-tau immune complex demonstrated increased MMP3 and MMP9, suggesting that activation of MMP9 requires the Fcγ receptor, the surface receptor activated by the anti-Aβ antibody [259]. Increased levels of CXCL1 following treatment with the anti-Aβ antibody, but not AL-002a, suggests enhanced infiltration of peripheral immune cells which may further exacerbate levels of pro-inflammatory cytokines with little benefit to the AD brain. Conversely, the absence of cerebrovascular pathology in the 5XFAD mice treated with AL-002a is likely due to increased levels of IL-10. As discussed previously, IL-10 inhibits the production of proinflammatory cytokines, thereby preventing the production of MMP3 and MMP9 and, in turn, tight junction breakdown and BBB leakage. Thus, activation of the microglial Fcγ receptor results in activation of MMP9, the expression of which is further activated by the chronic upregulation of TNFα and IL-1β, whereas activation of the microglial TREM2 receptor does not. The lack of cerebrovascular pathology following treatment with AL-002a demonstrates that agonizing TREM2 may be effective for the treatment of LOAD, and highlights the fact that, although treatment with AL-002a has implications for Aβ deposition, AL-002a does not directly target Aβ. Rather, AL-002a modulates the immune response in a way that appears to be beneficial and may have implications for other AD-associated pathologies. That being said, there are several limitations to our studies that are worth noting.

Firstly, some of the data presented here appears contradictory. Immunohistochemistry data presented in chapter 2 demonstrates reductions in Aβ

following treatment with AL-002a, however, follow-up studies presented in chapters 3 and 4 do not reproduce these findings. Instead data presented in chapter 3 demonstrates that acute treatment with AL-002a results in trending, but non-significant, reductions in Aβ whereas data presented in chapter 4 shows no reductions in Aβ following chronic treatment with AL-002a. These discrepancies in Aβ clearance may be attributable to the fact that two different anti-Aβ antibodies were used in these studies; immunohistochemistry data in chapter 2 was generated using an anti-Aβ antibody that binds the N terminus (amino acids 1-16) of the Aβ peptide, whereas data in chapters 3 and 4 were generated using the 4G8 antibody, which binds the middle portion of the Aβ peptide (amino acids 17-24). Given that the anti-Aβ antibody being injected binds the N terminus of the Aβ peptide it was necessary to use 4G8 in order to avoid potential antigen masking, however, this may have also contributed to the discrepancies in Aβ clearance observed between datasets.

The fact that acute administration of AL-002a showed trending, but non-significant, reductions in Aβ (chapter 3) while chronic administration of AL-002a failed to show any reductions in Aβ (chapter 4) is not trivial. These differences are likely due to the fact that in the acute administration study, AL-002a was directly injected into the brain whereas AL-002a was required to cross the BBB in the systemic study. Given that, on average, only 0.1% of systemically injected antibodies successfully cross the BBB this could represent a significant clinical challenge moving forward. It would be interesting to repeat these studies using

focused ultrasound, a non-invasive technology that enables reversible opening of the BBB to enhance the delivery of therapeutics.

Additionally, qPCR data presented in chapter 2 demonstrates that both intracranial (acute) and intraperitoneal (systemic) administration of AL-002a upregulates pro- and anti-inflammatory cytokines, and among those increased are TNFα and IL1β. This in and of itself is interesting given that anti-Aβ antibodies have only been shown to increase pro-inflammatory gene expression and, in some cases, decrease the anti-inflammatory gene expression. However, increases in levels of TNFα and IL1β were not recapitulated following systemic administration of AL-002a in a follow-up study (chapter 4). Rather, data presented in chapter 4 showed decreased levels of the aforementioned cytokines following treatment with AL-002a. This discrepancy is likely due to the fact that data presented in chapter 2 is indicative of gene expression levels whereas that from chapter 4 is indicative of protein expression levels and levels of mRNA transcripts alone are not sufficient to predict protein levels (Reviewed in [317]).

Furthermore, it is important to recognize that Alzheimer's disease effects the brain in a sexually dimorphic manner, adding a layer of complexity to the design of AD therapeutics. 5XFAD mice have been shown to exhibit sex-dependent differences in amyloid deposition [61, 217]. Thus, in order to avoid biasing our data, our study only used male mice. Considering in humans the incidence of Alzheimer's disease is higher in women than in men, these studies need to be repeated in female transgenic mice. As discussed, vascular amyloid load has been shown to affect the incidence of cerebrovascular adverse events. Unfortunately,

the CAA load in the 5XFAD model of AD is highly variable, making data interpretation somewhat unreliable. Repeating these studies in transgenic mice with vascular amyloid deposition is crucial for understanding the viability of TREM2 agonization as a therapeutic strategy for individuals with cardiovascular risk factors. By the same token, repeating these studies in amyloid-depositing transgenic mice crossed with mice expressing different humanized ApoE isoforms will also be critical in understanding the viability of AL-002a as a "one-size-fits-all" immunotherapy. Determining the effects of AL-002a treatment on the integrity of astrocytic end-feet will also be important for confirming that AL-002a does not negatively impact the vasculature. Finally, several studies have shown that TREM2 ameliorates neuronal tau pathology via the suppression of the microglial pro-inflammatory response, thereby implicating a neuroprotective role for TREM2 against tau pathology [318, 319]. Though data from previous anti-Aβ immunotherapy studies in humans suggest tau is largely unaffected by anti-Aβ antibodies, agonization of TREM2 using AL-002a may yield different results due to the altered microglial immune phenotype presented here. It will, therefore, be important to repeat these studies in a transgenic tau model to determine the effects of AL-002a treatment on tau pathology.

In conclusion, irrespective of these inherent limitations, our data advocate that agonism of TREM2 is a viable therapeutic strategy for the treatment of LOAD that lacks the limitation of cerebrovascular adverse events normally observed with existing anti-Aβ immunotherapies (Figure 5.2).

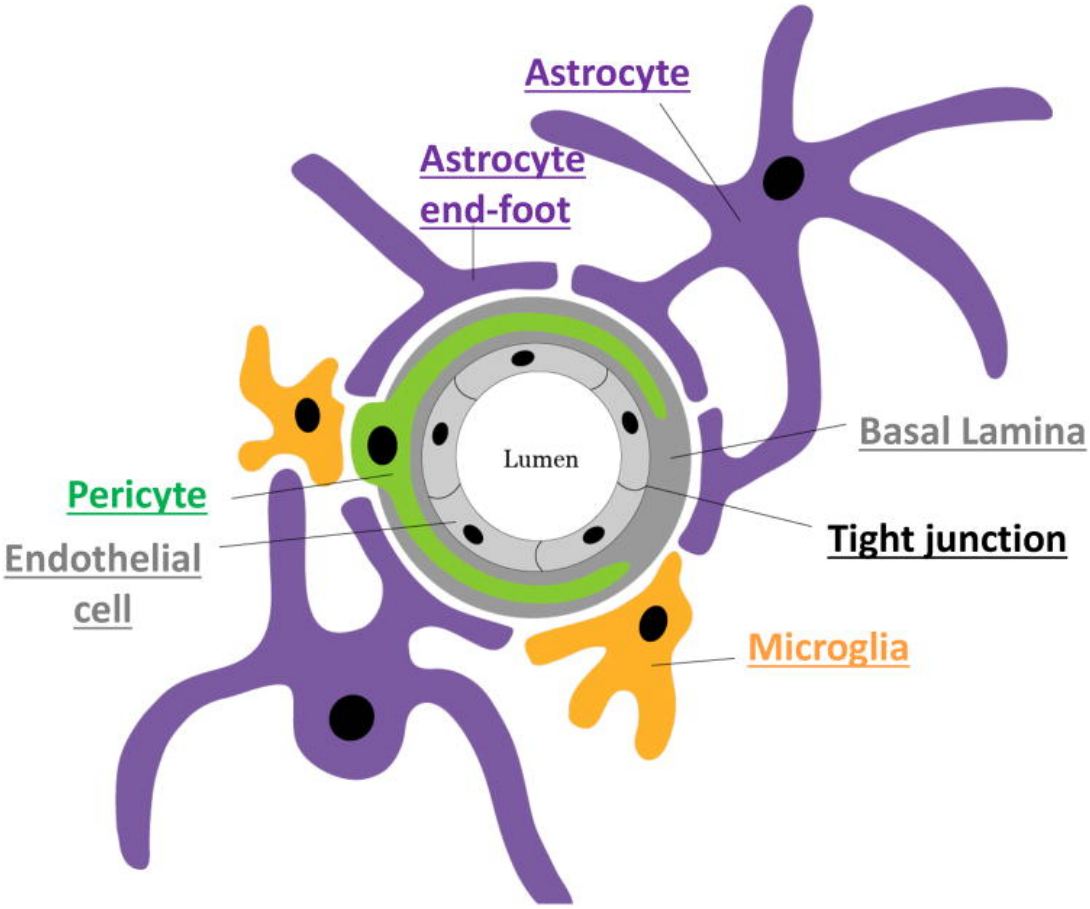

Figure 5.1: Schematic showing the arrangement of cells of the neurovascular unit.

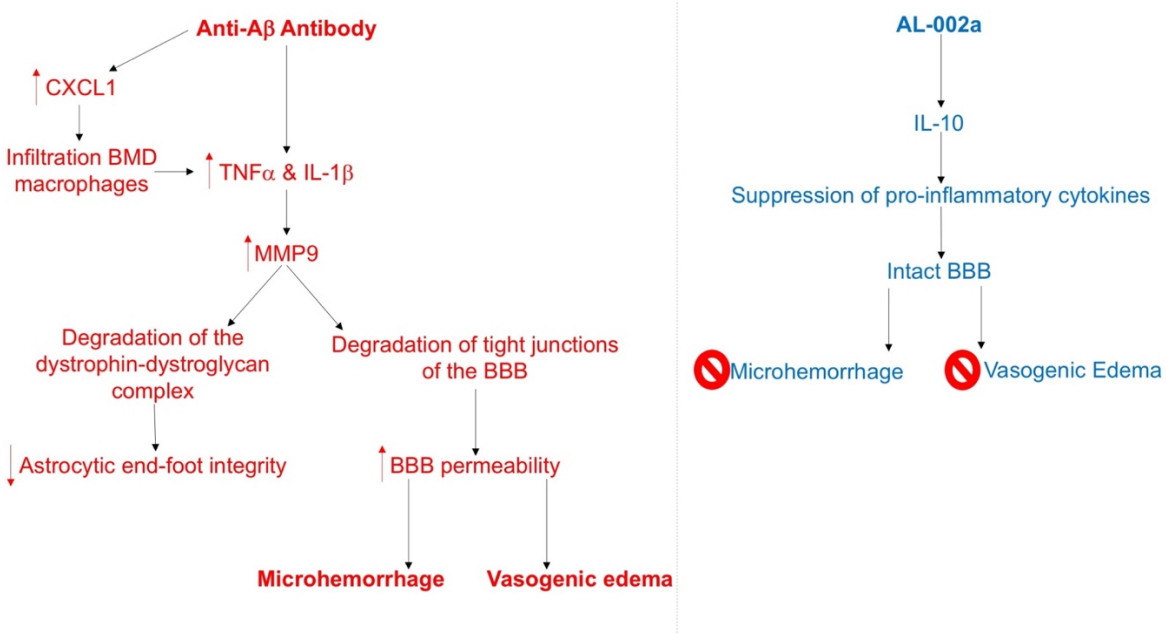

Figure 5.2: The proposed mechanisms by which the anti-Aβ antibody, but not AL-002a, induces cerebrovascular adverse events.

References

1. Alzheimer's, A., *2016 Alzheimer's disease facts and figures.* Alzheimers Dement, 2016. **12**(4): p. 459-509.
2. Alzheimer, A., et al., *An English translation of Alzheimer's 1907 paper, "Uber eine eigenartige Erkankung der Hirnrinde".* Clin Anat, 1995. **8**(6): p. 429-31.
3. Braak, H. and E. Braak, *Staging of Alzheimer's disease-related neurofibrillary changes.* Neurobiol Aging, 1995. **16**(3): p. 271-8; discussion 278-84.
4. Murphy, M.P. and H. LeVine, 3rd, *Alzheimer's disease and the amyloid-beta peptide.* J Alzheimers Dis, 2010. **19**(1): p. 311-23.
5. Verbeek, M.M., et al., *Cerebrospinal fluid amyloid beta(40) is decreased in cerebral amyloid angiopathy.* Ann Neurol, 2009. **66**(2): p. 245-9.
6. Brion, J.P., *Neurofibrillary tangles and Alzheimer's disease.* Eur Neurol, 1998. **40**(3): p. 130-40.
7. Guo, T., W. Noble, and D.P. Hanger, *Roles of tau protein in health and disease.* Acta Neuropathol, 2017. **133**(5): p. 665-704.
8. Braak, H. and E. Braak, *Demonstration of amyloid deposits and neurofibrillary changes in whole brain sections.* Brain Pathol, 1991. **1**(3): p. 213-6.
9. Braak, H. and E. Braak, *Neuropathological stageing of Alzheimer-related changes.* Acta Neuropathol, 1991. **82**(4): p. 239-59.
10. Thal, D.R., et al., *Phases of A beta-deposition in the human brain and its relevance for the development of AD.* Neurology, 2002. **58**(12): p. 1791-800.
11. Nelson, P.T., H. Braak, and W.R. Markesbery, *Neuropathology and cognitive impairment in Alzheimer disease: a complex but coherent relationship.* J Neuropathol Exp Neurol, 2009. **68**(1): p. 1-14.
12. Hardy, J.A. and G.A. Higgins, *Alzheimer's disease: the amyloid cascade hypothesis.* Science, 1992. **256**(5054): p. 184-5.
13. Hardy, J. and D.J. Selkoe, *The amyloid hypothesis of Alzheimer's disease: progress and problems on the road to therapeutics.* Science, 2002. **297**(5580): p. 353-6.
14. Marttinen, M., et al., *Molecular Mechanisms of Synaptotoxicity and Neuroinflammation in Alzheimer's Disease.* Front Neurosci, 2018. **12**: p. 963.
15. Kim, J., J.M. Basak, and D.M. Holtzman, *The role of apolipoprotein E in Alzheimer's disease.* Neuron, 2009. **63**(3): p. 287-303.
16. Mahley, R.W. and Y. Huang, *Apolipoprotein (apo) E4 and Alzheimer's disease: unique conformational and biophysical properties of apoE4 can modulate neuropathology.* Acta Neurol Scand Suppl, 2006. **185**: p. 8-14.
17. Corder, E.H., et al., *Protective effect of apolipoprotein E type 2 allele for late onset Alzheimer disease.* Nat Genet, 1994. **7**(2): p. 180-4.
18. Farrer, L.A., et al., *Effects of age, sex, and ethnicity on the association between apolipoprotein E genotype and Alzheimer disease. A meta-analysis. APOE and Alzheimer Disease Meta Analysis Consortium.* JAMA, 1997. **278**(16): p. 1349-56.
19. Down, J.L., *Observations on an ethnic classification of idiots. 1866.* Ment Retard, 1995. **33**(1): p. 54-6.

20. Lejeune, J., M. Gautier, and R. Turpin, *[Study of somatic chromosomes from 9 mongoloid children].* C R Hebd Seances Acad Sci, 1959. **248**(11): p. 1721-2.
21. Head, E., et al., *Alzheimer's Disease in Down Syndrome.* Eur J Neurodegener Dis, 2012. **1**(3): p. 353-364.
22. Mann, D.M., et al., *The topography of plaques and tangles in Down's syndrome patients of different ages.* Neuropathol Appl Neurobiol, 1986. **12**(5): p. 447-57.
23. Wisniewski, K.E., H.M. Wisniewski, and G.Y. Wen, *Occurrence of neuropathological changes and dementia of Alzheimer's disease in Down's syndrome.* Ann Neurol, 1985. **17**(3): p. 278-82.
24. Prasher, V.P., et al., *Molecular mapping of Alzheimer-type dementia in Down's syndrome.* Ann Neurol, 1998. **43**(3): p. 380-3.
25. Rovelet-Lecrux, A., et al., *APP locus duplication causes autosomal dominant early-onset Alzheimer disease with cerebral amyloid angiopathy.* Nat Genet, 2006. **38**(1): p. 24-6.
26. Luscher, C. and R.C. Malenka, *NMDA receptor-dependent long-term potentiation and long-term depression (LTP/LTD).* Cold Spring Harb Perspect Biol, 2012. **4**(6).
27. Matos, M., et al., *Amyloid-beta peptide decreases glutamate uptake in cultured astrocytes: involvement of oxidative stress and mitogen-activated protein kinase cascades.* Neuroscience, 2008. **156**(4): p. 898-910.
28. Ferreira, I.L., et al., *Amyloid beta peptide 1-42 disturbs intracellular calcium homeostasis through activation of GluN2B-containing N-methyl-d-aspartate receptors in cortical cultures.* Cell Calcium, 2012. **51**(2): p. 95-106.
29. Shankar, G.M., et al., *Natural oligomers of the Alzheimer amyloid-beta protein induce reversible synapse loss by modulating an NMDA-type glutamate receptor-dependent signaling pathway.* J Neurosci, 2007. **27**(11): p. 2866-75.
30. Guntupalli, S., J. Widagdo, and V. Anggono, *Amyloid-beta-Induced Dysregulation of AMPA Receptor Trafficking.* Neural Plast, 2016. **2016**: p. 3204519.
31. Decker, H., et al., *Amyloid-beta peptide oligomers disrupt axonal transport through an NMDA receptor-dependent mechanism that is mediated by glycogen synthase kinase 3beta in primary cultured hippocampal neurons.* J Neurosci, 2010. **30**(27): p. 9166-71.
32. Ronicke, R., et al., *Early neuronal dysfunction by amyloid beta oligomers depends on activation of NR2B-containing NMDA receptors.* Neurobiol Aging, 2011. **32**(12): p. 2219-28.
33. Danysz, W., et al., *Neuroprotective and symptomatological action of memantine relevant for Alzheimer's disease--a unified glutamatergic hypothesis on the mechanism of action.* Neurotox Res, 2000. **2**(2-3): p. 85-97.
34. Jin, M., et al., *Soluble amyloid beta-protein dimers isolated from Alzheimer cortex directly induce Tau hyperphosphorylation and neuritic degeneration.* Proc Natl Acad Sci U S A, 2011. **108**(14): p. 5819-24.
35. Shankar, G.M., et al., *Amyloid-beta protein dimers isolated directly from Alzheimer's brains impair synaptic plasticity and memory.* Nat Med, 2008. **14**(8): p. 837-42.

36. Davis, D.G., et al., *Alzheimer neuropathologic alterations in aged cognitively normal subjects.* J Neuropathol Exp Neurol, 1999. **58**(4): p. 376-88.
37. Price, J.L., et al., *Neuropathology of nondemented aging: presumptive evidence for preclinical Alzheimer disease.* Neurobiol Aging, 2009. **30**(7): p. 1026-36.
38. Villemagne, V.L., et al., *Longitudinal assessment of Abeta and cognition in aging and Alzheimer disease.* Ann Neurol, 2011. **69**(1): p. 181-92.
39. Klunk, W.E., et al., *Imaging brain amyloid in Alzheimer's disease with Pittsburgh Compound-B.* Ann Neurol, 2004. **55**(3): p. 306-19.
40. Chetelat, G., et al., *Amyloid imaging in cognitively normal individuals, at-risk populations and preclinical Alzheimer's disease.* Neuroimage Clin, 2013. **2**: p. 356-65.
41. Nicoll, J.A., et al., *Neuropathology of human Alzheimer disease after immunization with amyloid-beta peptide: a case report.* Nat Med, 2003. **9**(4): p. 448-52.
42. Nicoll, J.A., et al., *Abeta species removal after abeta42 immunization.* J Neuropathol Exp Neurol, 2006. **65**(11): p. 1040-8.
43. Holmes, C., et al., *Long-term effects of Abeta42 immunisation in Alzheimer's disease: follow-up of a randomised, placebo-controlled phase I trial.* Lancet, 2008. **372**(9634): p. 216-23.
44. Boche, D., et al., *Consequence of Abeta immunization on the vasculature of human Alzheimer's disease brain.* Brain, 2008. **131**(Pt 12): p. 3299-310.
45. Bombois, S., et al., *Absence of beta-amyloid deposits after immunization in Alzheimer disease with Lewy body dementia.* Arch Neurol, 2007. **64**(4): p. 583-7.
46. Ferrer, I., et al., *Neuropathology and pathogenesis of encephalitis following amyloid-beta immunization in Alzheimer's disease.* Brain Pathol, 2004. **14**(1): p. 11-20.
47. Masliah, E., et al., *Abeta vaccination effects on plaque pathology in the absence of encephalitis in Alzheimer disease.* Neurology, 2005. **64**(1): p. 129-31.
48. Duff, K., et al., *Increased amyloid-beta42(43) in brains of mice expressing mutant presenilin 1.* Nature, 1996. **383**(6602): p. 710-3.
49. Games, D., et al., *Alzheimer-type neuropathology in transgenic mice overexpressing V717F beta-amyloid precursor protein.* Nature, 1995. **373**(6514): p. 523-7.
50. Masliah, E., et al., *Neurofibrillary pathology in transgenic mice overexpressing V717F beta-amyloid precursor protein.* J Neuropathol Exp Neurol, 2001. **60**(4): p. 357-68.
51. Hsiao, K., et al., *Correlative memory deficits, Abeta elevation, and amyloid plaques in transgenic mice.* Science, 1996. **274**(5284): p. 99-102.
52. Kawarabayashi, T., et al., *Age-dependent changes in brain, CSF, and plasma amyloid (beta) protein in the Tg2576 transgenic mouse model of Alzheimer's disease.* J Neurosci, 2001. **21**(2): p. 372-81.
53. Frautschy, S.A., et al., *Microglial response to amyloid plaques in APPsw transgenic mice.* Am J Pathol, 1998. **152**(1): p. 307-17.

54. Lanz, T.A., D.B. Carter, and K.M. Merchant, *Dendritic spine loss in the hippocampus of young PDAPP and Tg2576 mice and its prevention by the ApoE2 genotype.* Neurobiol Dis, 2003. **13**(3): p. 246-53.
55. Jacobsen, J.S., et al., *Early-onset behavioral and synaptic deficits in a mouse model of Alzheimer's disease.* Proc Natl Acad Sci U S A, 2006. **103**(13): p. 5161-6.
56. Holcomb, L., et al., *Accelerated Alzheimer-type phenotype in transgenic mice carrying both mutant amyloid precursor protein and presenilin 1 transgenes.* Nat Med, 1998. **4**(1): p. 97-100.
57. Gordon, M.N., et al., *Time course of the development of Alzheimer-like pathology in the doubly transgenic PS1+APP mouse.* Exp Neurol, 2002. **173**(2): p. 183-95.
58. Arendash, G.W., et al., *Progressive, age-related behavioral impairments in transgenic mice carrying both mutant amyloid precursor protein and presenilin-1 transgenes.* Brain Res, 2001. **891**(1-2): p. 42-53.
59. Kurt, M.A., et al., *Hyperphosphorylated tau and paired helical filament-like structures in the brains of mice carrying mutant amyloid precursor protein and mutant presenilin-1 transgenes.* Neurobiol Dis, 2003. **14**(1): p. 89-97.
60. Sadowski, M., et al., *Amyloid-beta deposition is associated with decreased hippocampal glucose metabolism and spatial memory impairment in APP/PS1 mice.* J Neuropathol Exp Neurol, 2004. **63**(5): p. 418-28.
61. Oakley, H., et al., *Intraneuronal beta-amyloid aggregates, neurodegeneration, and neuron loss in transgenic mice with five familial Alzheimer's disease mutations: potential factors in amyloid plaque formation.* J Neurosci, 2006. **26**(40): p. 10129-40.
62. Lewis, J., et al., *Neurofibrillary tangles, amyotrophy and progressive motor disturbance in mice expressing mutant (P301L) tau protein.* Nat Genet, 2000. **25**(4): p. 402-5.
63. Lewis, J., et al., *Enhanced neurofibrillary degeneration in transgenic mice expressing mutant tau and APP.* Science, 2001. **293**(5534): p. 1487-91.
64. Oddo, S., et al., *Triple-transgenic model of Alzheimer's disease with plaques and tangles: intracellular Abeta and synaptic dysfunction.* Neuron, 2003. **39**(3): p. 409-21.
65. Oddo, S., et al., *Amyloid deposition precedes tangle formation in a triple transgenic model of Alzheimer's disease.* Neurobiol Aging, 2003. **24**(8): p. 1063-70.
66. Billings, L.M., et al., *Intraneuronal Abeta causes the onset of early Alzheimer's disease-related cognitive deficits in transgenic mice.* Neuron, 2005. **45**(5): p. 675-88.
67. Morris, R.G., et al., *Place navigation impaired in rats with hippocampal lesions.* Nature, 1982. **297**(5868): p. 681-3.
68. Alamed, J., et al., *Two-day radial-arm water maze learning and memory task; robust resolution of amyloid-related memory deficits in transgenic mice.* Nat Protoc, 2006. **1**(4): p. 1671-9.
69. Diamond, D.M., et al., *Exposing rats to a predator impairs spatial working memory in the radial arm water maze.* Hippocampus, 1999. **9**(5): p. 542-52.

70. Antunes, M. and G. Biala, *The novel object recognition memory: neurobiology, test procedure, and its modifications.* Cogn Process, 2012. **13**(2): p. 93-110.
71. Kinnavane, L., M.M. Albasser, and J.P. Aggleton, *Advances in the behavioural testing and network imaging of rodent recognition memory.* Behav Brain Res, 2015. **285**: p. 67-78.
72. Ennaceur, A. and J. Delacour, *A new one-trial test for neurobiological studies of memory in rats. 1: Behavioral data.* Behav Brain Res, 1988. **31**(1): p. 47-59.
73. Brown, M.W. and J.P. Aggleton, *Recognition memory: what are the roles of the perirhinal cortex and hippocampus?* Nat Rev Neurosci, 2001. **2**(1): p. 51-61.
74. Curzon, P., N.R. Rustay, and K.E. Browman, *Cued and Contextual Fear Conditioning for Rodents*, in *Methods of Behavior Analysis in Neuroscience*, nd and J.J. Buccafusco, Editors. 2009: Boca Raton (FL).
75. Gerlai, R., *Behavioral tests of hippocampal function: simple paradigms complex problems.* Behav Brain Res, 2001. **125**(1-2): p. 269-77.
76. Rozemuller, J.M., P. Eikelenboom, and F.C. Stam, *Role of microglia in plaque formation in senile dementia of the Alzheimer type. An immunohistochemical study.* Virchows Arch B Cell Pathol Incl Mol Pathol, 1986. **51**(3): p. 247-54.
77. Rogers, J., et al., *Expression of immune system-associated antigens by cells of the human central nervous system: relationship to the pathology of Alzheimer's disease.* Neurobiol Aging, 1988. **9**(4): p. 339-49.
78. Griffin, W.S., et al., *Brain interleukin 1 and S-100 immunoreactivity are elevated in Down syndrome and Alzheimer disease.* Proc Natl Acad Sci U S A, 1989. **86**(19): p. 7611-5.
79. Eikelenboom, P., et al., *Complement activation in amyloid plaques in Alzheimer's dementia.* Virchows Arch B Cell Pathol Incl Mol Pathol, 1989. **56**(4): p. 259-62.
80. McGeer, P.L., et al., *Immune system response in Alzheimer's disease.* Can J Neurol Sci, 1989. **16**(4 Suppl): p. 516-27.
81. Ishii, T. and S. Haga, *Immuno-electron-microscopic localization of complements in amyloid fibrils of senile plaques.* Acta Neuropathol, 1984. **63**(4): p. 296-300.
82. Kettenmann, H., F. Kirchhoff, and A. Verkhratsky, *Microglia: new roles for the synaptic stripper.* Neuron, 2013. **77**(1): p. 10-8.
83. Elkabes, S., E.M. DiCicco-Bloom, and I.B. Black, *Brain microglia/macrophages express neurotrophins that selectively regulate microglial proliferation and function.* J Neurosci, 1996. **16**(8): p. 2508-21.
84. Nimmerjahn, A., F. Kirchhoff, and F. Helmchen, *Resting microglial cells are highly dynamic surveillants of brain parenchyma in vivo.* Science, 2005. **308**(5726): p. 1314-8.
85. Sierra, A., et al., *The "Big-Bang" for modern glial biology: Translation and comments on Pio del Rio-Hortega 1919 series of papers on microglia.* Glia, 2016. **64**(11): p. 1801-40.
86. Ginhoux, F., et al., *Fate mapping analysis reveals that adult microglia derive from primitive macrophages.* Science, 2010. **330**(6005): p. 841-5.
87. Ajami, B., et al., *Local self-renewal can sustain CNS microglia maintenance and function throughout adult life.* Nat Neurosci, 2007. **10**(12): p. 1538-43.

88. Capotondo, A., et al., *Brain conditioning is instrumental for successful microglia reconstitution following hematopoietic stem cell transplantation.* Proc Natl Acad Sci U S A, 2012. **109**(37): p. 15018-23.
89. Lampron, A., M. Lessard, and S. Rivest, *Effects of myeloablation, peripheral chimerism, and whole-body irradiation on the entry of bone marrow-derived cells into the brain.* Cell Transplant, 2012. **21**(6): p. 1149-59.
90. Kierdorf, K., et al., *Bone marrow cell recruitment to the brain in the absence of irradiation or parabiosis bias.* PLoS One, 2013. **8**(3): p. e58544.
91. Giulian, D. and T.J. Baker, *Characterization of ameboid microglia isolated from developing mammalian brain.* J Neurosci, 1986. **6**(8): p. 2163-78.
92. Dale, D.C., L. Boxer, and W.C. Liles, *The phagocytes: neutrophils and monocytes.* Blood, 2008. **112**(4): p. 935-45.
93. Zhu, Z., et al., *Acidic mammalian chitinase in asthmatic Th2 inflammation and IL-13 pathway activation.* Science, 2004. **304**(5677): p. 1678-82.
94. Mosser, D.M. and J.P. Edwards, *Exploring the full spectrum of macrophage activation.* Nat Rev Immunol, 2008. **8**(12): p. 958-69.
95. Sternberg, E.M., *Neural regulation of innate immunity: a coordinated nonspecific host response to pathogens.* Nat Rev Immunol, 2006. **6**(4): p. 318-28.
96. McGeer, E.G. and P.L. McGeer, *The importance of inflammatory mechanisms in Alzheimer disease.* Exp Gerontol, 1998. **33**(5): p. 371-8.
97. Akiyama, H., et al., *Inflammation and Alzheimer's disease.* Neurobiol Aging, 2000. **21**(3): p. 383-421.
98. Schenk, D., et al., *Immunization with amyloid-beta attenuates Alzheimer-disease-like pathology in the PDAPP mouse.* Nature, 1999. **400**(6740): p. 173-7.
99. Janus, C., et al., *A beta peptide immunization reduces behavioural impairment and plaques in a model of Alzheimer's disease.* Nature, 2000. **408**(6815): p. 979-82.
100. Morgan, D., et al., *A beta peptide vaccination prevents memory loss in an animal model of Alzheimer's disease.* Nature, 2000. **408**(6815): p. 982-5.
101. Head, E., et al., *A two-year study with fibrillar beta-amyloid (Abeta) immunization in aged canines: effects on cognitive function and brain Abeta.* J Neurosci, 2008. **28**(14): p. 3555-66.
102. Lemere, C.A., et al., *Alzheimer's disease abeta vaccine reduces central nervous system abeta levels in a non-human primate, the Caribbean vervet.* Am J Pathol, 2004. **165**(1): p. 283-97.
103. Schenk, D., *Amyloid-beta immunotherapy for Alzheimer's disease: the end of the beginning.* Nat Rev Neurosci, 2002. **3**(10): p. 824-8.
104. Orgogozo, J.M., et al., *Subacute meningoencephalitis in a subset of patients with AD after Abeta42 immunization.* Neurology, 2003. **61**(1): p. 46-54.
105. Wilcock, D.M., et al., *Intracranially administered anti-Abeta antibodies reduce beta-amyloid deposition by mechanisms both independent of and associated with microglial activation.* J Neurosci, 2003. **23**(9): p. 3745-51.

106. Wilcock, D.M., et al., *Microglial activation facilitates Abeta plaque removal following intracranial anti-Abeta antibody administration.* Neurobiol Dis, 2004. **15**(1): p. 11-20.
107. Wilcock, D.M., et al., *Passive amyloid immunotherapy clears amyloid and transiently activates microglia in a transgenic mouse model of amyloid deposition.* J Neurosci, 2004. **24**(27): p. 6144-51.
108. Pfeifer, M., et al., *Cerebral hemorrhage after passive anti-Abeta immunotherapy.* Science, 2002. **298**(5597): p. 1379.
109. Wilcock, D.M., et al., *Passive immunotherapy against Abeta in aged APP-transgenic mice reverses cognitive deficits and depletes parenchymal amyloid deposits in spite of increased vascular amyloid and microhemorrhage.* J Neuroinflammation, 2004. **1**(1): p. 24.
110. Racke, M.M., et al., *Exacerbation of cerebral amyloid angiopathy-associated microhemorrhage in amyloid precursor protein transgenic mice by immunotherapy is dependent on antibody recognition of deposited forms of amyloid beta.* J Neurosci, 2005. **25**(3): p. 629-36.
111. Schroeter, S., et al., *Immunotherapy reduces vascular amyloid-beta in PDAPP mice.* J Neurosci, 2008. **28**(27): p. 6787-93.
112. Black, R.S., et al., *A single ascending dose study of bapineuzumab in patients with Alzheimer disease.* Alzheimer Dis Assoc Disord, 2010. **24**(2): p. 198-203.
113. Salloway, S., et al., *A phase 2 multiple ascending dose trial of bapineuzumab in mild to moderate Alzheimer disease.* Neurology, 2009. **73**(24): p. 2061-70.
114. Sperling, R., et al., *Amyloid-related imaging abnormalities in patients with Alzheimer's disease treated with bapineuzumab: a retrospective analysis.* Lancet Neurol, 2012. **11**(3): p. 241-9.
115. Salloway, S., et al., *Two phase 3 trials of bapineuzumab in mild-to-moderate Alzheimer's disease.* N Engl J Med, 2014. **370**(4): p. 322-33.
116. Sperling, R.A., et al., *Amyloid-related imaging abnormalities in amyloid-modifying therapeutic trials: recommendations from the Alzheimer's Association Research Roundtable Workgroup.* Alzheimers Dement, 2011. **7**(4): p. 367-85.
117. Bard, F., et al., *Peripherally administered antibodies against amyloid beta-peptide enter the central nervous system and reduce pathology in a mouse model of Alzheimer disease.* Nat Med, 2000. **6**(8): p. 916-9.
118. Wilcock, D.M. and C.A. Colton, *Immunotherapy, vascular pathology, and microhemorrhages in transgenic mice.* CNS Neurol Disord Drug Targets, 2009. **8**(1): p. 50-64.
119. DeMattos, R.B., et al., *Peripheral anti-A beta antibody alters CNS and plasma A beta clearance and decreases brain A beta burden in a mouse model of Alzheimer's disease.* Proc Natl Acad Sci U S A, 2001. **98**(15): p. 8850-5.
120. Solomon, B., et al., *Disaggregation of Alzheimer beta-amyloid by site-directed mAb.* Proc Natl Acad Sci U S A, 1997. **94**(8): p. 4109-12.
121. Zago, W., et al., *Neutralization of soluble, synaptotoxic amyloid beta species by antibodies is epitope specific.* J Neurosci, 2012. **32**(8): p. 2696-702.

122. Keren-Shaul, H., et al., *A Unique Microglia Type Associated with Restricting Development of Alzheimer's Disease.* Cell, 2017. **169**(7): p. 1276-1290 e17.
123. Wang, Y., et al., *TREM2 lipid sensing sustains the microglial response in an Alzheimer's disease model.* Cell, 2015. **160**(6): p. 1061-71.
124. Takahashi, K., C.D. Rochford, and H. Neumann, *Clearance of apoptotic neurons without inflammation by microglial triggering receptor expressed on myeloid cells-2.* J Exp Med, 2005. **201**(4): p. 647-57.
125. Li, X., et al., *Different mechanisms of apolipoprotein E isoform-dependent modulation of prostaglandin E2 production and triggering receptor expressed on myeloid cells 2 (TREM2) expression after innate immune activation of microglia.* FASEB J, 2015. **29**(5): p. 1754-62.
126. Kiialainen, A., et al., *Dap12 and Trem2, molecules involved in innate immunity and neurodegeneration, are co-expressed in the CNS.* Neurobiol Dis, 2005. **18**(2): p. 314-22.
127. Hsieh, C.L., et al., *A role for TREM2 ligands in the phagocytosis of apoptotic neuronal cells by microglia.* J Neurochem, 2009. **109**(4): p. 1144-56.
128. Hickman, S.E. and J. El Khoury, *TREM2 and the neuroimmunology of Alzheimer's disease.* Biochem Pharmacol, 2014. **88**(4): p. 495-8.
129. Forabosco, P., et al., *Insights into TREM2 biology by network analysis of human brain gene expression data.* Neurobiol Aging, 2013. **34**(12): p. 2699-714.
130. Thrash, J.C., B.E. Torbett, and M.J. Carson, *Developmental regulation of TREM2 and DAP12 expression in the murine CNS: implications for Nasu-Hakola disease.* Neurochem Res, 2009. **34**(1): p. 38-45.
131. Jiang, T., et al., *Upregulation of TREM2 ameliorates neuropathology and rescues spatial cognitive impairment in a transgenic mouse model of Alzheimer's disease.* Neuropsychopharmacology, 2014. **39**(13): p. 2949-62.
132. Sessa, G., et al., *Distribution and signaling of TREM2/DAP12, the receptor system mutated in human polycystic lipomembraneous osteodysplasia with sclerosing leukoencephalopathy dementia.* Eur J Neurosci, 2004. **20**(10): p. 2617-28.
133. Jay, T.R., V.E. von Saucken, and G.E. Landreth, *TREM2 in Neurodegenerative Diseases.* Mol Neurodegener, 2017. **12**(1): p. 56.
134. Ulrich, J.D., et al., *Elucidating the Role of TREM2 in Alzheimer's Disease.* Neuron, 2017. **94**(2): p. 237-248.
135. Atagi, Y., et al., *Apolipoprotein E Is a Ligand for Triggering Receptor Expressed on Myeloid Cells 2 (TREM2).* J Biol Chem, 2015. **290**(43): p. 26043-50.
136. Bailey, C.C., L.B. DeVaux, and M. Farzan, *The Triggering Receptor Expressed on Myeloid Cells 2 Binds Apolipoprotein E.* J Biol Chem, 2015. **290**(43): p. 26033-42.
137. Yeh, F.L., et al., *TREM2 Binds to Apolipoproteins, Including APOE and CLU/APOJ, and Thereby Facilitates Uptake of Amyloid-Beta by Microglia.* Neuron, 2016. **91**(2): p. 328-40.
138. Song, W., et al., *Alzheimer's disease-associated TREM2 variants exhibit either decreased or increased ligand-dependent activation.* Alzheimers Dement, 2017. **13**(4): p. 381-387.

139. Daws, M.R., et al., *Pattern recognition by TREM-2: binding of anionic ligands.* J Immunol, 2003. **171**(2): p. 594-9.
140. Kawabori, M., et al., *Triggering receptor expressed on myeloid cells 2 (TREM2) deficiency attenuates phagocytic activities of microglia and exacerbates ischemic damage in experimental stroke.* J Neurosci, 2015. **35**(8): p. 3384-96.
141. Kober, D.L., et al., *Neurodegenerative disease mutations in TREM2 reveal a functional surface and distinct loss-of-function mechanisms.* Elife, 2016. **5**.
142. Colonna, M., *TREMs in the immune system and beyond.* Nat Rev Immunol, 2003. **3**(6): p. 445-53.
143. Colonna, M. and Y. Wang, *TREM2 variants: new keys to decipher Alzheimer disease pathogenesis.* Nat Rev Neurosci, 2016. **17**(4): p. 201-7.
144. Nasu, T., Y. Tsukahara, and K. Terayama, *A lipid metabolic disease-"membranous lipodystrophy"-an autopsy case demonstrating numerous peculiar membrane-structures composed of compound lipid in bone and bone marrow and various adipose tissues.* Acta Pathol Jpn, 1973. **23**(3): p. 539-58.
145. Hakola, H.P., *Neuropsychiatric and genetic aspects of a new hereditary disease characterized by progressive dementia and lipomembranous polycystic osteodysplasia.* Acta Psychiatr Scand Suppl, 1972. **232**: p. 1-173.
146. Kaneko, M., et al., *Nasu-Hakola disease: The first case reported by Nasu and review: The 50th Anniversary of Japanese Society of Neuropathology.* Neuropathology, 2010. **30**(5): p. 463-70.
147. Sasaki, A., et al., *Variable expression of microglial DAP12 and TREM2 genes in Nasu-Hakola disease.* Neurogenetics, 2015. **16**(4): p. 265-76.
148. Bianchin, M.M., et al., *Nasu-Hakola disease (polycystic lipomembranous osteodysplasia with sclerosing leukoencephalopathy--PLOSL): a dementia associated with bone cystic lesions. From clinical to genetic and molecular aspects.* Cell Mol Neurobiol, 2004. **24**(1): p. 1-24.
149. Satoh, J., et al., *Immunohistochemical characterization of microglia in Nasu-Hakola disease brains.* Neuropathology, 2011. **31**(4): p. 363-75.
150. Paloneva, J., et al., *Mutations in two genes encoding different subunits of a receptor signaling complex result in an identical disease phenotype.* Am J Hum Genet, 2002. **71**(3): p. 656-62.
151. Guerreiro, R., et al., *TREM2 variants in Alzheimer's disease.* N Engl J Med, 2013. **368**(2): p. 117-27.
152. Jonsson, T. and K. Stefansson, *TREM2 and neurodegenerative disease.* N Engl J Med, 2013. **369**(16): p. 1568-9.
153. Neumann, H. and M.J. Daly, *Variant TREM2 as risk factor for Alzheimer's disease.* N Engl J Med, 2013. **368**(2): p. 182-4.
154. Guerreiro, R.J., et al., *Using exome sequencing to reveal mutations in TREM2 presenting as a frontotemporal dementia-like syndrome without bone involvement.* JAMA Neurol, 2013. **70**(1): p. 78-84.
155. Jonsson, T., et al., *Variant of TREM2 associated with the risk of Alzheimer's disease.* N Engl J Med, 2013. **368**(2): p. 107-16.

156. Ghani, M., et al., *Mutation analysis of the MS4A and TREM gene clusters in a case-control Alzheimer's disease data set.* Neurobiol Aging, 2016. **42**: p. 217 e7-217 e13.
157. Cuyvers, E., et al., *Investigating the role of rare heterozygous TREM2 variants in Alzheimer's disease and frontotemporal dementia.* Neurobiol Aging, 2014. **35**(3): p. 726 e11-9.
158. Kim, J.H., et al., *Gene-based rare allele analysis identified a risk gene of Alzheimer's disease.* PLoS One, 2014. **9**(10): p. e107983.
159. Hooli, B.V., et al., *The rare TREM2 R47H variant exerts only a modest effect on Alzheimer disease risk.* Neurology, 2014. **83**(15): p. 1353-8.
160. Bertram, L., A.R. Parrado, and R.E. Tanzi, *TREM2 and neurodegenerative disease.* N Engl J Med, 2013. **369**(16): p. 1565.
161. Sirkis, D.W., et al., *Rare TREM2 variants associated with Alzheimer's disease display reduced cell surface expression.* Acta Neuropathol Commun, 2016. **4**(1): p. 98.
162. Roussos, P., et al., *The triggering receptor expressed on myeloid cells 2 (TREM2) is associated with enhanced inflammation, neuropathological lesions and increased risk for Alzheimer's dementia.* Alzheimers Dement, 2015. **11**(10): p. 1163-70.
163. Jin, S.C., et al., *Coding variants in TREM2 increase risk for Alzheimer's disease.* Hum Mol Genet, 2014. **23**(21): p. 5838-46.
164. Yu, J.T., et al., *Triggering receptor expressed on myeloid cells 2 variant is rare in late-onset Alzheimer's disease in Han Chinese individuals.* Neurobiol Aging, 2014. **35**(4): p. 937 e1-3.
165. Jiang, T., et al., *A rare coding variant in TREM2 increases risk for Alzheimer's disease in Han Chinese.* Neurobiol Aging, 2016. **42**: p. 217 e1-3.
166. Wang, Y., et al., *TREM2-mediated early microglial response limits diffusion and toxicity of amyloid plaques.* J Exp Med, 2016. **213**(5): p. 667-75.
167. Kleinberger, G., et al., *TREM2 mutations implicated in neurodegeneration impair cell surface transport and phagocytosis.* Sci Transl Med, 2014. **6**(243): p. 243ra86.
168. Peng, Q., et al., *TREM2- and DAP12-dependent activation of PI3K requires DAP10 and is inhibited by SHIP1.* Sci Signal, 2010. **3**(122): p. ra38.
169. Otero, K., et al., *TREM2 and beta-catenin regulate bone homeostasis by controlling the rate of osteoclastogenesis.* J Immunol, 2012. **188**(6): p. 2612-21.
170. Yuan, P., et al., *TREM2 Haplodeficiency in Mice and Humans Impairs the Microglia Barrier Function Leading to Decreased Amyloid Compaction and Severe Axonal Dystrophy.* Neuron, 2016. **92**(1): p. 252-264.
171. Gao, X., et al., *Silencing of triggering receptor expressed on myeloid cells-2 enhances the inflammatory responses of alveolar macrophages to lipopolysaccharide.* Mol Med Rep, 2013. **7**(3): p. 921-6.
172. Bouchon, A., et al., *A DAP12-mediated pathway regulates expression of CC chemokine receptor 7 and maturation of human dendritic cells.* J Exp Med, 2001. **194**(8): p. 1111-22.

173. Wu, K., et al., *TREM-2 promotes macrophage survival and lung disease after respiratory viral infection.* J Exp Med, 2015. **212**(5): p. 681-97.
174. Zheng, H., et al., *TREM2 Promotes Microglial Survival by Activating Wnt/beta-Catenin Pathway.* J Neurosci, 2017. **37**(7): p. 1772-1784.
175. Mazaheri, F., et al., *TREM2 deficiency impairs chemotaxis and microglial responses to neuronal injury.* EMBO Rep, 2017. **18**(7): p. 1186-1198.
176. N'Diaye, E.N., et al., *TREM-2 (triggering receptor expressed on myeloid cells 2) is a phagocytic receptor for bacteria.* J Cell Biol, 2009. **184**(2): p. 215-23.
177. Chen, L.C., et al., *Regulation of TREM expression in hepatic macrophages and endothelial cells during acute endotoxemia.* Exp Mol Pathol, 2008. **84**(2): p. 145-55.
178. Cella, M., et al., *Impaired differentiation of osteoclasts in TREM-2-deficient individuals.* J Exp Med, 2003. **198**(4): p. 645-51.
179. Schmid, C.D., et al., *Heterogeneous expression of the triggering receptor expressed on myeloid cells-2 on adult murine microglia.* J Neurochem, 2002. **83**(6): p. 1309-20.
180. Chouery, E., et al., *Mutations in TREM2 lead to pure early-onset dementia without bone cysts.* Hum Mutat, 2008. **29**(9): p. E194-204.
181. Klunemann, H.H., et al., *The genetic causes of basal ganglia calcification, dementia, and bone cysts: DAP12 and TREM2.* Neurology, 2005. **64**(9): p. 1502-7.
182. Rajagopalan, P., D.P. Hibar, and P.M. Thompson, *TREM2 and neurodegenerative disease.* N Engl J Med, 2013. **369**(16): p. 1565-7.
183. Cruchaga, C., et al., *GWAS of cerebrospinal fluid tau levels identifies risk variants for Alzheimer's disease.* Neuron, 2013. **78**(2): p. 256-68.
184. Luis, E.O., et al., *Frontobasal gray matter loss is associated with the TREM2 p.R47H variant.* Neurobiol Aging, 2014. **35**(12): p. 2681-2690.
185. Pottier, C., et al., *TYROBP genetic variants in early-onset Alzheimer's disease.* Neurobiol Aging, 2016. **48**: p. 222 e9-222 e15.
186. Condello, C., et al., *Microglia constitute a barrier that prevents neurotoxic protofibrillar Abeta42 hotspots around plaques.* Nat Commun, 2015. **6**: p. 6176.
187. Yeh, F.L., D.V. Hansen, and M. Sheng, *TREM2, Microglia, and Neurodegenerative Diseases.* Trends Mol Med, 2017. **23**(6): p. 512-533.
188. Jay, T.R., et al., *TREM2 deficiency eliminates TREM2+ inflammatory macrophages and ameliorates pathology in Alzheimer's disease mouse models.* J Exp Med, 2015. **212**(3): p. 287-95.
189. Xiang, X., et al., *TREM2 deficiency reduces the efficacy of immunotherapeutic amyloid clearance.* EMBO Mol Med, 2016. **8**(9): p. 992-1004.
190. Roe, C.M., et al., *Amyloid imaging and CSF biomarkers in predicting cognitive impairment up to 7.5 years later.* Neurology, 2013. **80**(19): p. 1784-91.
191. Blaser, R. and C. Heyser, *Spontaneous object recognition: a promising approach to the comparative study of memory.* Front Behav Neurosci, 2015. **9**: p. 183.
192. Dodel, R., et al., *Human antibodies against amyloid beta peptide: a potential treatment for Alzheimer's disease.* Annals of neurology, 2002. **52**(2): p. 253-6.

193. Carter, M.D., G.A. Simms, and D.F. Weaver, *The development of new therapeutics for Alzheimer's disease.* Clinical pharmacology and therapeutics, 2010. **88**(4): p. 475-86.
194. Himmelstein, D.S., et al., *Tau as a therapeutic target in neurodegenerative disease.* Pharmacology and Therapeutics, 2012. **136**(1): p. 8-22.
195. Apostolova, L.G., *Alzheimer disease: A quantitative trait approach to GWAS pays dividends.* Nat Rev Neurol, 2017. **13**(6): p. 321-322.
196. DiCarlo, G., et al., *Intrahippocampal LPS injections reduce Abeta load in APP+PS1 transgenic mice.* Neurobiol Aging, 2001. **22**(6): p. 1007-12.
197. Morgan, D., et al., *Dynamic complexity of the microglial activation response in transgenic models of amyloid deposition: implications for Alzheimer therapeutics.* J Neuropathol Exp Neurol, 2005. **64**(9): p. 743-53.
198. Wilcock, D.M., et al., *Diverse inflammatory responses in transgenic mouse models of AD and the effect of immunotherapy on these responses.* ASN neuro, 2011.
199. Naert, G. and S. Rivest, *CC chemokine receptor 2 deficiency aggravates cognitive impairments and amyloid pathology in a transgenic mouse model of Alzheimer's disease.* J Neurosci, 2011. **31**(16): p. 6208-20.
200. Reale, M., et al., *Peripheral chemokine receptors, their ligands, cytokines and Alzheimer's disease.* J Alzheimers Dis, 2008. **14**(2): p. 147-59.
201. Wan, Y.Y., *GATA3: a master of many trades in immune regulation.* Trends Immunol, 2014. **35**(6): p. 233-42.
202. Zheng, C., X.W. Zhou, and J.Z. Wang, *The dual roles of cytokines in Alzheimer's disease: update on interleukins, TNF-alpha, TGF-beta and IFN-gamma.* Transl Neurodegener, 2016. **5**: p. 7.
203. Rivera-Escalera, F., et al., *Interleukin-1beta mediated amyloid plaque clearance is independent of CCR2 signaling in the APP/PS1 mouse model of Alzheimer's disease.* Neurobiol Dis, 2014. **69**: p. 124-33.
204. Guillot-Sestier, M.V., et al., *Il10 deficiency rebalances innate immunity to mitigate Alzheimer-like pathology.* Neuron, 2015. **85**(3): p. 534-48.
205. Herber, D.L., et al., *Time-dependent reduction in Abeta levels after intracranial LPS administration in APP transgenic mice.* Experimental neurology, 2004. **190**(1): p. 245-53.
206. Chakrabarty, P., et al., *IL-10 alters immunoproteostasis in APP mice, increasing plaque burden and worsening cognitive behavior.* Neuron, 2015. **85**(3): p. 519-33.
207. Sudduth, T.L., et al., *Lithium Treatment of APPSwDI/NOS2-/- Mice Leads to Reduced Hyperphosphorylated Tau, Increased Amyloid Deposition and Altered Inflammatory Phenotype.* PloS one, 2012. **7**(2): p. e31993.
208. Vorhees, C.V. and M.T. Williams, *Assessing spatial learning and memory in rodents.* ILAR J, 2014. **55**(2): p. 310-32.
209. Vorhees, C.V. and M.T. Williams, *Value of water mazes for assessing spatial and egocentric learning and memory in rodent basic research and regulatory studies.* Neurotoxicol Teratol, 2014. **45**: p. 75-90.

210. Doens, D. and P.L. Fernandez, *Microglia receptors and their implications in the response to amyloid beta for Alzheimer's disease pathogenesis.* J Neuroinflammation, 2014. **11**: p. 48.
211. Fuller, J.P., J.B. Stavenhagen, and J.L. Teeling, *New roles for Fc receptors in neurodegeneration-the impact on Immunotherapy for Alzheimer's Disease.* Front Neurosci, 2014. **8**: p. 235.
212. Sheng, J.G., R.E. Mrak, and W.S. Griffin, *Neuritic plaque evolution in Alzheimer's disease is accompanied by transition of activated microglia from primed to enlarged to phagocytic forms.* Acta Neuropathol, 1997. **94**(1): p. 1-5.
213. Tanaka, F., et al., *Clinical outcome and survival of secondary (AA) amyloidosis.* Clin Exp Rheumatol, 2003. **21**(3): p. 343-6.
214. Ard, M.D., et al., *Scavenging of Alzheimer's amyloid beta-protein by microglia in culture.* J Neurosci Res, 1996. **43**(2): p. 190-202.
215. Kopec, K.K. and R.T. Carroll, *Alzheimer's beta-amyloid peptide 1-42 induces a phagocytic response in murine microglia.* J Neurochem, 1998. **71**(5): p. 2123-31.
216. Peress, N.S., et al., *Identification of Fc gamma RI, II and III on normal human brain ramified microglia and on microglia in senile plaques in Alzheimer's disease.* J Neuroimmunol, 1993. **48**(1): p. 71-9.
217. Bundy, J.L., et al., *Sex-biased hippocampal pathology in the 5XFAD mouse model of Alzheimer's disease: A multi-omic analysis.* J Comp Neurol, 2018.
218. Sevigny, J., et al., *The antibody aducanumab reduces Abeta plaques in Alzheimer's disease.* Nature, 2016. **537**(7618): p. 50-6.
219. Wilcock, D.M., M.N. Gordon, and D. Morgan, *Quantification of cerebral amyloid angiopathy and parenchymal amyloid plaques with Congo red histochemical stain.* Nat Protoc, 2006. **1**(3): p. 1591-5.
220. Murphy, M.P., et al., *FAD-linked mutations in presenilin 1 alter the length of Abeta peptides derived from betaAPP transmembrane domain mutants.* Biochim Biophys Acta, 2002. **1586**(2): p. 199-209.
221. Wilcock, D.M. and C.A. Colton, *Anti-amyloid-beta immunotherapy in Alzheimer's disease: relevance of transgenic mouse studies to clinical trials.* J Alzheimers Dis, 2008. **15**(4): p. 555-69.
222. Haskill, S., et al., *Identification of three related human GRO genes encoding cytokine functions.* Proc Natl Acad Sci U S A, 1990. **87**(19): p. 7732-6.
223. Soulet, D. and S. Rivest, *Bone-marrow-derived microglia: myth or reality?* Curr Opin Pharmacol, 2008. **8**(4): p. 508-18.
224. Massengale, M., et al., *Hematopoietic cells maintain hematopoietic fates upon entering the brain.* J Exp Med, 2005. **201**(10): p. 1579-89.
225. Priller, J., et al., *Targeting gene-modified hematopoietic cells to the central nervous system: use of green fluorescent protein uncovers microglial engraftment.* Nat Med, 2001. **7**(12): p. 1356-61.
226. Simard, A.R. and S. Rivest, *Bone marrow stem cells have the ability to populate the entire central nervous system into fully differentiated parenchymal microglia.* FASEB J, 2004. **18**(9): p. 998-1000.

227. Vallieres, L. and P.E. Sawchenko, *Bone marrow-derived cells that populate the adult mouse brain preserve their hematopoietic identity.* J Neurosci, 2003. **23**(12): p. 5197-207.
228. Perry, V.H. and S. Gordon, *Macrophages and microglia in the nervous system.* Trends Neurosci, 1988. **11**(6): p. 273-7.
229. Lawson, L.J., V.H. Perry, and S. Gordon, *Turnover of resident microglia in the normal adult mouse brain.* Neuroscience, 1992. **48**(2): p. 405-15.
230. El Khoury, J., et al., *Ccr2 deficiency impairs microglial accumulation and accelerates progression of Alzheimer-like disease.* Nat Med, 2007. **13**(4): p. 432-8.
231. Town, T., et al., *Blocking TGF-beta-Smad2/3 innate immune signaling mitigates Alzheimer-like pathology.* Nat Med, 2008. **14**(6): p. 681-7.
232. Simard, A.R., et al., *Bone marrow-derived microglia play a critical role in restricting senile plaque formation in Alzheimer's disease.* Neuron, 2006. **49**(4): p. 489-502.
233. Malm, T.M., et al., *Bone-marrow-derived cells contribute to the recruitment of microglial cells in response to beta-amyloid deposition in APP/PS1 double transgenic Alzheimer mice.* Neurobiol Dis, 2005. **18**(1): p. 134-42.
234. Stalder, A.K., et al., *Invasion of hematopoietic cells into the brain of amyloid precursor protein transgenic mice.* J Neurosci, 2005. **25**(48): p. 11125-32.
235. Zhang, K., et al., *CXCL1 contributes to beta-amyloid-induced transendothelial migration of monocytes in Alzheimer's disease.* PLoS One, 2013. **8**(8): p. e72744.
236. Xia, M. and B.T. Hyman, *GROalpha/KC, a chemokine receptor CXCR2 ligand, can be a potent trigger for neuronal ERK1/2 and PI-3 kinase pathways and for tau hyperphosphorylation-a role in Alzheimer's disease?* J Neuroimmunol, 2002. **122**(1-2): p. 55-64.
237. Streit, W.J., *Microglia and Alzheimer's disease pathogenesis.* J Neurosci Res, 2004. **77**(1): p. 1-8.
238. Suzuki, N., et al., *High tissue content of soluble beta 1-40 is linked to cerebral amyloid angiopathy.* Am J Pathol, 1994. **145**(2): p. 452-60.
239. Kumar-Singh, S., *Cerebral amyloid angiopathy: pathogenetic mechanisms and link to dense amyloid plaques.* Genes Brain Behav, 2008. **7 Suppl 1**: p. 67-82.
240. Poduslo, J.F., G.L. Curran, and C.T. Berg, *Macromolecular permeability across the blood-nerve and blood-brain barriers.* Proc Natl Acad Sci U S A, 1994. **91**(12): p. 5705-9.
241. Shibata, M., et al., *Clearance of Alzheimer's amyloid-ss(1-40) peptide from brain by LDL receptor-related protein-1 at the blood-brain barrier.* J Clin Invest, 2000. **106**(12): p. 1489-99.
242. Deane, R., Z. Wu, and B.V. Zlokovic, *RAGE (yin) versus LRP (yang) balance regulates alzheimer amyloid beta-peptide clearance through transport across the blood-brain barrier.* Stroke, 2004. **35**(11 Suppl 1): p. 2628-31.
243. Weller, R.O., et al., *Perivascular drainage of amyloid-beta peptides from the brain and its failure in cerebral amyloid angiopathy and Alzheimer's disease.* Brain Pathol, 2008. **18**(2): p. 253-66.

244. Amor, S. and M.N. Woodroofe, *Innate and adaptive immune responses in neurodegeneration and repair.* Immunology, 2014. **141**(3): p. 287-91.
245. Amor, S., et al., *Inflammation in neurodegenerative diseases--an update.* Immunology, 2014. **142**(2): p. 151-66.
246. Lobo-Silva, D., et al., *Balancing the immune response in the brain: IL-10 and its regulation.* J Neuroinflammation, 2016. **13**(1): p. 297.
247. Murray, P.J., *Understanding and exploiting the endogenous interleukin-10/STAT3-mediated anti-inflammatory response.* Curr Opin Pharmacol, 2006. **6**(4): p. 379-86.
248. Moore, K.W., et al., *Interleukin-10 and the interleukin-10 receptor.* Annu Rev Immunol, 2001. **19**: p. 683-765.
249. Ledeboer, A., et al., *Expression and regulation of interleukin-10 and interleukin-10 receptor in rat astroglial and microglial cells.* Eur J Neurosci, 2002. **16**(7): p. 1175-85.
250. Balasingam, V. and V.W. Yong, *Attenuation of astroglial reactivity by interleukin-10.* J Neurosci, 1996. **16**(9): p. 2945-55.
251. Norden, D.M., et al., *TGFbeta produced by IL-10 redirected astrocytes attenuates microglial activation.* Glia, 2014. **62**(6): p. 881-95.
252. Zhou, Z., et al., *Interleukin-10 provides direct trophic support to neurons.* J Neurochem, 2009. **110**(5): p. 1617-27.
253. Candelario-Jalil, E., et al., *Matrix metalloproteinases are associated with increased blood-brain barrier opening in vascular cognitive impairment.* Stroke, 2011. **42**(5): p. 1345-50.
254. Hernandez-Guillamon, M., et al., *Matrix metalloproteinase 2 (MMP-2) degrades soluble vasculotropic amyloid-beta E22Q and L34V mutants, delaying their toxicity for human brain microvascular endothelial cells.* J Biol Chem, 2010. **285**(35): p. 27144-58.
255. Yan, P., et al., *Matrix metalloproteinase-9 degrades amyloid-beta fibrils in vitro and compact plaques in situ.* J Biol Chem, 2006. **281**(34): p. 24566-74.
256. Vecil, G.G., et al., *Interleukin-1 is a key regulator of matrix metalloproteinase-9 expression in human neurons in culture and following mouse brain trauma in vivo.* J Neurosci Res, 2000. **61**(2): p. 212-24.
257. Galis, Z.S., et al., *Cytokine-stimulated human vascular smooth muscle cells synthesize a complement of enzymes required for extracellular matrix digestion.* Circ Res, 1994. **75**(1): p. 181-9.
258. Klein, T. and R. Bischoff, *Physiology and pathophysiology of matrix metalloproteases.* Amino Acids, 2011. **41**(2): p. 271-90.
259. Wilcock, D.M., et al., *Activation of matrix metalloproteinases following anti-Abeta immunotherapy; implications for microhemorrhage occurrence.* J Neuroinflammation, 2011. **8**: p. 115.
260. Kettenmann, H., et al., *Physiology of microglia.* Physiol Rev, 2011. **91**(2): p. 461-553.
261. Ji, K., et al., *Microglia actively regulate the number of functional synapses.* PLoS One, 2013. **8**(2): p. e56293.

262. Parkhurst, C.N., et al., *Microglia promote learning-dependent synapse formation through brain-derived neurotrophic factor.* Cell, 2013. **155**(7): p. 1596-609.
263. Bamberger, M.E., et al., *A cell surface receptor complex for fibrillar beta-amyloid mediates microglial activation.* J Neurosci, 2003. **23**(7): p. 2665-74.
264. Paresce, D.M., R.N. Ghosh, and F.R. Maxfield, *Microglial cells internalize aggregates of the Alzheimer's disease amyloid beta-protein via a scavenger receptor.* Neuron, 1996. **17**(3): p. 553-65.
265. Stewart, C.R., et al., *CD36 ligands promote sterile inflammation through assembly of a Toll-like receptor 4 and 6 heterodimer.* Nat Immunol, 2010. **11**(2): p. 155-61.
266. Liu, Y., et al., *LPS receptor (CD14): a receptor for phagocytosis of Alzheimer's amyloid peptide.* Brain, 2005. **128**(Pt 8): p. 1778-89.
267. Hickman, S.E., E.K. Allison, and J. El Khoury, *Microglial dysfunction and defective beta-amyloid clearance pathways in aging Alzheimer's disease mice.* J Neurosci, 2008. **28**(33): p. 8354-60.
268. Mawuenyega, K.G., et al., *Decreased clearance of CNS beta-amyloid in Alzheimer's disease.* Science, 2010. **330**(6012): p. 1774.
269. Yan, S.D., et al., *RAGE and amyloid-beta peptide neurotoxicity in Alzheimer's disease.* Nature, 1996. **382**(6593): p. 685-91.
270. El Khoury, J., et al., *Microglia, scavenger receptors, and the pathogenesis of Alzheimer's disease.* Neurobiol Aging, 1998. **19**(1 Suppl): p. S81-4.
271. Heneka, M.T., et al., *Neuroinflammation in Alzheimer's disease.* Lancet Neurol, 2015. **14**(4): p. 388-405.
272. Leissring, M.A., et al., *Enhanced proteolysis of beta-amyloid in APP transgenic mice prevents plaque formation, secondary pathology, and premature death.* Neuron, 2003. **40**(6): p. 1087-93.
273. Streit, W.J., et al., *Dystrophic microglia in the aging human brain.* Glia, 2004. **45**(2): p. 208-12.
274. Krabbe, G., et al., *Functional impairment of microglia coincides with Beta-amyloid deposition in mice with Alzheimer-like pathology.* PLoS One, 2013. **8**(4): p. e60921.
275. Lucin, K.M., et al., *Microglial beclin 1 regulates retromer trafficking and phagocytosis and is impaired in Alzheimer's disease.* Neuron, 2013. **79**(5): p. 873-86.
276. Veerhuis, R., H.M. Nielsen, and A.J. Tenner, *Complement in the brain.* Mol Immunol, 2011. **48**(14): p. 1592-603.
277. Levi-Strauss, M. and M. Mallat, *Primary cultures of murine astrocytes produce C3 and factor B, two components of the alternative pathway of complement activation.* J Immunol, 1987. **139**(7): p. 2361-6.
278. Walker, D.G. and P.L. McGeer, *Complement gene expression in human brain: comparison between normal and Alzheimer disease cases.* Brain Res Mol Brain Res, 1992. **14**(1-2): p. 109-16.

279. Walker, D.G., S.U. Kim, and P.L. McGeer, *Complement and cytokine gene expression in cultured microglial derived from postmortem human brains.* J Neurosci Res, 1995. **40**(4): p. 478-93.
280. Veerhuis, R., et al., *Complement C1-inhibitor expression in Alzheimer's disease.* Acta Neuropathol, 1998. **96**(3): p. 287-96.
281. Veerhuis, R., et al., *Cytokines associated with amyloid plaques in Alzheimer's disease brain stimulate human glial and neuronal cell cultures to secrete early complement proteins, but not C1-inhibitor.* Exp Neurol, 1999. **160**(1): p. 289-99.
282. Fonseca, M.I., et al., *Absence of C1q leads to less neuropathology in transgenic mouse models of Alzheimer's disease.* J Neurosci, 2004. **24**(29): p. 6457-65.
283. Rogers, J., et al., *Complement activation and beta-amyloid-mediated neurotoxicity in Alzheimer's disease.* Res Immunol, 1992. **143**(6): p. 624-30.
284. McGeer, P.L., et al., *Activation of the classical complement pathway in brain tissue of Alzheimer patients.* Neurosci Lett, 1989. **107**(1-3): p. 341-6.
285. Medeiros, R. and F.M. LaFerla, *Astrocytes: conductors of the Alzheimer disease neuroinflammatory symphony.* Exp Neurol, 2013. **239**: p. 133-8.
286. Olabarria, M., et al., *Concomitant astroglial atrophy and astrogliosis in a triple transgenic animal model of Alzheimer's disease.* Glia, 2010. **58**(7): p. 831-8.
287. Sofroniew, M.V. and H.V. Vinters, *Astrocytes: biology and pathology.* Acta Neuropathol, 2010. **119**(1): p. 7-35.
288. Liddelow, S.A. and B.A. Barres, *Reactive Astrocytes: Production, Function, and Therapeutic Potential.* Immunity, 2017. **46**(6): p. 957-967.
289. Liddelow, S.A., et al., *Neurotoxic reactive astrocytes are induced by activated microglia.* Nature, 2017. **541**(7638): p. 481-487.
290. Furman, J.L., et al., *Targeting astrocytes ameliorates neurologic changes in a mouse model of Alzheimer's disease.* J Neurosci, 2012. **32**(46): p. 16129-40.
291. Hartz, A.M., et al., *Amyloid-beta contributes to blood-brain barrier leakage in transgenic human amyloid precursor protein mice and in humans with cerebral amyloid angiopathy.* Stroke, 2012. **43**(2): p. 514-23.
292. Carrano, A., et al., *Neuroinflammation and blood-brain barrier changes in capillary amyloid angiopathy.* Neurodegener Dis, 2012. **10**(1-4): p. 329-31.
293. Kapasi, A. and J.A. Schneider, *Vascular contributions to cognitive impairment, clinical Alzheimer's disease, and dementia in older persons.* Biochim Biophys Acta, 2016. **1862**(5): p. 878-86.
294. Stanimirovic, D.B. and A. Friedman, *Pathophysiology of the neurovascular unit: disease cause or consequence?* J Cereb Blood Flow Metab, 2012. **32**(7): p. 1207-21.
295. Keaney, J. and M. Campbell, *The dynamic blood-brain barrier.* FEBS J, 2015. **282**(21): p. 4067-79.
296. Amiry-Moghaddam, M., et al., *An alpha-syntrophin-dependent pool of AQP4 in astroglial end-feet confers bidirectional water flow between blood and brain.* Proc Natl Acad Sci U S A, 2003. **100**(4): p. 2106-11.
297. Simard, M. and M. Nedergaard, *The neurobiology of glia in the context of water and ion homeostasis.* Neuroscience, 2004. **129**(4): p. 877-96.

298. Dunn, K.M. and M.T. Nelson, *Potassium channels and neurovascular coupling.* Circ J, 2010. **74**(4): p. 608-16.
299. Strohschein, S., et al., *Impact of aquaporin-4 channels on K+ buffering and gap junction coupling in the hippocampus.* Glia, 2011. **59**(6): p. 973-80.
300. Noell, S., et al., *Evidence for a role of dystroglycan regulating the membrane architecture of astroglial endfeet.* Eur J Neurosci, 2011. **33**(12): p. 2179-86.
301. Gondo, A., et al., *Sustained down-regulation of beta-dystroglycan and associated dysfunctions of astrocytic endfeet in epileptic cerebral cortex.* J Biol Chem, 2014. **289**(44): p. 30279-88.
302. Newman, E.A., D.A. Frambach, and L.L. Odette, *Control of extracellular potassium levels by retinal glial cell K+ siphoning.* Science, 1984. **225**(4667): p. 1174-5.
303. Neusch, C., et al., *Lack of the Kir4.1 channel subunit abolishes K+ buffering properties of astrocytes in the ventral respiratory group: impact on extracellular K+ regulation.* J Neurophysiol, 2006. **95**(3): p. 1843-52.
304. Wallraff, A., et al., *Distinct types of astroglial cells in the hippocampus differ in gap junction coupling.* Glia, 2004. **48**(1): p. 36-43.
305. Badaut, J., et al., *Aquaporins in brain: distribution, physiology, and pathophysiology.* J Cereb Blood Flow Metab, 2002. **22**(4): p. 367-78.
306. Price, B.R., et al., *An emerging role of astrocytes in vascular contributions to cognitive impairment and dementia.* J Neurochem, 2018. **144**(5): p. 644-650.
307. Xu, Z., et al., *Deletion of aquaporin-4 in APP/PS1 mice exacerbates brain Abeta accumulation and memory deficits.* Mol Neurodegener, 2015. **10**: p. 58.
308. Tarasoff-Conway, J.M., et al., *Clearance systems in the brain-implications for Alzheimer disease.* Nat Rev Neurol, 2015. **11**(8): p. 457-70.
309. Michaluk, P., et al., *Beta-dystroglycan as a target for MMP-9, in response to enhanced neuronal activity.* J Biol Chem, 2007. **282**(22): p. 16036-41.
310. Sudduth, T.L., et al., *Time-course of glial changes in the hyperhomocysteinemia model of vascular cognitive impairment and dementia (VCID).* Neuroscience, 2017. **341**: p. 42-51.
311. Eng, J.A., et al., *Clinical manifestations of cerebral amyloid angiopathy-related inflammation.* Ann Neurol, 2004. **55**(2): p. 250-6.
312. Scolding, N.J., et al., *Abeta-related angiitis: primary angiitis of the central nervous system associated with cerebral amyloid angiopathy.* Brain, 2005. **128**(Pt 3): p. 500-15.
313. Kinnecom, C., et al., *Course of cerebral amyloid angiopathy-related inflammation.* Neurology, 2007. **68**(17): p. 1411-6.
314. Nakata-Kudo, Y., et al., *Microbleeds in Alzheimer disease are more related to cerebral amyloid angiopathy than cerebrovascular disease.* Dement Geriatr Cogn Disord, 2006. **22**(1): p. 8-14.
315. Goos, J.D., et al., *Incidence of cerebral microbleeds: a longitudinal study in a memory clinic population.* Neurology, 2010. **74**(24): p. 1954-60.
316. Gregoire, S.M., et al., *MRI detection of new microbleeds in patients with ischemic stroke: five-year cohort follow-up study.* Stroke, 2010. **41**(1): p. 184-6.

317. Liu, Y., A. Beyer, and R. Aebersold, *On the Dependency of Cellular Protein Levels on mRNA Abundance.* Cell, 2016. **165**(3): p. 535-50.
318. Bemiller, S.M., et al., *TREM2 deficiency exacerbates tau pathology through dysregulated kinase signaling in a mouse model of tauopathy.* Mol Neurodegener, 2017. **12**(1): p. 74.
319. Jiang, T., et al., *TREM2 Ameliorates Neuronal Tau Pathology Through Suppression of Microglial Inflammatory Response.* Inflammation, 2018. **41**(3): p. 811-823.

Vita

Brittani R. Price, B.S.
Doctoral Candidate
Department of Physiology
Sanders Brown Center on Aging
University of Kentucky College of Medicine

1. EDUCATION

Undergraduate

B.Sc (Magna Cum Laude): Morehead State University, Morehead, Kentucky. Biomedical Science. 2015

Professional / Graduate

Graduate Certificate in Clinical and Translational Sciences: CCTS, University of Kentucky. 2018.

Graduate Certificate in Medical Physiology Teaching: Department of Physiology, University of Kentucky. 2018.

Ph.D. Neurophysiology: Department of Physiology, University of Kentucky. 2019.

2. TEACHING

University of Kentucky

PGY 207 – Case Studies in Physiology. 28 lectures on basic physiology and pathophysiology. Fall semester 2017.

HON 152 – Biology of Aging. 1 lecture on Alzheimer's Disease. Spring semester 2018.

Area Health Education Center (AHEC) Summer Camp – Human Physiology. 8 2-hour lectures on basic physiology and pathophysiology. Summer 2018.

3. HONORS AND AWARDS

National Neurotrauma Society Travel Award Recipient. 2016
Alzheimer's Association International Conference Travel Award Recipient. 2016.
Markesbury Symposium Outstanding Poster Presentation Award Recipient. 2016.
Alzheimer's Association International Conference Volunteer Travel Award Recipient. 2017.
Alzheimer's Association Student Poster Competition Finalist. 2017.
Alzheimer's Association Immunity and Neurodegeneration PIA Invited Speaker. 2017.
T32 Predoctoral Fellow. 2017.

4. PUBLIC SERVICE AND PROFESSIONAL DEVELOPMENT

Professional Memberships:

Bluegrass Society for Neuroscience. 2016-Present.
Society for Neuroscience. 2016-Present.
International Society to Advance Alzheimer's Research and Treatment. 2016-Present.

Service:

Executive Committee Member. University of Kentucky Women in Medicine and Science (WIMS). 2016.
Professional Development Committee Chair. University of Kentucky Biomedical Graduate Student Organization. 2017-Present.
Planning Committee. Everything is Science Lexington, Science Festival. 2017-Present.
Vascular Cognitive Disorders Professional Interest Area (VPIA) Student Representative. Alzheimer's Association. 2018-Present.
Immunity and Neurodegeneration Professional Interest Area Student Representative. Alzheimer's Association. 2018-Present.
Free Memory Screens. Lexington Senior Center. 2018-Present.

5. SPEAKING ENGAGEMENTS

International

Alzheimer's Association International Conference Invited Seminar, London, UK 2017.

6. RESEARCH AND INTELLECTUAL CONTRIBUTIONS

Peer-reviewed Publications:

1. Tiffany L. Sudduth, Erica M. Weekman, **Brittani R. Price**, Jennifer L. Gooch, Abigail Woolums, Christopher M. Norris, Donna M. Wilcock. Time-course of glial changes in the hyperhomocysteinemia model of vascular cognitive impairment and dementia. Neuroscience, 2017.
2. **Brittani R. Price**, Christopher M. Norris, Donna M. Wilcock. The Role of Astrocytes in Vascular Cognitive Impairment. Journal of Neurochemistry, 2017. *Invited Review.*
3. **Brittani R. Price,** Donna M. Wilcock, Erica M Weekman. Hyperhomocysteinemia as a Risk Factor for Vascular Contributions to Cognitive Impairment and Dementia. Frontiers, 2018. *Invited Review*.
4. **Brittani R. Price**, Tiffany L. Sudduth, Erica M. Weekman, Abigail Woolums, Danielle Hawthorne, Arnon Rosenthal, Donna M. Wilcock. Therapeutic targeting of TREM2 by an activating antibody ameliorates amyloid-beta deposition and improves cognition. *Under Review*.
5. Erica M. Weekman, Tiffany L. Sudduth, **Brittani R. Price**, Abigail Woolums, Danielle Hawthorne, Charles E. Seaks, Donna M. Wilcock. Time-course of neuropathological events in hyperhomocysteinemic amyloid depositing mice reveals early neuroinflammatory changes that precede amyloid changes and cerebrovascular events. *Under Review*.

7. SPONSORED GRANTS AND CONTRACTS

Current

5T32 NS077889 Hall, ED (PI) 08/29/2017-09/01/2019
NIH/NINDS
Neurobiology of CNS Injury and Repair Training Grant.